An Investigation into the Effect of Agitation on Polymer Properties in Emulsion Polymerisation.

by

Brian Graham Clarkson.

Submitted for the degree of Master of Philosophy
of the University of London
and for the
Dimploma of Imperial College.

Department of Chemical Engineering
and Chemical Technology,
Imperial College,
University of London.

September 1988.

Abstract.

Traditionally the important physical processes in emulsion polymerisation have been considered to be dominated solely by the chemistry involved. A description of the physical chemistry of emulsion polymerisation with a review of the historical developments is presented as a basis for a discussion of the role of agitation in emulsion polymerisation.

Agitation effects have been examined in two types of reactor, a continuous flow recycle loop reactor and a batch autoclave, providing two different types of flow field. The development of the loop reactor in commercial emulsion polymerisation is reviewed. Previous modelling work on loop reactors has been adapted and examined experimentally. The construction and instrumentation of a 4.3 litre pilot plant scale loop reactor is described together with the modifications made during the course of this work. Results of the characterisation of flow rates, mixing and temperature distribution within the reactor together with descriptions of emulsion polymerisations of styrene monomer in batch operation are given. These are used to support conclusions on the design of loop reactors for successful use in emulsion polymerisation.

A description of batch emulsion polymerisations of styrene performed in a glass autoclave with paddle agitator is given. The polymer latex produced was characterised by conversion, particle size distribution, and molecular weight distribution. A discussion of the affect of agitation on these polymer properties is presented.

Molecular weight distributions were measured by Gel Permeation Chromatography. A review of resolution problems inherent with G.P.C. is presented and a practical description of how to overcome them and obtain true molecular weights distributions from G.P.C. chromatograms is reported.

Acknowledgements.

I would like to extend my thanks and appreciation to:

My supervisors, Dr G.C.Maitland and Dr S.M.Richardson, for their advice and guidance throughout the course of this work;

The technical support staff in the Department of Chemical Engineering;

The Science and Engineering Research Council for their financial support;

Unilever Research Port Sunlight Laboratory for the facilites to produce this thesis;

and finally, to my wife Angela for her love and encouragement, without which I could not have completed this work.

"When I applied my mind to know wisdom and observe man's labour on earth, his eyes not seeing sleep day or night, then I saw all that God has done. No-one can comprehend what goes on under the sun. Despite all his efforts to search it out, man cannot discover its meaning. Even if a wise man claims he knows, he cannot really comprehend it."

Ecclesiastes 8:16,17

Table of Contents.

	Title Page.	1
	Abstract.	2
	Acknowledgements.	3
	Table of Contents.	4
	List of Tables.	6
	List of Figures.	7
1	Introduction.	9
2	A Review of Emulsion Polymerisation.	11
2.1	Nature of Polymerisation.	11
2.2	Emulsion Polymerisation.	13
2.3	Advantages and Disadvantages.	18
2.4	Quantitative Theory.	19
3	Batch Autoclave Polymerisation of Styrene	27
3.1	Aims of Autoclave Experiments.	27
3.2	Reactor Scaling.	27
3.3	Experimental Method.	28
3.4	Measurements upon Polymer Latex.	31
3.5	Results and Discussion.	33
4	The Loop Reactor Process.	44
4.1	Introduction.	44
4.2	History of the Process.	45
4.3	A Loop Reactor Mixing Model.	49
4.4	An Experimental Loop Reactor.	64
4.5	Temperature Distribution	70
4.6	Mixing Measurements.	74
4.7	Emulsion Polymerisation of Styrene.	84
4.8	Reagents and Procedure.	86
4.9	Observations and Results.	87
4.10	Comments on the design of Loop Reactors for Emulsion Polymerisation.	91

5	Measurement of Molecular Weight Distribution.	93
5.1	Experimental Measurements.	102
5.2	Chromatograms to Molecular Weight.	105
6	Conclusions	113
	References.	115

List of Tables.

Table:

3.1 Effect of Agitation Speed and Surfactant Concentration upon Polymer Properties. 34

3.2 Effect of Agitation Speed and Surfactant Concentration upon Polymer Properties with Slow Monomer Addition. 37

3.3 Effect of Initial Agitator Speed upon the Polymer Properties. 41

4.1 Flow Conditions in Loop Reactor for Styrene Emulsion Polymerisation Experiments. 89

List of Figures.

Figure:

2.1	Physical Picture in Emulsion Polymerisation.	16,17
3.1	Experimental Batch Reactor.	29
3.2	Effect of Agitation Speed and Surfactant Concentration upon Polymer Properties with Slow Monomer Addition.	38
3.3	Effect of Initial Agitator Speed upon the Polymer Properties.	42
4.1	Internal and External Circulation Loop Reactors.	46
4.2	Schematic Diagram for Loop Reactor Model.	50
4.3	Batch Mixing in a Loop Reactor with a Bodenstein Number of 25 and 50.	53
4.4	Batch Mixing in a Loop Reactor with a Bodenstein Number of 100 and 200.	54
4.5	Batch Mixing in a Loop Reactor with a Bodenstein Number of 400 and 800.	55
4.6	Mixing Time in a Batch Loop Reactor with Bodenstain Number as a Parameter.	57
4.7	Mixing Time against Bodenstein Number.	58
4.8	Mixing in a Continuous Loop Reactor with a Bodenstein Number of 50 and Circulation Numbers of 10 and 20.	60
4.9	Mixing in a Continuous Loop Reactor with a Bodenstein Number of 50 and Circulation Numbers of 40 and 80.	61
4.10	Mixing in a Continuous Loop Reactor with a Bodenstein Number of 200 and Circulation Numbers of 10 and 20.	62

4.11 Mixing in a Continuous Loop Reactor with a Bodenstein Number of 200 and Circulation Numbers of 40 and 80. 63
4.12 Comparison of Inhomogeneity Calculations with Bodenstein Number as a Parameter. 65
4.13 Mixing Time in a Continuous Loop Reactor with Circulation Number as a Parameter. 66
4.14 Schematic Diagram of the Experimental Loop Reactor. 68
4.15 Line Diagram of the Experimental Loop Reactor. 69
4.16 Loop Reactor Measurement Port. 71
4.17 Radial Temperature Profiles. 72
4.18 Static Mixers. 73
4.19 Experimental Batch Mixing Traces. 75
4.20 Comparison with Experimental Results. 77
4.21 Experimental Continuous Mixing Traces. 78
4.22 Comparison with Experimental Results. 79
4.23 Experimental Mixing Times, No Static Mixers. 80
4.24 Experimental Mixing Times, One Static Mixers. 81
4.25 Experimental Mixing Times, Two Static Mixers. 82
4.26 Experimental Mixing Times, Four Static Mixers. 83
4.27 Effective Longitudinal Dispersion Coefficient against Reynolds Number. 85

5.1 Column Dispersion of a Gaussian Distribution. 96
5.2 Gamma Distribution form its Moments, Mono-Modal Distribution. 103
5.3 Gamma Distribution form its Moments, Bi-Modal Distribution. 104
5.4 Calibration Curve for G.P.C. Columns 106
5.4 Typical Output from Chromatogram Program. 109
5.5 Corrected G.P.C. Chromatogram. 111

1.0 Introduction.

Polymerisation of vinyl monomers in aqueous emulsion has been performed since the 1920s, and is an important method of producing synthetic rubbers and polymer latices. The stability of the monomer in water emulsion is usually maintained by micelle forming soap-like compounds or non-ionic surfactants. The importance of this process has lead to much research into the mechanism of polymerisation, from the monomer emulsion to the final polymer latex. However, the method of formation of the monomer emulsion and affect of the agitation conditions on the properties of the final polymer latex has received considerably less attention and is not well understood[1.1,1.2,1.3,1.4].

The majority of the annual tonnage of emulsion polymer latex is produced in large semi-batch reactors in the form of a stirred tank with baffles, cooling coils or external heat exchangers, and microprocessor control. The development of a continuous process for emulsion polymerisation would be advantageous in that annual tonnages could be increased and use of on line quality control could overcome the problems of batch to batch inconsistency. From the standpoint of reactor design and scale-up, for both batch and continuous reactors, an understanding of the effect of agitation upon the quality of the latex products would be very useful.

The objectives of this work were to examine how agitation conditions affect the course of emulsion polymerisation in both batch and continuous reactors, and to investigate the feasibility of a continuous emulsion polymerisation process.

The role of agitation in the initial dispersion of monomer and its effect on the latex produced was examined experimentally with a styrene in water emulsion system. An isothermal bench scale batch stirred tank reactor was used, with systematic variation of the agitator speed and emulsifier concentration.

When characterising the polymer latices produced in these experiments, a practical and easily implemented method of analysing the molecular weight distribution from Gel Permeation Chromatography chromatograms was developed and is described in chapter five.

A Loop Reactor was used to examine continuous flow emulsion polymerisation, and is a fundamentally different type of reactor from the traditional semi-batch stirred tank. In the Loop Reactor there is no active agitator in the traditional sense, such as a paddle, to disperse the monomer and aid heat and mass transfer. The polymerising reagents are circulated around a continuous length of pipe, into which fresh reagents are pumped and from which product is extracted. Since the Loop Reactor is basically a pipe, the flow fields within it are well defined and uniform, so growing polymer particles will experience similar, known, agitation histories. This gave a second type of flow regime under which the affect of agitation could be studied. The macro-mixing within Loop Reactor is modelled and examined experimentally, and the conclusions are used to suggest guidelines for the design of Loop Reactors for emulsion polymerisation.

2.0 A Review of Emulsion Polymerisation.

2.1 Nature of Polymerisation.

A polymer is a compound whose molecule is formed from a large number of repeated units of one or more compounds of low molecular weight, called monomers. Synthetic polymers can be produced from a wide range of monomers in many different reaction conditions. There are two main mechanisms by which polymerisation can proceed; chain growth or addition; and step growth or condensation. In addition polymerisation, unsaturated monomer molecules react by the rearrangement of multiple bonds to create an essentially linear sequence of monomer units. Growth of the polymer molecules can only occur in an active chain where there is a free radical, to which monomer units are added. Free radicals are formed by a catalyst-like compound called an initiator. High molecular weight molecules are formed quickly, and long reaction times are required for a high conversion of monomer, as the concentration of growing chains is low. In condensation polymerisation chemically bi-functional monomers react with the elimination of a small molecule, for example water, the chemical nature of the polymer being different from the monomers. Growth of the polymer molecule can occur when any two of the reaction species are present. Monomer disappears early in the reaction, but long reaction times are required for high molecular weights. The way in which these polymerisations are performed affects the nature of the polymer product, for example: molecular weight, morphology and rheology. Polymerisation methods can be classified as follows:

I. Liquid Phase.

i. Bulk Polymerisation.

- Polymer soluble in monomer: polystyrene, polymethlymethacrylate, polyvinylacetate.
- Polymer insoluble in monomer: polyvinylchloride, polyacrylonitrile.
- Polymer swollen by monomer: polyethylene.

ii. Solution Polymerisation.
- Polymer soluble in solvent: polyethylene in cyclo-octane.
- Polymer insoluble in solvent: polyethylene in iso-octane.

iii. Suspension Polymerisation.
Initiator soluble in monomer,
particle diameter 10-1000 μm.

iv. Emulsion Polymerisation.
Initiator soluble in continuous phase,
particle diameter 50-100 nm.

II. Vapour Phase.
Ziegler Natta polymerisation of olefins: high density polyethylene, polypropylene.

III. Solid Phase.
Radiation induced polymerisation in crystalline state: polydimethylsiloxane.

The simplest of these methods is the liquid phase bulk polymerisation, which will be used to illustrate some of the problems encountered in polymerisation. Essentially monomer is placed in a stirred reaction vessel with a mechanism for heating and/or cooling, such as a jacket or coils. As the reaction proceeds the viscosity of the reacting mixture increases which impedes mixing. As most polymerisations are exothermic and polymers have a low thermal conductivity, heat removal is poor and control of the rate of reaction is difficult. The properties of the polymer produced will vary significantly throughout the reactor, which can make the product commercially useless. Each of the other methods of liquid phase polymerisation attempts to overcome these problems by diluting the reactants and improving the heat transfer.

2.2 Emulsion Polymerisation.

Emulsion Polymerisation has been a major way of producing synthetic rubber since it was first reported as a polymerisation method in 1927[2.1]. Published literature on the various aspects of emulsion polymerisation is extensive, and has been reviewed many times. Two such comprehensive reviews are by Blackley[2.2] and Piirma[2.3]. No attempt is made here to produce such a comprehensive review of emulsion polymerisation, only to describe the physical processes and outline the important historical developments. Emulsion polymerisation is one method of performing addition polymerisations. It is a heterogeneous polymerisation process in which monomer is dispersed in a continuous phase by an emulsifying agent, with an initiator that is soluble in the continuous phase. An emulsion polymerisation will typically contain a minimum of four basic components:

i. Monomer.
ii. Continuous phase.
iii. Emulsifying agent.
iv. Initiator.

The continuous phase is usually aqueous and, since most monomers are sparingly soluble, the solubility limit of the monomers will have been exceeded leading to two distinct phases: the monomer phase and the aqueous phase. The aqueous phase contains the soap-like micelle forming emulsifying agent, and can be considered as two phases: the micelle phase and the true aqueous phase.

From this it can be see that there exist several sites, or loci, at which polymerisation could be considered to proceed:

i. the monomer droplets;
ii. the monomer droplet / aqueous phase interface;
iii. the true aqueous phase;
iv. the micelle phase.

The earliest successful qualitative theory to explain the mechanism of emulsion polymerisation was that of Harkins[2.4,2.5]. The essential features of the theory are:

i. Monomer droplets are reservoirs of monomer, from which it diffuses into the aqueous phase, then to micelles or polymer particles.

ii. Particle initiation occurs in monomer swollen micelles, by radical oligomers formed in the true aqueous phase from dissolved monomer and initiator. Monomer is then absorbed from the aqueous phase and the particles grow as polymerisation proceeds.

iii. The main loci of polymerisation are polymer particles formed from initiated and swollen micelles. Polymerisation is not in the monomer particles as these are very much bigger than the final polymer particles formed.

iv. A small amount of initiation occurs in the true aqueous phase, becoming less significant with the increase emulsifier concentration.

v. Growth in polymer particles leads to the adsorption of emulsifier from the true aqueous phase, and the dissociation of non-initiated micelles. Micelles disappear early in the reaction, between 10% and 20% conversion.

vi. Continual monomer absorption into polymer particles leads to the disappearance of monomer droplets, leaving only monomer swollen polymer particles.

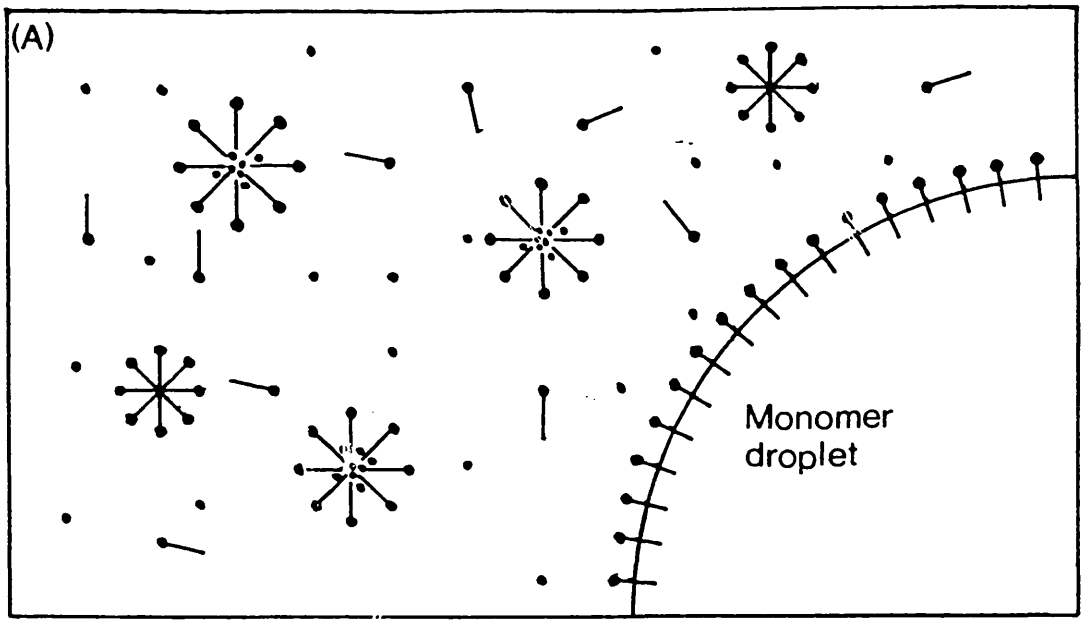
The course of an emulsion polymerisation is shown diagramatically in figures 2.1A, 2.1B, 2.1C & 2.1D. Before initiation, figure 2.1A, monomer is dispersed in the aqueous phase and stabilised by emulsifier molecules. Micelles are formed if the emulsifier concentration is above the critical micelle concentration; some micelles will contain absorbed monomer. The aqueous phase will contain free emulsifier molecules and dissolved monomer. When initiator is added, $R^{\cdot}$ in figure 2.1B, its highly ionic nature makes it unlikely that it will be absorbed directly into micelles. The first step in initiation involves initiator radicals adding some monomer molecules, from the aqueous phase, to become sufficiently oil soluble to be absorbed. Once radicals are absorbed into micelles, growing polymer particles receive monomer by mass transfer and diffusion, via the aqueous phase, from monomer droplets. As polymerisation continues, these particles get bigger and require more emulsifier to stabilise them. This comes from the aqueous phase and the uninitiated micelles, until all free emulsifier is used up. When all the micelles have gone particle initiation ends; this is traditionally called Interval one.

Interval two, figure 2.1C, is characterised by a constant number of growing polymer particles, which implies a constant rate of polymerisation. Monomer droplets are depleted giving up monomer and emulsifier to growing particles. The disappearance of monomer droplets marks the start of the final stage, Interval three, figure 2.1D. Polymer particles are swollen by monomer, which is the only source of monomer, and so the rate of polymerisation falls off as monomer becomes less accessible to the active end of the growing chain. Polymerisation is completed when all the absorbed monomer has reacted. The system now contains a dispersion of small polymer particles stabilised by emulsifying agent.

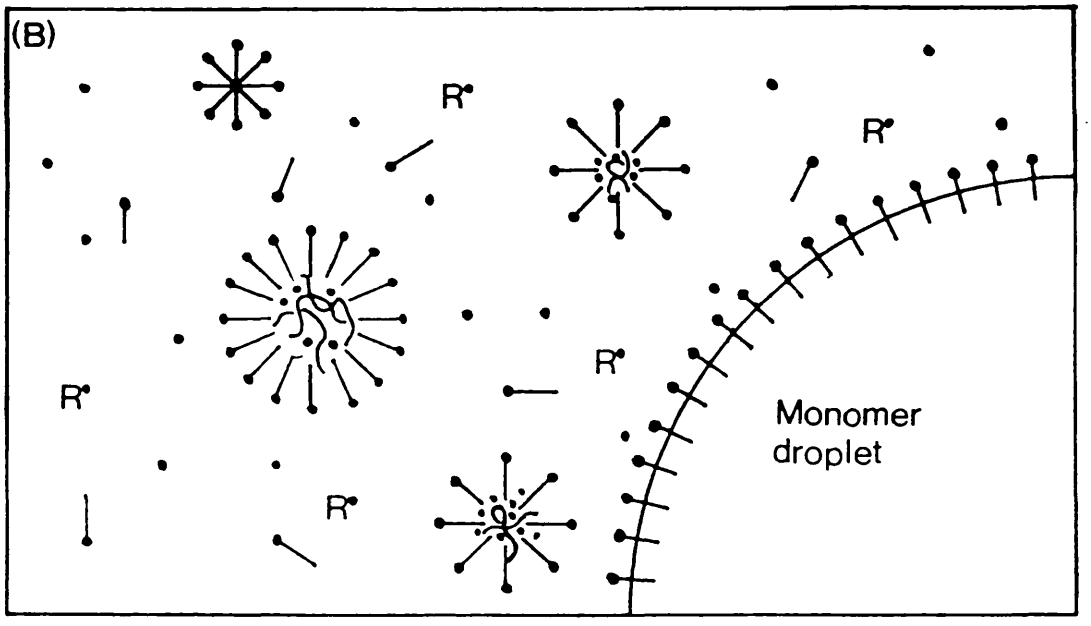
Figure 2.1

Physical Picture in Emulsion Polymerisation

Pre-Initiation



Interval I



• monomer

•— emulsifier

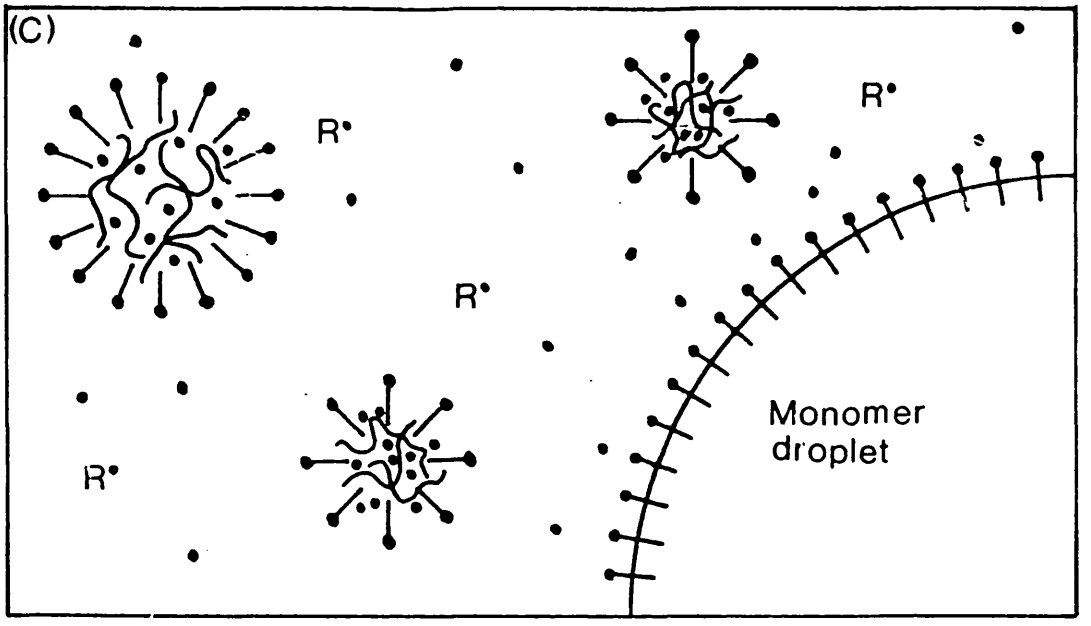
R• free radical

~~ polymer chain

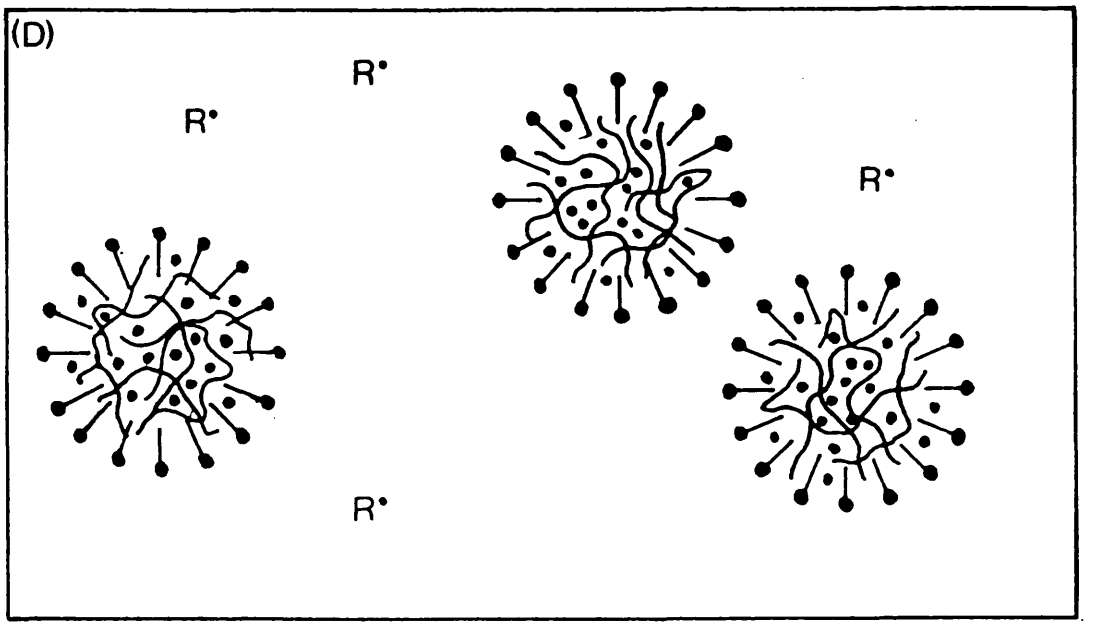
Figure 2.1

Physical Picture in Emulsion Polymerisation

Interval II



Interval III



• monomer

•— emulsifier

R• free radical

~~ polymer chain

2.3 Advantages and Disadvantages of Emulsion Polymerisation.

Since the polymerising system remains fluid throughout the course of the reaction, removing the heat of reaction is less of a problem than in a bulk polymerisation. Provided a correctly formulated recipe is used there is no tendency for particle coalescence. The product is a polymer latex which is advantageous if the product is to be used for coatings or adhesives.

In contrast to most polymerisation processes, emulsion polymerisation produces very high molecular weight polymer at relatively fast reaction rates. This is due to the large number of protected colloidal particles maintaining the concentration of reacting radicals in the system, and hence a fast reaction rate. As each colloidal particle usually contains only one radical at a time, (since if a second radical enters, terminate will rapidly ensue), only a small number of large polymer chains are produced in each particle, giving a high molecular weight. Products like synthetic rubbers require these high molecular weights, and a fast reaction rate reduces production costs. However, high molecular weights are not always desirable, as with adhesives, so chain transfer agents can be added in order to reduce it.

Emulsion polymerisation has the disadvantage that if the bulk polymer is required it must be separated from the aqueous phase, which is not trivial process. The polymer produced like this will also have a significant proportion of non-polymer content, the surfactant. A further industrial disadvantage that is shared with suspension and solution polymerisation is that the effective reactor volume is reduced by the dispersion medium.

2.4 Quantitative theory.

Historically, the quantitative theory to have the most significant impact on emulsion polymerisation modelling is that of Smith and Ewart[2,6]. It has become a bench-mark to which other developments have been compared and a starting point of more sophisticated theories. Based on the Harkin model, it attempts predict the rate of reaction and the number of reaction loci, in terms of the concentrations of certain reaction components. The rate of polymerisation in a single polymer particle, during Interval two, was explained in terms of:

-Rate of formation of free radicals.
-Rate of escape of free radicals from the reaction locus.
-Rate of termination of free radicals in reaction locus and aqueous phase.
-Rate of polymerisation of free radicals in a reaction locus.

Assuming steady state on the number of particles with i free radicals in them, a balance of the above rate gave recursion formula on the number of free radicals per polymer particle. These formula were not solved explicitly but three limiting cases were examined:

Case 1. Where the mean number of free radicals per polymer particle is small compared with unity. This would occur if the rate of transfer out of a particle is larger than the termination rate or the rate of transfer into a particle.

Case 2. Where the mean number of free radicals per polymer particle is approximately one half. This would occur if termination in particles is instantaneous, or at least fast compared with successive entries, and radical transfer back into the aqueous phase is negligible.

Case 3. Where the mean number of free radicals per polymer particle is large compared with unity. This would occur if the rate of termination is slow, which may be due to increased viscosity.

For each of these cases an expression for the rate of polymerisation was derived. The most successful of which is that for Case 2, which applies to the emulsion polymerisation of styrene and methyl methacrylate under normal conditions[2.7,2.8]. The rate of polymerisation per unit volume of emulsion is given by the simple expression:

$$\frac{d[M]}{dt} = -\frac{k_p[M]N_p\bar{n}}{2}$$

equation 2.1

where: k_p = propagation rate constant
$[M]$ = monomer concentration in the particle
N_p = number of polymer particles per unit volume
$\bar{n}$ = mean number of free radicals per particle

In order to determine how many polymer particles are formed, Harkins original idea, that most of the soap is present in the form of micelles containing dissolved monomer, was developed. To simplify the problem of the effectiveness of the micelles in capturing the monomer, two extremes were considered:

First it was assumed that all the free radicals produced go into micelles as long as micelles are still present. This would give too many loci since some radicals mutually terminate.

Secondly it was assumed that a given interfacial area always has the same effectiveness in collecting free radicals, and is independent of the size of the particle. This gives too few reaction loci as, from Fick's first law of diffusion, the radical absorption rate is proportional to the particle surface area divided by the radius. So small particles absorb more radicals per unit area than large particles do.

These two approaches yielded similar results for the number of particles, N_p,

$$N_p = k\left\{\frac{\rho}{\mu}\right\}^{2/5}\left\{\alpha S\right\}^{3/5}$$

equation 2.2

where ρ = rate of formation of free radicals per unit volume.
μ = rate of increase in volume of a particle, assumed constant.
α = specific surface area per unit of emulsifier.
S = emulsifier concentration.

The only difference in the two approaches was in the value of k, k=0.53 was obtained in the first situation, whereas k=0.37 was obtained in the second. As these two values represent extremes of the situation the true value will lie between them, $0.37 < k < 0.53$. This equations leads to the following conclusions about the emulsion polymerisation reaction:

i. the steady rate of polymerisation should be of order 2/5 with respect to the initial initiator concentration;

ii. the steady rate of polymerisation should be of order 3/5 with respect to the concentration of the micelle generating substance;

iii. the steady rate of polymerisation per unit mass of soap should be inversely proportional to the 2/5th power of the concentration of micelle forming substance. Thus a given mass of soap should be more efficient at promoting polymerisation in a dilute solution than in a concentrated solution.

Implicit in the Harkins theory, and here, is that there will be no polymerisation if micelles are not present.

The Smith-Ewart theory has been successful in describing some experimental systems, particularly Case 2 kinetics which are considered the 'ideal' model of emulsion polymerisation. In many situations emulsion polymerisation does not follow Smith-Ewart kinetics. Thus variations upon their theory and different approaches have been published to account for this. These deviations arise from the chemistry of the polymerisation systems used departing from the 'ideal' assumptions, and include:

i. Polymerisation in monomer droplets when monomer soluble initiators are used, polymerisation being similar to the suspension process.

ii. Precipitation out of the aqueous phase of oligomers that form polymerisation loci, as in solution polymerisations.

iii. Micelle regeneration due to polymer chain ends stabilising growing particles and releasing emulsifier in Intervals 2 & 3.

iv. The 'Gel effect' due to increase viscosity within the polymer particle, particularly in Interval 3.

v. Particle morphology changes due to polymer insolubility in its monomer.

In a review on the mathematical modelling of emulsion polymerisation, Min & Ray[2.9] concluded that all previous models were inadequate. They presented a comprehensive mathematical description of emulsion polymerisation which included all the previous models as special cases. This description considered virtually all physical processes that could take place in an emulsion polymerisation, which lead to complex multivariate population balance equations coupled to material and energy balances for the reactor.

Min[2.10] did not attempt to solve the full set of equations due to their complexity, but considered a specific polymerising system. Assumption, based on experimental experience, were made about which physical processes that are important for the system, and which should be included into the model. The equation subset was further simplified by restricting the detail required from the population balances, giving a solvable set of descriptive equations. An example of this approach was given by Min & Ray[2.11] for the batch homo emulsion polymerisation of methyl methacrylate. Assumptions made for this system included:

i. The kinetics followed the free radical scheme,

Initiation $I \longrightarrow 2R$

$R + M \longrightarrow P_1$

Propagation $P_n + M \longrightarrow P_{n+1}$

Chain Transfer $P_n + M \longrightarrow P_1 + M_n$

$P_n + T_r \longrightarrow P_1 + M_n$

Termination $P_n + P_m \longrightarrow M_{n+m}$

$P_n + P_m \longrightarrow M_n + M_m$

where: I = Initiator R = Free Radicals M = Monomer

T_r = Chain Transfer agent

P_n = Growing polymer of length n monomer units

M_n = Dead polymer of length n monomer units

ii. There is excellent temperature control so that the system is isothermal.

iii. The polymer particles are homogeneous with no internal structure.

iv. New polymer particles may arise both from micelles and from aqueous phase oligomer precipitation.

v. Polymer particles are stabilised both by emulsifier and by polymer chain ends on the particle surface.

vi. Polymer particle agglomeration is important.

vii. The gel effect is present at high conversion.

viii. The monomer concentration in polymer particles depends on particle size and aqueous phase monomer concentration.

For computational reasons the particle size distribution was considered together with two subsets. The first subset represented small particles reappearing in Interval three. The second subset represented the particles in Interval one singly impregnated with growing radicals. The total particle balance is of the form:

$$\begin{bmatrix}\text{change of total}\\ \text{number of particles}\\ \text{with time}\end{bmatrix} + \begin{bmatrix}\text{rate of change}\\ \text{by volume increase}\\ \text{of growing particles}\end{bmatrix} =$$

$$\begin{bmatrix}\text{rate of formation of particles}\\ \text{of volume V to V+dV}\\ \text{by coalescence}\end{bmatrix} - \begin{bmatrix}\text{rate of disappearance of}\\ \text{particles of volume V to}\\ \text{V+dV by coalescence}\end{bmatrix}$$

$$+ \begin{bmatrix}\text{rate of change of population}\\ \text{by coalescence between}\\ \text{micelles and polymer particles}\end{bmatrix} + \begin{bmatrix}\text{rate of new particle}\\ \text{formation of volume Vo}\\ \text{by oligomer precipitation}\end{bmatrix}$$

$$+ \begin{bmatrix}\text{rate of new particle formation}\\ \text{of volume Vm by radical entry}\\ \text{into micelles}\end{bmatrix}$$

The particle size distribution also contained, a radical number distribution, a growing polymer chain length distribution and a dead polymer chain length distribution. These six distributions formed a set of coupled partial differential and integral equations that were solved numerically.

Due to the wide variety of time scales of the various physical processes in the model, the system of equations are stiff. To overcome the stiffness a quasi steady sate approximation was made wherever possible, for example: in the growing polymer chain length distribution, aqueous and particle phases; in the radical number distribution in both phases; and in the dead polymer concentration in the aqueous phase.

The method of solution was to calculate the leading moments of the various distributions. The advantage of this is that moments can easily be compared with experimental data, and it reduces the equations to ordinary differential or algebraic equations, which are readily solved numerically. Explicit distributions are obtained by moment expansions.

The fist task in modelling a specific system is to determine values for the appropriate system parameters. Here kinetic parameters, dependence of the gel effect on conversion, collision frequency factor for coalescence and physical properties were taken or calculated from the available literature. Result from this simulation showed a good comparison with experimental results.

In many of the models of emulsion polymerisation the nucleation of particles and their growth are considered from the point at which monomer is dispersed in the continuous phase and maintained by some form of agitation and surfactant. However, the role which agitation has to play in the course of polymerisation and on the properties of the final polymer latex is not well understood[2.12,2.13,2.14]. For reactor design and scale-up it would very useful to understand how agitation effects the polymerisation process.

As has been explained above the rate of polymerisation is a function of the number of polymer particles, which are supplied with monomer from stabilised droplets via the continuous phase. Agitation will influence the physical processes involved in maintaining the stability of the particle and the mass transfer of species. In the following chapter the batch emulsion polymerisation of styrene at low surfactant concentrations is described, and the effect of agitation upon the polymer properties investigated.

3.0 Batch Emulsion Polymerisation of Styrene.

3.1 Aim of the Batch Polymerisation Experiments.

The majority of commercially produced emulsion latex is made in semi-batch reactor, in which successful recipes and procedure are used, together with experience, to maintain product quality. There are many areas of operation in which a variation may produce differences between batches of latex, such as the surface chemistry, roughness or fouling of the reactor walls, ambient weather conditions, the quality of the feed stock, or agitation conditions.

This work was designed to investigate whether changes in agitation conditions would produce detectable changes in the properties of the polymer latex produced.

3.2 Reactor Scaling.

A typical commercial reactor would have a reaction volume of twenty cubic meters and be stirred by a four bladed paddle agitator two meters in diameter turning at between twenty and eighty revolutions per minute. In order to have similar agitation conditions within an experimental reactor as are experienced in a commercial reactor, scaling criteria need to be used[3.1].

If the power drawn by a given agitator, P, is measured at various agitator speeds, N, in water, and the results are plotted logarthmically, a line with a slope of 3.0 is obtained. When agitators of different diameter but of the same design are used in proportionally larger tanks, then P varies with agitator diameter, D, to the fifth power. It can also be shown that P varies directly with fluid density, ρ. Combining these in the form of a dimensionless quantity gives the power number, N_p:

$$N_P = \frac{P}{N^3 D^5 \rho}$$

equation 3.1

When scaling the reactor a constant power number and constant power dissipation per unit volume, P/V, were assumed, that is scale up on a basis of constant droplet break up. Since the reagents will be the same the fluid density is constant, so for given reactor geometries the ratio of agitation speeds will be given by:

$$\left[\frac{N_2}{N_1}\right]^3 = \left[\frac{V_2}{V_1}\right] \cdot \left[\frac{D_1}{D_2}\right]^5$$

equation 3.2

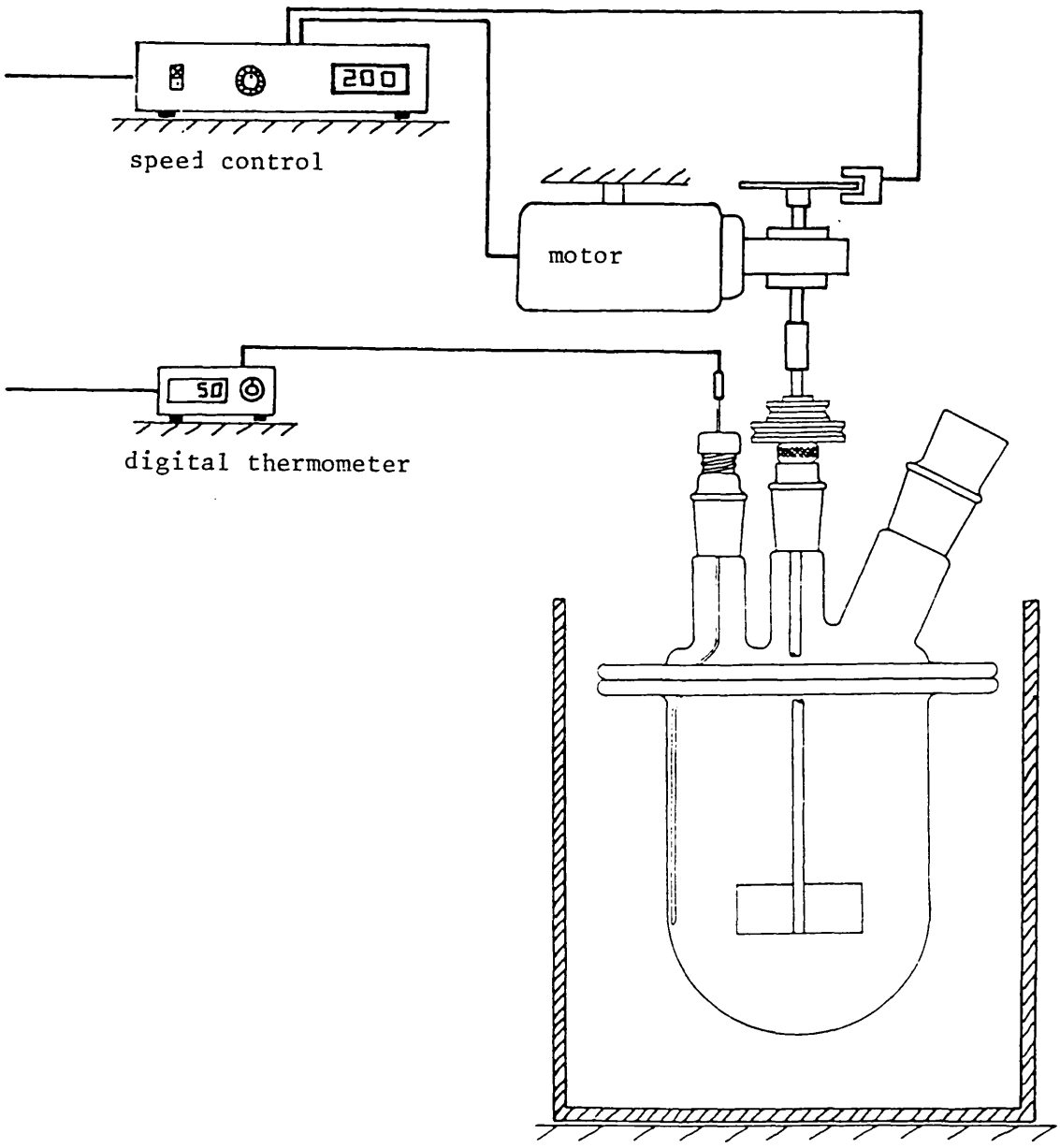
Maintaining a similar agitator diameter to reactor diameter ratio, the glass reaction vessel used, which had a half litre reaction volume, required a 50 mm diameter agitator. Using the values for the above commercial reactor the experimental agitator speeds should run between 270 and 1100 rpm, to give similar agitation conditions.

3.3 Experimental Method.

An illustration of the apparatus used to perform the polymerisation experiments appears in figure 3.1. A Quickfit round bottomed glass reaction vessel was suspended in a thermostatically controlled water bath which was maintained at the required reaction temperature of 50°C. The reaction vessel was fitted, coaxially, with a stainless steel paddle agitator, the height of the centre of the paddles was a distance from the bottom of the flask equal to the radius of curvature of the flask. The agitator was driven by a variable speed electric motor, the speed of which was controlled by a negative feedback control loop, which allowed speeds from 0 to 1200 rpm to be selected and maintained. The temperature of the reactor contents was measured using a 1 mm diameter stainless steel sheathed thermocouple, connected to a digital thermometer and/or a B.B.C. microcomputer for data logging.

Figure 3.1

Experimental Batch Reactor.



A simple recipe was used containing only the basic components for an emulsion polymerisation. The reagents were supplied by B.D.H. Ltd.

The monomer used was Styrene which was supplied containing an inhibitor, 10-20ppm tert-butylcatechol. This was removed by distillation in a reduced pressure nitrogen atmosphere. The flask containing the styrene being distilled was submerged in a thermostatically controlled water bath at 47°C, to provide a constant and stable mode of heating and prevented the styrene becoming super heated. Twenty millimetres of mercury nitrogen pressure was maintained using a vacuum pump and a nitrogen supply, monitored by a mercury manometer.

The surfactant used was Sodium dodecyl Sulphate, minimum assay 99%, used as supplied and made up to the required concentration with distilled water.

The Initiator was analytical quality Potassium persulphate, minimum assay 98%. It was used as supplied and made up to the required concentration with distilled water.

A typical recipe used would be:

Monomer	: 22.80 w/w%	(114.00 g)	(125.8 ml)
Surfactant	: 0.64 w/w%	(3.20 g)	
Initiator	: 0.39 w/w%	(1.95 g)	
Water	: 76.17 w/w%	(380.85 g)	(381.6 ml)

The initiator was dissolved in 100 ml of the distilled water, the rest of which was used to dissolve the surfactant. The surfactant solution was then placed into the reactor and a stream of nitrogen blown over it with the agitator set to the required speed. The initiator solution was placed into a flask in the thermostatic bath, and both solutions were allowed to reach the reaction temperature of 50°C. When the surfactant solution had reached this temperature, the measured volume of styrene was added. Agitation and the nitrogen purge were maintained. Reagents were allowed to reach the reaction

temperature or stirred for a set length of time, depending upon the experiment that is to be performed, then the initiator solution would be added and the reaction would proceed. After three hours the reaction would be quenched by placing the sealed reactor vessel in cold water and adding 50ml of 1% 1,4 di-hydroxy-benzene in aqueous solution, samples of latex were then taken for measurements.

3.4 Measurements upon Polymer Latex.

To characterise the polymer latex produced, and examine whether any change had been produced by the different agitation conditions, three measurements were made: the conversion of monomer into polymer; the particle size distribution; and the molecular weight distribution.

Conversion was defined as the percentage of monomer that had been converted into solid emulsified polymer. In order to measure this the contents of the reactor were poured into a separating funnel and allowed to settle. A 100 ml sample was drawn off at the bottom, (any un-emulsified monomer would have risen to the top), and the solid polymer recovered in one of two ways. The first method was to dry the latex in an oven at 40°C to constant mass. If there was residual monomer within the latex, which occurred at low conversions, this method proved not to be reproducible, as polymerisation would take place in the oven. For low conversions a second method was used in which polymer was precipitated out of the latex by adding excess methanol, in which polystyrene is essentially insoluble. The solids could then be filtered and dried. The second method was always reproducible to within one percent conversion, at high and low conversions. The mass of added solids, surfactant and initiator, per 100 ml of latex was subtracted from the mass of recovered polymer, which was then divided by the mass of styrene added per 100 ml of latex to get percentage conversion.

A full particle size distribution would have been the ideal way of examining the effect agitation had on particle growth and the coalescence and breakage mechanism. Three methods of particle size measurement were used: a Coulter Counter, a HIAC particle counter, and a Malvern photon correlation spectrometer. The Coulter counter and HIAC particle counter both rely on individual particles passing through, or past, a small orifice one at a time, then measuring a drop in electrical conductivity or light transmission which was correlated to the particle size. The number of particles were accumulated into channels, each channel represents a group of particle diameters, giving a histogram of the particle size distribution. However, with these two instruments the size of the orifice was the limiting factor, since with the smallest orifices available 90% of the sample was confined to the lowest channel and so a distribution or mean particle size could not be obtained.

With the photon correlation spectrometer that was available the mean particle radius, circa 500 Å, could be measured. A quality parameter, which was some measure of the polydispersity of the sample, was also given, but a full particle size distribution could not be produced on this instrument. To measure the particle size a sample of latex, diluted with filtered distilled water, was placed in an optical cell in the instrument. Laser light scattered through 90° was detected in a photomultiplier and an autocorrelation function was generated by the associated electronics and computer. The mean diffusion coefficient of the particles was obtained from the autocorrelation function, and from this the mean hydrodynamic radius[3,2].

The molecular weight distribution was measured on a Gel Permeation Chromatograph; a full description of the technique used is given in chapter five. The complete molecular weight distribution could be obtained by this method, but, for convenience, only the weight average molecular weight and the polydispersity will be used here.

3.5 Results and Discussion.

A series of polymerisations were performed for a range of agitation speeds and for two concentrations of surfactant. Table 3.1 contains a summary of the experimental results. Surfactant concentration is expressed in multiples of the critical micelle concentration, cmc, where 1.2 g of sodium dodecyl sulphate would give the cmc in the above recipe. Apart from the surfactant concentration the proportions of the other reagents remained the same.

On examining these results certain strongly correlated trends appear. Looking at conversion as a function of surfactant concentration, at constant agitator speed, an increase in surfactant leads to an increase in conversion, accompanied with a smaller particle size and a higher molecular weight. As agitator speed is increased, at constant surfactant concentration, conversion decreases and mean particle size increases. However, at the lower surfactant concentration the conversion decrease with increased agitator speed is only very slight, if at all. The repeated experiments show some variation in results, which was thought to be due to the inhibiting effect of atmospheric oxygen, as variations were more pronounced at higher agitation speeds. A more pure nitrogen purge was used in subsequent experiments which overcame the effect.

At low conversion there will be a lot of free monomer in the form of droplets which will require the majority of the surfactant. Thus at low surfactant concentrations there will not be enough surfactant to stabilise a large number of small polymerising particles, so polymerisation continues in the relatively few loci formed, producing large particles as they continue to be well supplied with monomer throughout the polymerisation. Thus for a fixed reaction time the conversion will be lower than in a situation where there are more polymerisation loci. It was observed here that for nominally the same conditions both high and low conversions, with the respective small and large particles, was observed. Thus it is important to know how the surfactant is distributed between micelles and monomer droplets.

Table 3.1 : Effect of Agitation Speed and Surfactant Concentration upon Polymer Properties.

Agitator Speed /rpm	Surfactant Concentration /cmc	Conversion /%	Molecular Weight / 10**5	Hydrodynamic Radius /angstrom
300	2	96	2.4	480
300	2	98	1.1	630
300	2	90	2.7	420
300	1	20	1.2	810
300	1	21	1.3	1,000
400	2	84	9.2	430
400	2	82	8.4	440
400	2	80	7.5	580
400	1	16	0.8	4,200
400	1	18	1.1	2,050
400	1	15	1	1,800
550	1	20	3.1	480
1,000	2	52	1.2	770
1,000	2	45	1.1	1,000
1,000	2	82	1.2	490
1,000	2	88	1.3	470
1,200	1	19	0.6	890

A possible experiment that could be performed to investigate whether or not this explanation is correct is as follows. Add the monomer to the water without the surfactant and stir, at a fixed rate for a set time, to disperse the monomer. Then add enough surfactant to cover the monomer droplets in one step or at regular intervals. Compare the results of these experiments with a similar series where the surfactant is added first, at the same level as above, and then the monomer is added later. In the first case starving monomer droplets of surfactant should give less free surfactant and hence cause fewer polymerisation loci to be formed. Thus there should be a low conversion rate with large particles. In the second case an initial excess of surfactant may allow the formation of many polymerisation loci, leading to a high conversion rate.

The time taken for diffusion of monomer and initiator from the surface of a particle to the centre goes up with the square of the radius. Thus, in large particles, with a diffusion controlled reaction rate, the rate of conversion will be slower than in a small particle. Hence large particles will be associated with low conversion rates and small particles with a high conversion rates.

To summaries the result in table 3.1 the following statements can be made:

Low conversion correlates with large particle radius.
High conversion correlates with small particle radius.
Low surfactant concentration correlates with low conversion.
High surfactant concentration correlates with high conversion.
Low molecular weight correlates with large particle radius.
High molecular weight correlates with low particle radius.

With the experience of the above experiments showing a sensitivity of the conversion, particle size and molecular weight, to the distribution of the surfactant by agitation, a second set of experiment was designed to investigate this. In these the same recipes were used, but the monomer was added slowly, over a five minute period, to an aqueous phase containing the surfactant and

initiator. Each reaction was performed over three hours at 50°C. The results of these experiments appear in table 3.2 and graphically in figure 3.2. These results show a significant effect due to agitation upon the conversion and molecular weight, both increasing with increased agitation speed. There is also an increase in both these parameters as the surfactant concentration is increased, for a fixed agitator speed. It is interesting to note that the particle size does not vary significantly with agitation speed in these experiments.

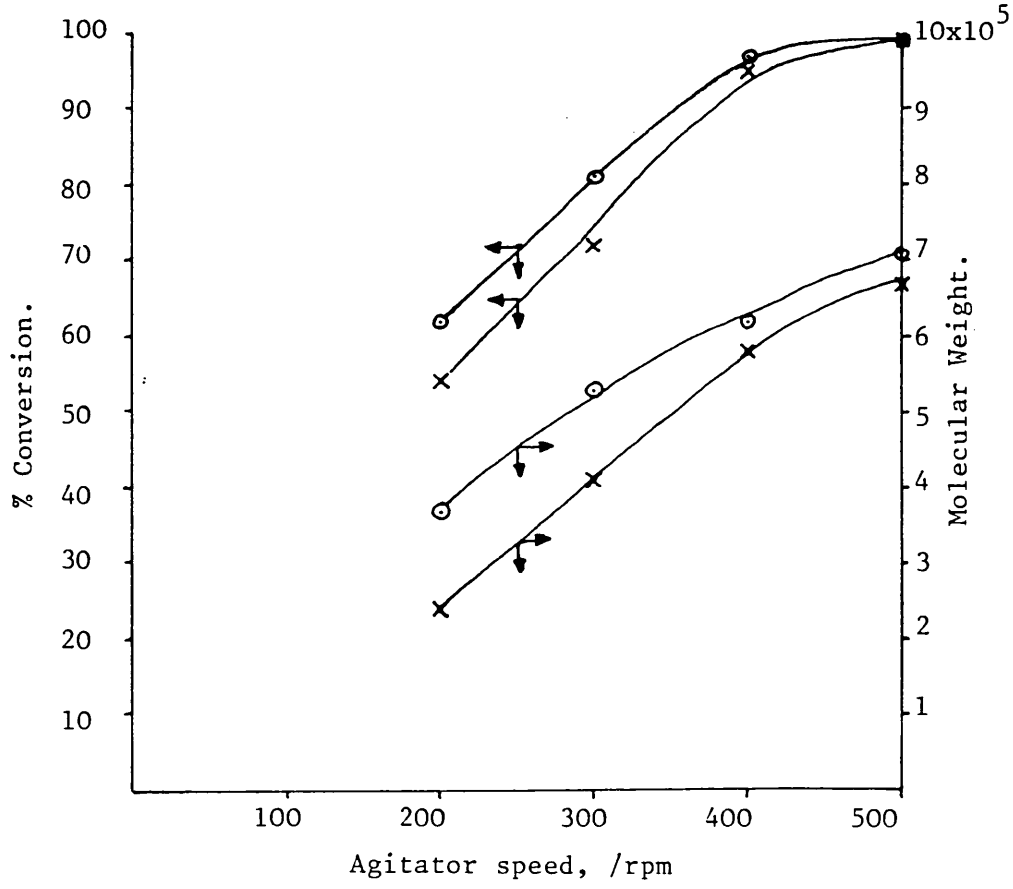
Since each of the experiments took place over the same time, an increase in conversion implies a faster rate of reaction, as more polymer is formed in a fixed time. The increase in conversion caused by the increase in surfactant concentration, at constant agitator speed, is in agreement with the Smith & Ewart theory. The increase in conversion with agitator speed could be caused by a range of phenomena. Equations 2.1 & 2.2 show that the rate of reaction is a function of monomer concentration in the polymer particles, the number of particles, the mean number of free radicals per particle, the rate of formation of free radicals and the surfactant concentration.

If the rate of reaction is mass transfer limited, that is the polymer particles are monomer starved, then improved monomer supply to the particle will increase the reaction rate and thus the conversion for a fixed reaction time. The extent to which this effect occurs will be limited by the rate of reaction, since supplying monomer faster than the rate of consumption will not increase the rate of reaction. To examine whether or not the reaction is mass transfer limited a series of experiment could be performed in which the monomer is added at known rates and the conversion as a function of time determined. If the rate of reaction determined from the conversion curve is limited by the rate of monomer addition then the potential rate of reaction is higher. This should be repeated for the range of agitation speeds and the rate of monomer addition which limits the rate of reaction determined. From this the agitation speed at which the rate of reaction is mass transfer limited can be determined.

Table 3.2 : Effect of Agitation Speed and Surfactant Concentration upon the Polymer Properties with Slow Monomer Addition.

Agitator Speed /rpm	Surfactant Concentration /cmc	Conversion /%	Molecular Weight / 10**5	Polydispersity	Hydrodynamic Radius /angstrom
500	1	99	6.7	3.6	488
400	1	95	5.8	3.4	475
300	1	72	4.1	3.2	505
200	1	54	2.4	3	425
500	2	99	7.1	3.5	472
400	2	97	6.2	3.4	510
300	2	81	5.3	3.1	463
200	2	62	3.7	2.9	428

Figure 3.2 : Effect of Agitation Speed and Surfactant Concentration upon the Polymer Properties with Slow Monomer Addition.



x : One times cmc
o : Two times cmc

The number of polymer particles is assumed to be constant after the initial particle nucleation period of the Smith & Ewart theory. During this initial period particles will be formed from initiated micelles and precipitating oligomers coagulating and adsorbing surfactant. During the particle nucleation phase agitation will play an important role since the formation of the emulsion requires sufficient shear to break up the monomer into micron size droplets. The shear field will promote coagulation of oligomers in the particle nucleation stage, thus helping to form polymer particles, but could also increase particle coagulation throughout the course of the reaction reducing the number of reaction loci. No evidence is seen here, tables 3.1 & 3.2, that particle break up at high shear rates is a significant mechanism.

The initiator used in these experiments was water soluble, and added as an aqueous solution, so it would be well dispersed throughout the aqueous phase. The rate of formation of free radicals from the initiator would depend upon the thermal decomposition of the initiator, which would go as a first order decay since the reaction is isothermal. Thus for each of the experiments in table 3.2 there was a consistent initiator concentration profile between each reaction, as the same amount of initiator was used. How this consistent initiator concentration affected the number of free radicals per particle would depend upon the number and size of particle present. If there are a small number of particles then the concentration of initiator per particle would be high, and potentially so would the average number of free radicals per particle, but there would be fewer reaction loci. With a large number of particles the average number of free radicals per particle would be lower and there would be more reaction loci.

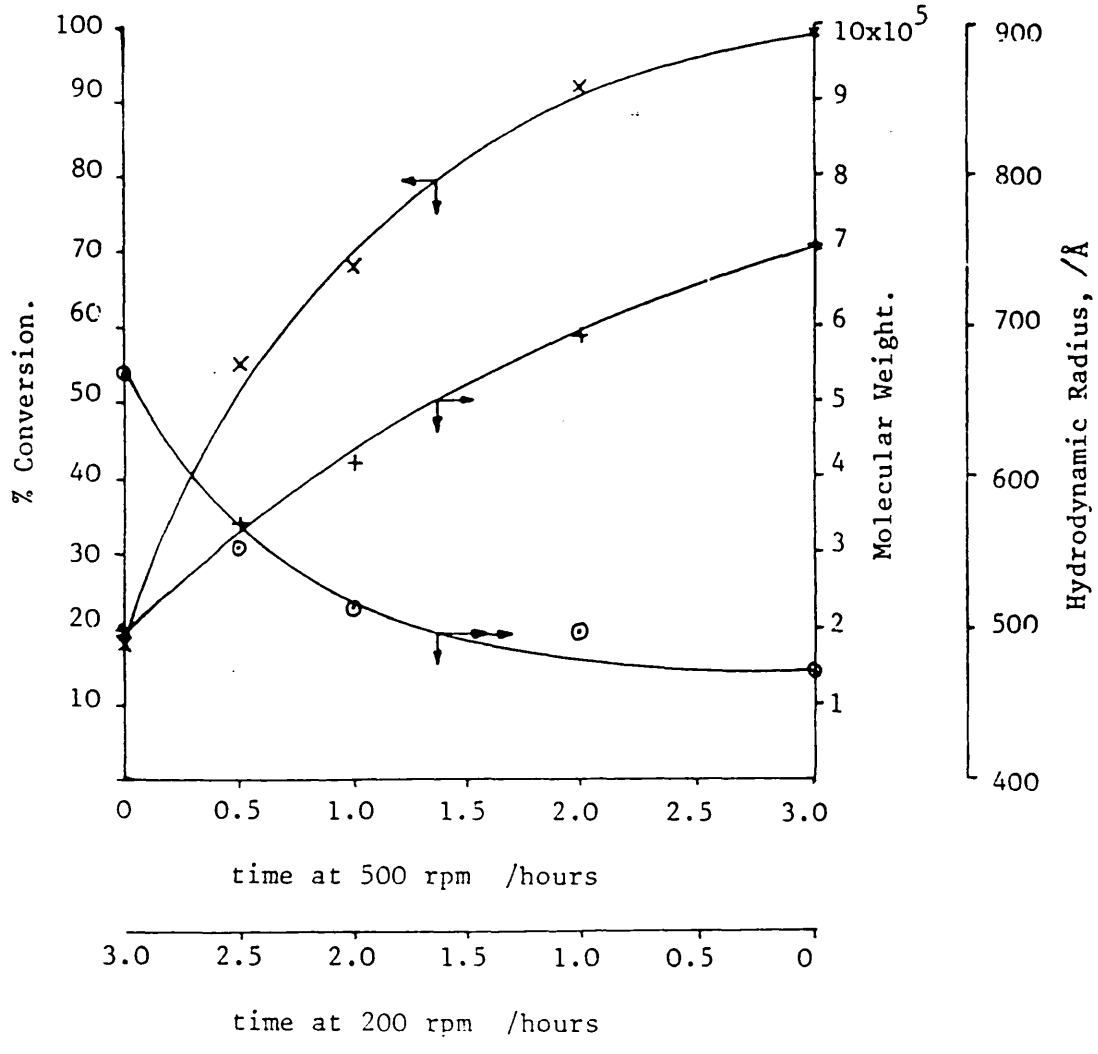
The increase in molecular weight with increased agitator speed suggests that number of free radicals per particle is decreasing since larger molecules are forming within the particles. As the conversion increases with agitator speed at an approximately constant final particle radius, then the number of polymer particles formed in the initial period increases with agitator speed. The increase in number of particles with a constant supply of initiator would lead to a decrease in the average number of free radicals per particle as agitator speed is increased, and thus higher molecular weights are achieved. This is confirmed by the increase in molecular weight with increased surfactant concentration since there are more polymer particles formed.

At low agitation speed a significant quantity of residual monomer was observed after the latex was allowed to settle, which indicates that the majority of surfactant was bound up on polymer particles and the monomer droplets were maintained in suspension mechanically. As was suggested above, the role of agitation in the initial particle nucleation stage is important in forming the emulsion and the polymer particles. To investigate the role of agitation in this initial stage a set of polymerisation were performed in which the agitation history was not uniform, as it had been so far. In these experiments the reactor contents were stirred at 500 rpm for an initial period, then at 200 rpm for the remainder of the three hour reaction time. The monomer was added in one step to the aqueous phase containing both surfactant, at twice the critical micelle concentration, and initiator. The result of these experiments appear in table 3.3 and graphically in figure 3.3. These experiments confirm trend of increased conversion and molecular weight when agitation is improved, that were observed in table 3.2, and demonstrates the importance of having a well dispersed monomer phase early in the reaction. Although increased agitation speed at the start of the reaction improved conversion, maintaining the agitation throughout the polymerisation caused higher conversions again. This indicates that the low surfactant concentrations used in these experiments the mechanical stabilisation of the monomer droplet has an important effect on the course of the polymerisation.

Table 3.3 : Effect of Initial Agitator Speed upon the Polymer Properties.

Time at 500 rpm /hour	Time at 200 rpm /hour	Conversion /%	Molecular Weight / 10**5	Polydispersity	Hydrodynamic Radius /angstrom
0	3	18	1.9	2.2	671
0.5	2.5	55	3.4	2.4	545
1	2	68	4.2	2.7	514
2	1	92	5.9	3.1	498
3	0	99	7.1	3.5	472

Figure 3.3 : Effect of Initial Agitator Speed upon the Polymer Properties.



Slow addition of monomer to the surfactant solution at low agitation speeds increases the overall conversion, as compared with adding the monomer in a single batch. This is due to more of the surfactant being available for particle formation via micelles or precipitating oligomers during the initial period, rather than being used for monomer droplet stabilisation.

In all of these experiments low surfactant concentrations have been used, since it is under these conditions that emulsion polymerisation is most sensitive to the effects of agitation as the colloidal particles have little protection. This work show that emulsion polymerisation under such conditions is not independent of the type of agitation used, and there are three important affects of agitation that must be considered when performing emulsion polymerisation:

i. Agitation has a significant affect on the course of reaction when the atmosphere above the reaction contains oxygen.

ii. The distribution of surfactant between micelles or reaction loci and the monomer droplets during the particle nucleation stage determines the number and size of the polymer particles, and thus the rate of reaction and molecular weight. The role of agitation during this stage is important in causing monomer droplet formation and stabilisation, and the coagulation of precipitating oligomers to form reaction loci, as well as distribution of the surfactant between the various phases.

iii. At lower agitation speeds the rate of reaction is controlled by the monomer transport rate from the monomer droplets to the reaction loci.

From a standpoint of reactor design and reactor scale-up it would be very useful to understand these effect. Further study of this area would not only benefit commercial operations of emulsion polymerisation reactors, but also increase the understanding of the mechanisms involved in emulsion polymerisation.

4.0 The Loop Reactor Process.

4.1 Introduction.

Commercial production of emulsion polymers started in the 1930s and traditionally has taken place in batch autoclaves, fitted with agitators, baffles and cooling coils. The Loop process is fundamentally different. It consists of a continuous length of piping connecting the outlet of the circulating pump back to its inlet. Raw materials are pumped into the reactor in the required proportions, and as the reactor is always full, the overflow forms the product stream at a rate equal to the introduction of new raw material. The outlet pipe usually incorporates a restriction valve which allows the reactor to be pressurised. The pressure capability of the pumps and pipework makes the Loop process ideal for handling gaseous monomers. Thus, excluding peripheral equipment, the capital cost of a Loop Reactor may be one third that of an autoclave for liquid monomer and up to one tenth of the price of a pressurised autoclave. Since a Loop Reactor is compact and light, a smaller building and less supporting framework are required. Having no head space, the process is intrinsically safe with toxic and/or explosive gaseous monomers, for example vinyl chloride and ethylene. Although continuous operation allows increased production for the volume of the reactor, the annual tonnage for a single reactor is restrictive as they have a smaller reaction volume than an autoclave.

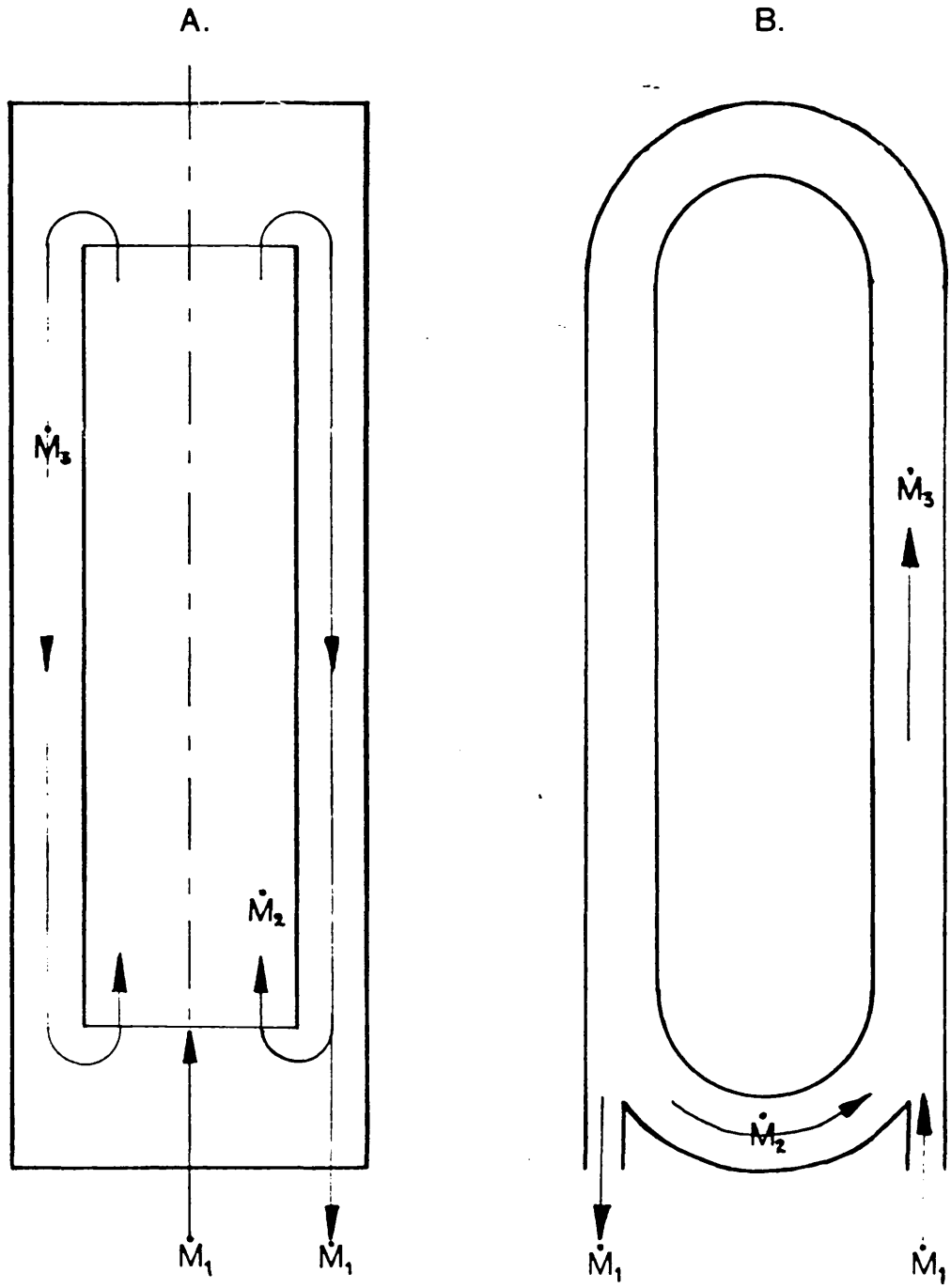
4.2 History of the Process.

A Loop Reactor is a chemical reactor in which there is a definitely directed circulation flow on which a through flow can be superimposed to give a continuous operation. There are two principle types of loop reactor, illustrated in figures 4.1A & 4.1B. The internal circulation Loop Reactor, used mainly in biochemical applications, and the external flow Loop Reactor. It is the development of the external flow Loop Reactor for emulsion polymerisation that will be considered here.

In 1966 Dr.R.Lanthier[4.1] was studying the half-lives of redox initiators in emulsion polymerisation using a steady state technique to overcome problems associated with the rate of decomposition of the materials. In this technique he connected the outlet of a pump to its inlet, and by altering the rate of introduction of new materials, the mean residence time could be varied. As the tubes were always full the overflow was an ideal sampling point for analysis of the reaction products. Experiments went well and results were produced, but so was a significant volume of emulsion latex by-product, it was realised that a new process had been discovered. Gulf Oil Canada Limited, for whom Dr.R.Lanthier worked, took out a patent on the process as a continuous method of vinyl polymerisation[4.2].

The patent covers redox and peroxide initiators, and states that it is crucial that they form sufficient free radicals to initiate polymerisation within one circulation of the charge, so to ensure that an accumulation of monomer and initiator does not occur and to lead to an uncontrolled polymerisation. As the charge is described as rapidly circulating, the half lives of the initiators should be of the same order as the circulation time, and short compared with the polymerisation time. An external flow Loop Reactor is described, and it is pointed out that the overflow outlet should be situated such that the withdrawn material will have been circulated for at least the largest part of one cycle. This would place the reactant inlet and the product outlet close together, the outlet being upstream of the inlet.

Figure 4.1 Loop Reactors.



Internal circulation.

External circulation.

To achieve substantially complete conversions, circulation rate much greater then the feed rate were used, this increased the mean residence time within the reactor. For a large conversion of monomer to polymer a recycle ratio, R = Circulation flow rate/ Product flow rate, R=100 was considered more than adequate. It was found that R=40 was a minimum value for the polymerisation of vinyl acetate, which has a relatively short reaction time compared to some other monomers, for example vinyl chloride. It was considered that regardless of the degree of conversion required the recycle ratio should be greater than ten, R>10, to provide the desired ratio of polymer to dispersing medium in the product.

The patent is illustrated with with twenty four example experiments performed on two reactor assemblies. The first reactor used a centrifugal pump capable of pumping 6820ml/min of emulsion, viscosity 28cp. The loop is formed from 4m of 0.01m OD tubing, the inlet to the reactor is at the inlet to the pump, and the overflow is a tee joint just before the pump inlet. Total reactor capacity was 800ml, of which the pump accounted for over half. The feed rate was 62ml/min vinyl acetate with 2% polyoxypropylene, and 50ml/min aqueous initiator solution, which gave a recycle ratio of R=60.

Mixing of reagents would have been by several processes in the reactor. The flow in the tubing was laminar, with a Reynolds number of about 500, this would provide axial mixing, and since vinyl acetate has a significant solubility in water, this could have been quite effective due to radial diffusion of the vinyl acetate across the concentration gradient produced by the parabolic flow profile. However, the centrifugal pump would have acted as a stirred tank and, as it had such a relatively large capacity, would have provided most of the mixing required.

The second reactor described used a positive displacement pump with 4.4m of 0.01m OD stainless steel pressure tubing, for the polymerisation of vinyl chloride. A circulation rate of 20000ml/min could be produced in a reactor with a total volume of 2000ml, of which the pump accounted for 1650ml. The experiments described were not emulsion polymerisations, but one solution polymerisation and one bulk vinyl chloride polymerisation, both of which had recycle ratios greater than one thousand. Again here most of the mixing was provided within the pump, bulk viscosity and density were not given for the reactor contents, but if they were similar to the first case the pipe flow would still have been laminar.

In both of these reactors the fraction of the total reactor volume accounted for by the pump is significant when examining the mixing processes within the reactor. In the first example 60% of the volume was in the centrifugal pump. In the second case over 80% of the volume was in the positive displacement pump. The characteristic advantage of a Loop Reactor, that is the well defined flow in the pipe work, is therefore lost as most of the reaction and mixing took place within the pumps, within which the flow is not at all well defined. The nature of the pipe flow would not be a dominant effect in the emulsification of the monomer. However, if a Loop Reactor with a significant proportion of its total volume in pipe work was to be used, would laminar flow conditions be sufficient to emulsify non-soluble monomers and maintain favourable heat transfer conditions?

Another important points the patent specification raises is the connection between recycle ratio and conversion. These points need to be examined in the design Loop Reactors for emulsion polymerisation.

4.3 A Loop Reactor Mixing Model.

It is desirable in an emulsion polymerisation to disperse the reactants throughout the volume of the reactor as rapidly and uniformly as possible, and to maintain a uniform temperature distribution. In a Loop Reactor there are two main mixing mechanisms superimposed upon each other: longitudinal mixing caused by the stream profile, reactor geometry and molecular diffusion; and backmixing due to the recycle flow.

Mixing in Loop Reactors has been modelled in various ways. Warnecke[4.3] used a model in which the loop was split into two reactors, as in figure 4.2. A variety of models were suggested for each of the reactors, continuous stirred tanks, a cascade of CSTR's, plug flow tubular reactors and a tubular reactors with axial dispersion. The transfer function of the latter was used for both reactors to obtain the moments of the residence time distribution for the overall Loop Reactor.

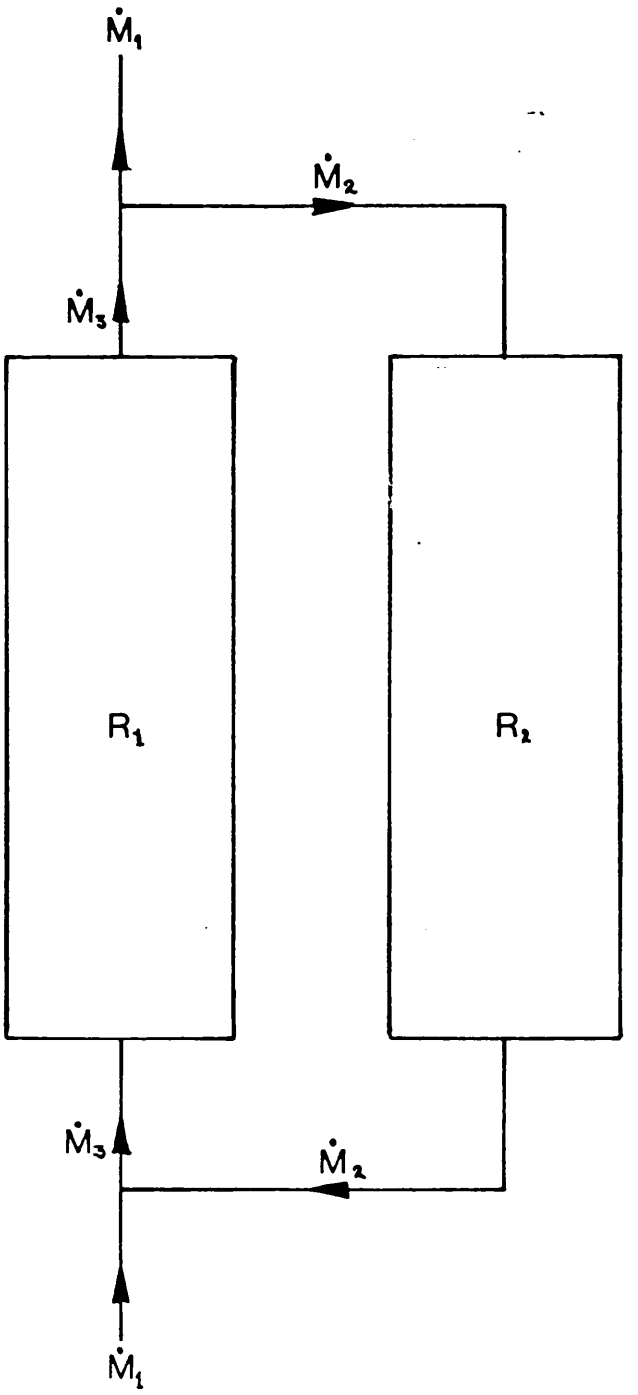
A different approach was taken by Blenke[4.4] where a diffusion model was used. This approach is relatively simple and gives insight into the mixing process within Loop Reactors. All the various causes of longitudinal mixing may be lumped together in a longitudinal dispersion coefficient, D. The diffusion model is characterised by the Bodenstein number:

$$Bo = w.L/D \qquad \text{equation 4.1}$$

where: w = mean liquid velocity.
and L = length of one circulation.

The Bodenstein number is a measure of the relationship between mass transport due to plug flow, (w.L), and that due to longitudinal mixing, (D). As Bo increases the flow approaches that of ideal plug flow, that is no longitudinal mixing: it is thus an analogue of the Peclet Number, in which D represents the mass diffusivity.

Figure 4.2 Loop Reactor Model.



To analyse the mixing within a Loop Reactor, transform the circulation flow into linear tubular flow and inject a pulse of tracer into the stream at x=0 at time t=0, which will spread along the flow path due to longitudinal mixing. Consider the rate of change in concentration, C(x,t), of tracer in a cross sectional control volume of area A and thickness δx. Tracer will be carried into and out of the control volume by the flow, with mean velocity w, and by the longitudinal flux, N. Thus:

$$\frac{\partial C(x,t)}{\partial t} = \left[\frac{N(x,t).A}{A.\delta x} + \frac{w.A.C(x,t)}{A.\delta x} \right] - \left[\frac{N(x+\delta x,t).A}{A.\delta x} + \frac{w.A.C(x+\delta x,t)}{A.\delta x} \right]$$

equation 4.2

From Fick's law of diffusion:

$$N(x,t) = -D.\frac{\partial C(x,t)}{\partial x}$$

equation 4.3

Thus equation 4.2 becomes:

$$\frac{\partial C(x,t)}{\partial t} + w.\frac{\partial C(x,t)}{\partial x} = D.\frac{\partial^2 C(x,t)}{\partial x^2}$$

equation 4.4

To make equation 4.4 dimensionless the following quantities are defined:

a relative flow path: $x_u = x/L$ equation 4.5

a relative concentration: $c_r = C(x,t)/c_\infty$ equation 4.6

where: c_∞ = concentration if the tracer were uniformly distributed throughout the reactor volume.

a relative time: $\tau = t/\hat{t}$ equation 4.7

where: $\hat{t}$ = mean circulation time = L/w

Thus the local temporal change in concentration in dimensionless form becomes:

$$\frac{\partial c_r}{\partial \tau} + \frac{\partial c_r}{\partial x_u} = \frac{1}{Bo}\frac{\partial^2 c_r}{\partial x_u^2}$$

equation 4.8

The solution of equation 4.8 for an instantaneous plane source is given by Carslaw[4.5] and describes the tracer distribution as a function of time, τ, at a positions, x_u:

$$(c_r)_{x_u} = \left(\frac{Bo}{4\pi\tau}\right)^{1/2} . \exp\left\{ - \frac{(x_u-\tau)^2 . Bo}{4\tau} \right\}$$

equation 4.9

To introduce backmixing all the positions down the imaginary straight tube that represent one, two, three, etc. circulations, (x_u=1,2,3,...), are considered to come together at one point, thus reforming the loop. The change in concentration of tracer at any point in the loop as a function of time, will be the summation of equation 4.9 for each complete circulation around the loop, (x_u=1,2,3,...), that contributes to the overall concentration:

$$c_r = \sum_{x_u=\tau-2}^{x_u=\tau+2} \left(\frac{Bo}{4\pi\tau}\right)^{1/2} . \exp\left\{ - \frac{(x_u-\tau)^2 . Bo}{4\tau} \right\}$$

equation 4.10

The contribution of the third, forth, etc., circulation away from that under consideration has a negligible contribution.

This summing of the longitudinal mixing effect represents the characteristic backmixing of the Loop Reactor, and combines the two mixing effects to give the total effect of circulation flow in batch conditions. Figures 4.3, 4.4 & 4.5 show the effect of increasing Bodenstein number on the concentration profile, as calculated from equation 4.10. As Bo increases the flow becomes more plug like and so more circulations are required to achieve a uniform concentration.

Comparisons in mixing need to be based on the same degree of mixing throughout the mixing space. In order to quantify a degree of mixing, the inhomogeneity, h, is defined as:

$$h = \frac{\hat{c} - c_\infty}{c_\infty} = \hat{c}_r - 1$$

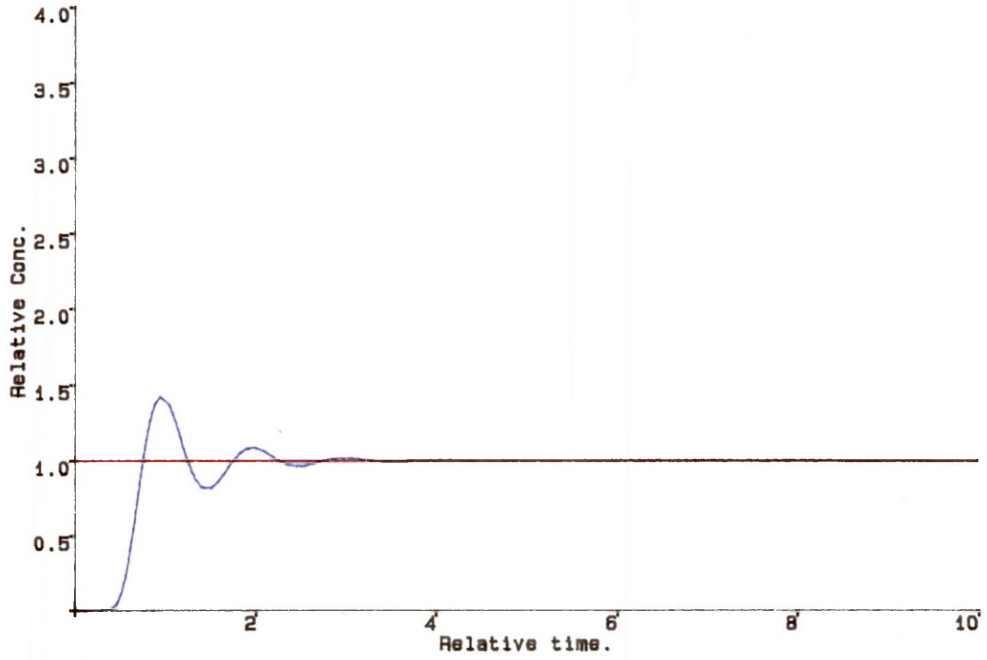
equation 4.11

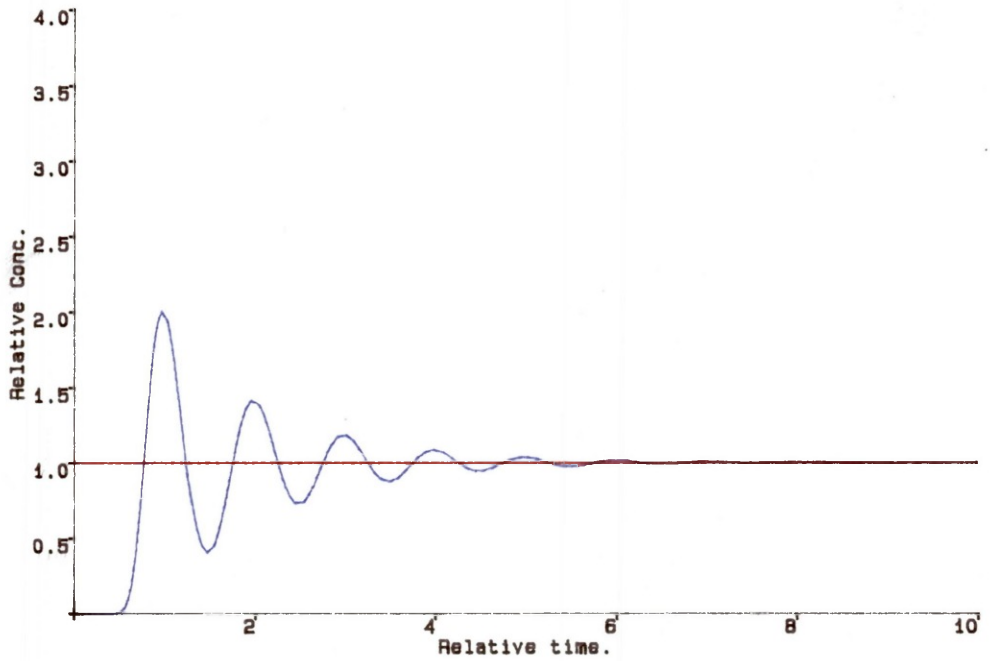
where: $\hat{c}$ = peak concentration.

Figure 4.3

Batch Mixing in a Loop Reactor

Bodenstein Number : 25.0



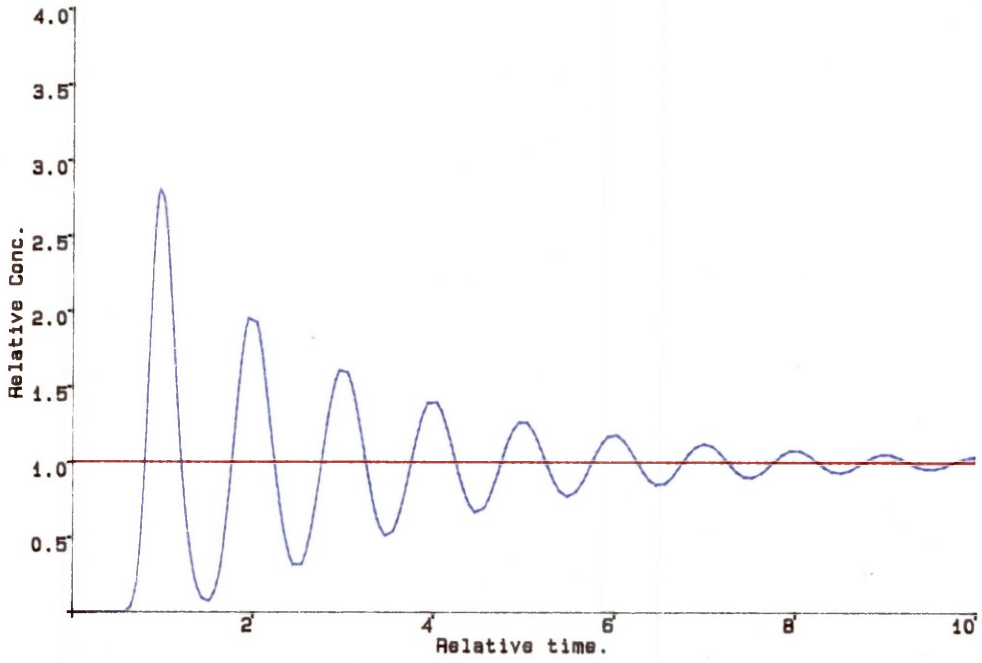


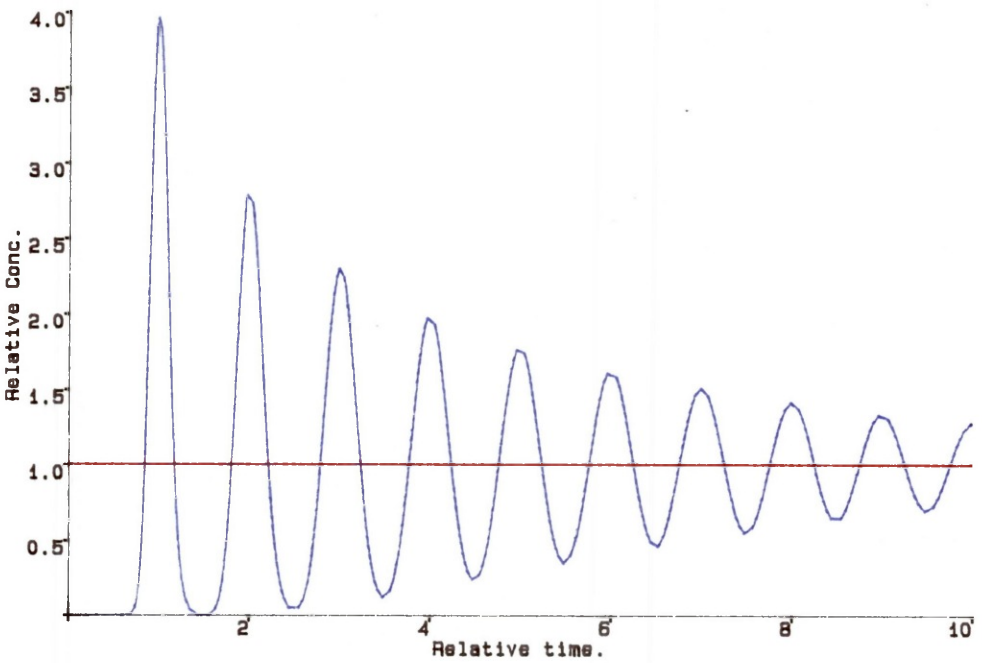
Bodenstein Number : 50.0

Figure 4.4

Batch Mixing in a Loop Reactor

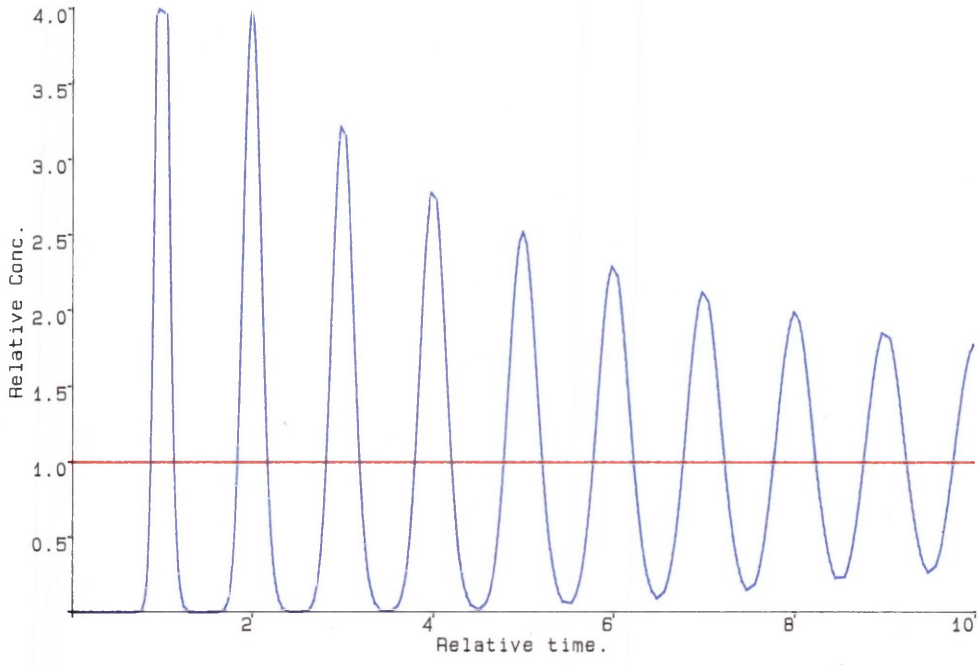
Bodenstein Number : 100.0

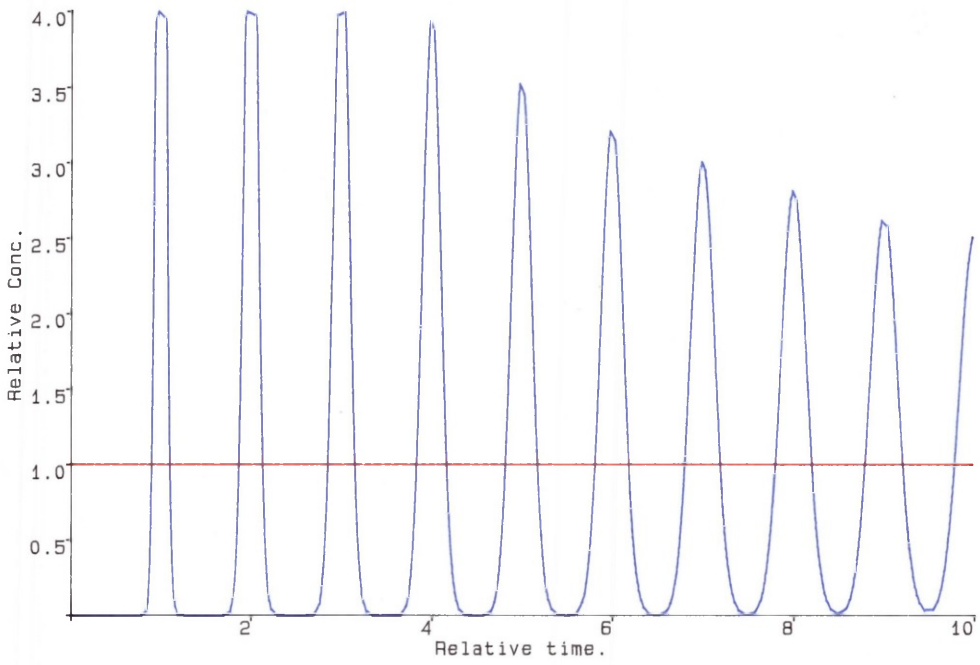




Bodenstein Number : 200.0

Figure 4.5
Batch Mixing in a Loop Reactor
Bodenstein Number : 400.0





Bodenstein Number : 800.0

The smaller the value of h, the more homogeneous the reactor contents. To compare mixers a relative mixing time is defined as the relative time taken to reach a specified inhomogeneity. The way in which inhomogeneity characterises relative mixing time as a function of Bodenstein number in the Loop Reactor is seen in figure 4.6. Comparing figures 4.3, 4.4 & 4.5 with figure 4.6 shows that an inhomogeneity around 0.02 represents an essentially uniform concentration distribution. It can also be seen from figure 4.6 that mixing time increases linearly with Bodenstein number for a given inhomogeneity, and this is plotted on figure 4.7.

Equation 4.10 represents continual circulation of the reactor contents, however, one of the main advantages of the Loop Reactor for emulsion polymerisation is that it can be operated as a continuous process. To include this into the mixing model a circulation number, n, is defined:

$$n = \frac{M_3}{M_1} = \frac{M_1 + M_2}{M_1} = 1 + \frac{M_2}{M_1} = 1 + R$$

equation 4.12

where: M_1,M_2 & M_3 are mass flow rates defined in figure 4.1

Thus the circulation number is simply related to the recycle ratio. After each circulation the tracer mass is assumed to divide in the same ratio as the rest of the stream, so after one circulation the fraction of original tracer still in the loop will be:

$$\frac{M_2}{M_3} = \frac{n - 1}{n}$$

equation 4.13

Figure 4.6
Mixing Time in a Batch Loop Reactor
with Bodenstein Number as a Parameter.

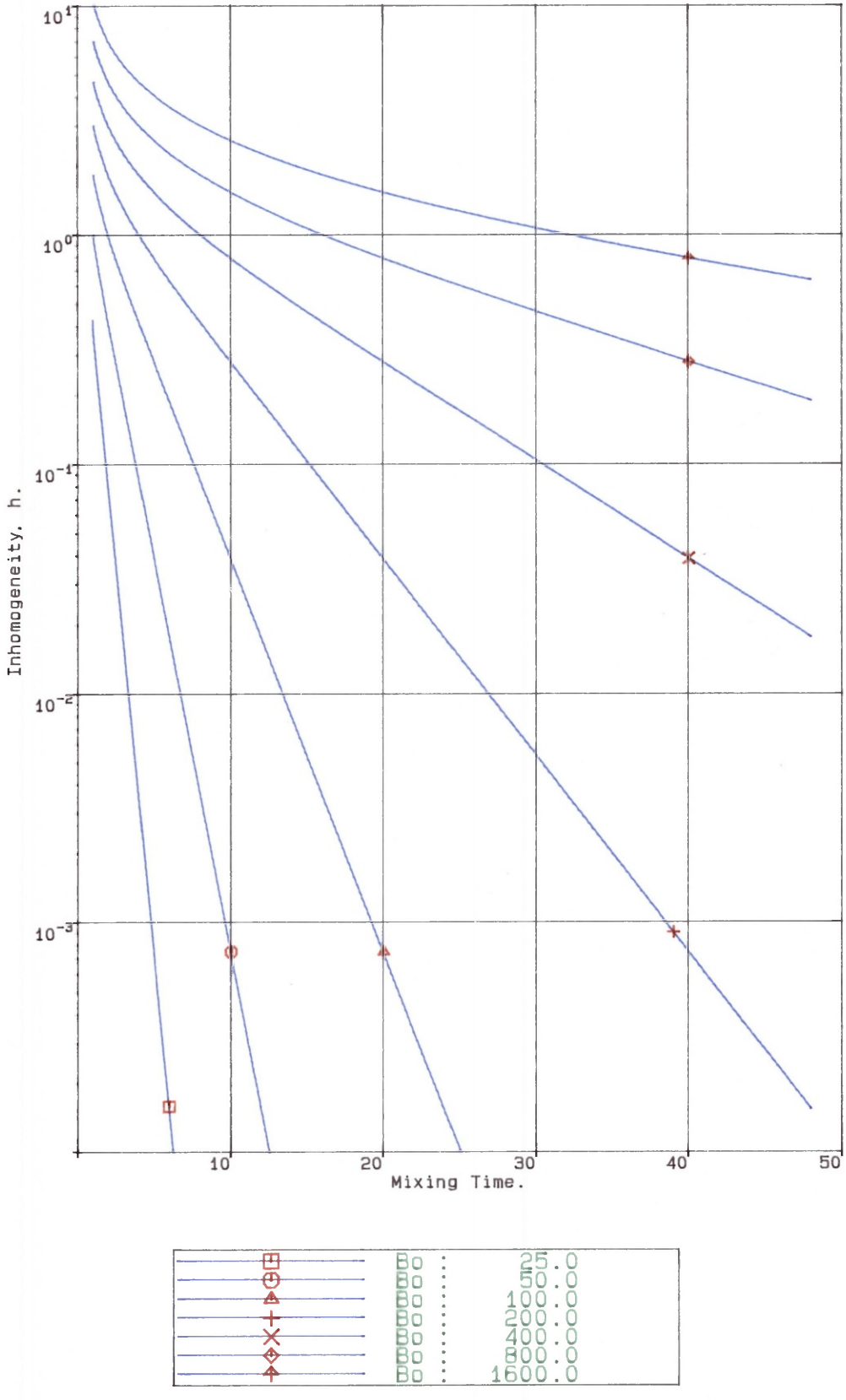
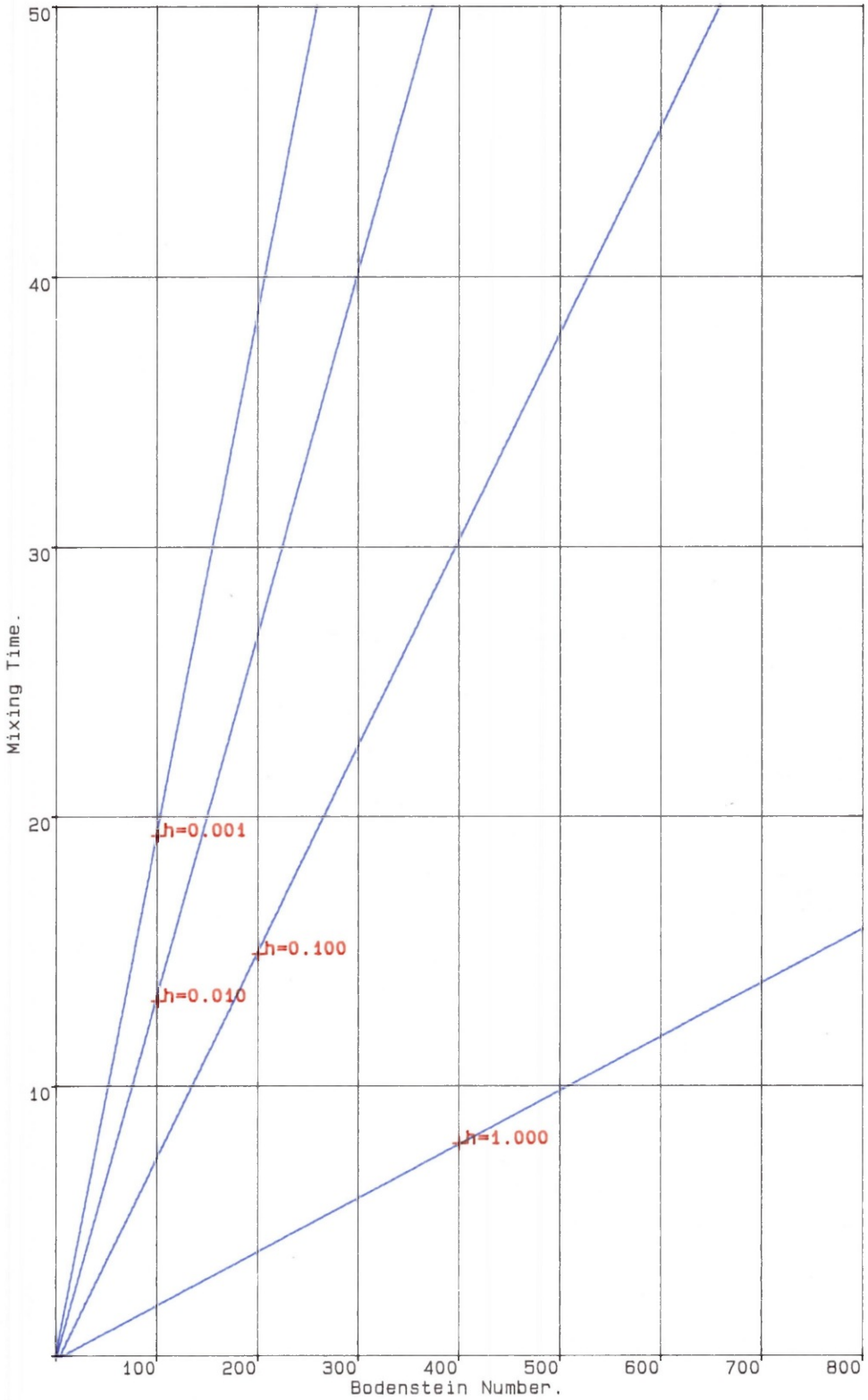


Figure 4.7
Mixing Time against Bodenstein Number.



And after each subsequent circulation the mass of tracer will decrease by the same fraction. To include this into equation 4.10, x_u is considered to be an integer number of circulations, so the continuous operation concentration profile will be given by:

$$c_r = \sum_{x_u=\tau-2}^{x_u=\tau+2} \left(\frac{n-1}{n}\right)^{x_u} \left(\frac{Bo}{4\pi\tau}\right)^{1/2} .\exp\left\{ - \frac{(x_u-\tau)^2.Bo}{4\tau} \right\}$$

equation 4.14

This also represents the residence time distribution of a loop reactor, and can be seen in figures 4.8, 4.9, 4.10 & 4.11, for two Bodenstein numbers and a range of circulation numbers. The circulation number does not have strong effect upon the degree of mixing, but obviously does on renewal of reactor contents. Blenke states that the same mixing times as in batch operation are used for a specified inhomogeneity, because, due to renewal, concentration of tracer drops to the same extent as the reference concentration. However, the value of the reference concentration at any given time is not easily evaluated experimentally, so the change in inhomogeneity cannot be calculated, with respect to time, from equation 4.11. To overcome this a different definition of inhomogeneity can be used. In figures 4.3, 4.4 & 4.5 it can be seen that in batch operation that the peaks and troughs oscillate about the reference concentration. Thus a reference concentration based on the mean of successive peak and trough concentrations is used to evaluate the inhomogeneity. Substituting this reference concentration into equation 4.8 gives:

$$h = \frac{c_{max} - c_{min}}{c_{max} + c_{min}}$$

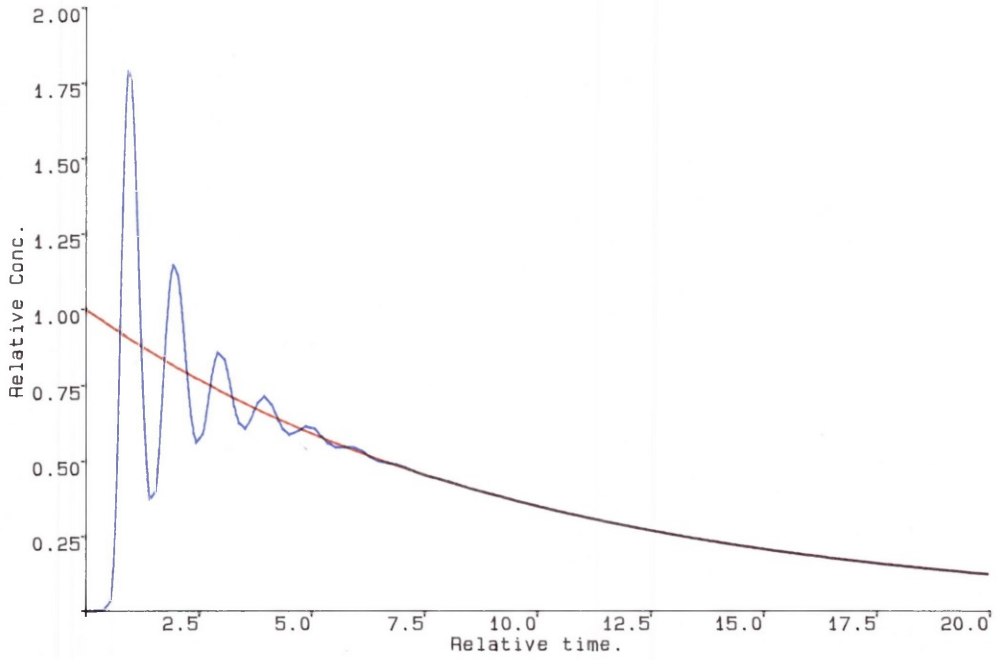
equation 4.15

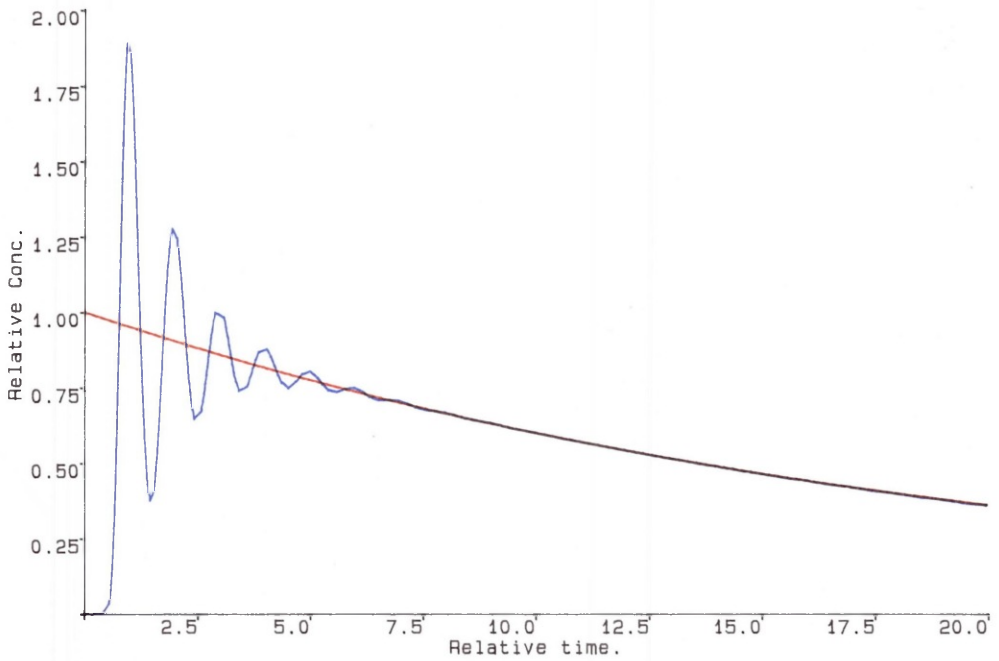
Figure 4.8

Mixing in a Continuous Loop Reactor

Bodenstein Number : 50.0

Circulation Number : 10.0

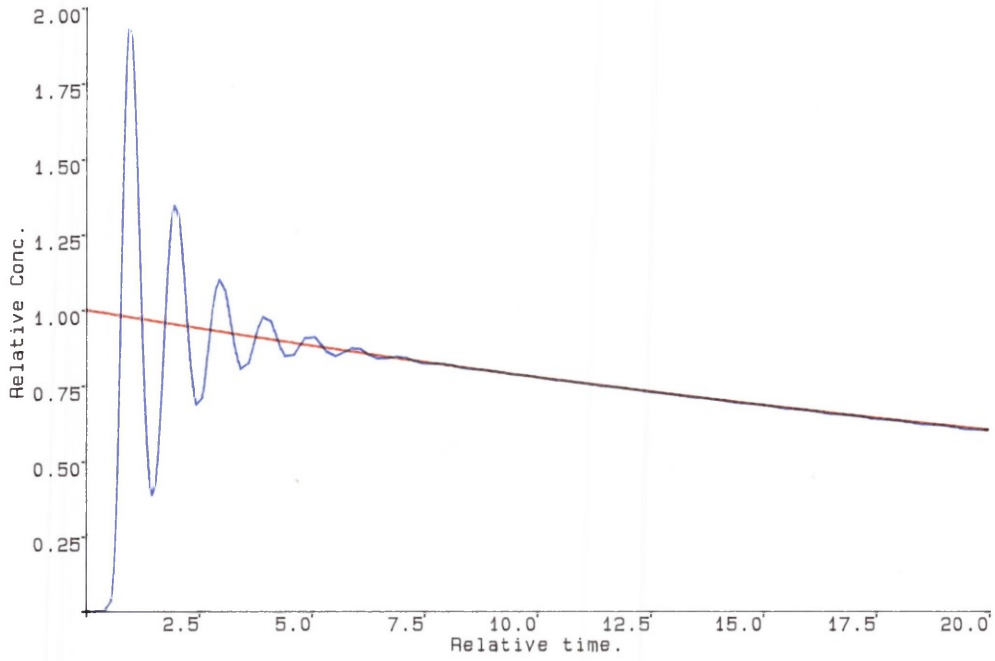


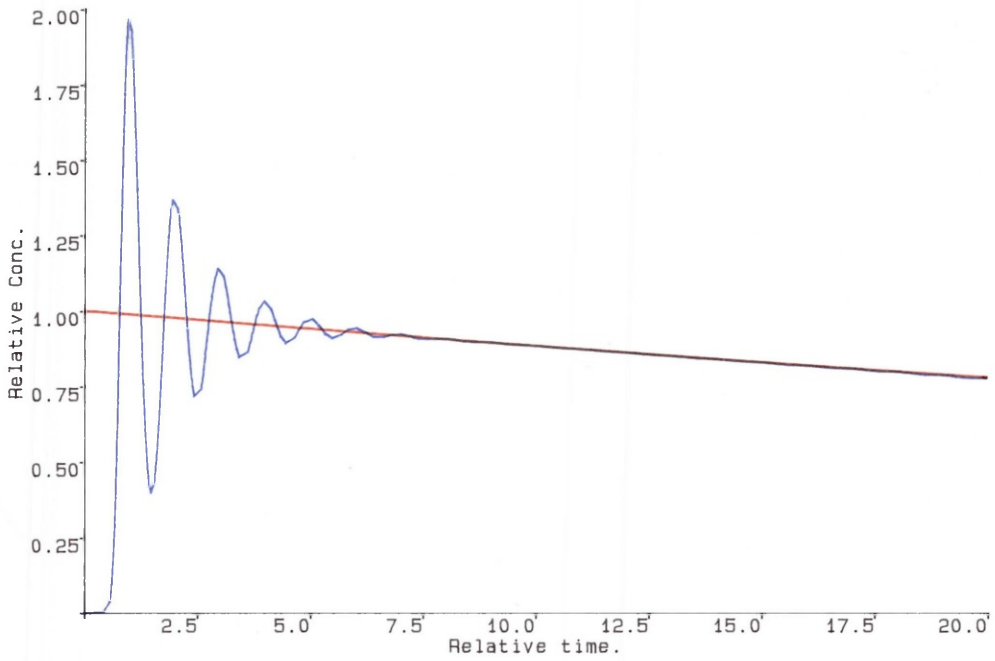


Bodenstein Number : 50.0

Circulation Number : 20.0

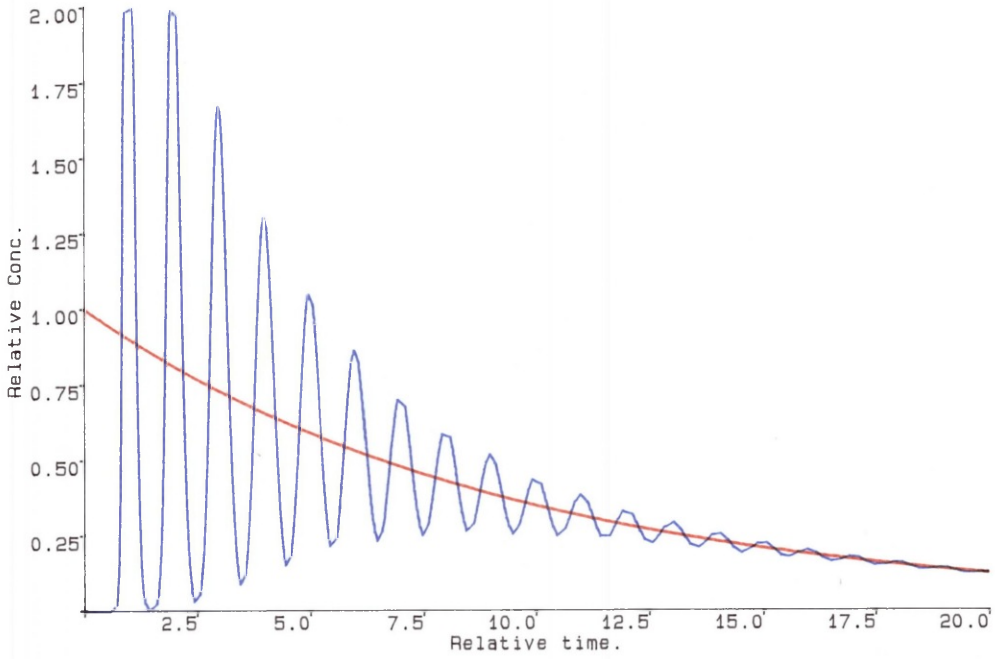
Figure 4.9
Mixing in a Continuous Loop Reactor
Bodenstein Number : 50.0
Circulation Number : 40.0

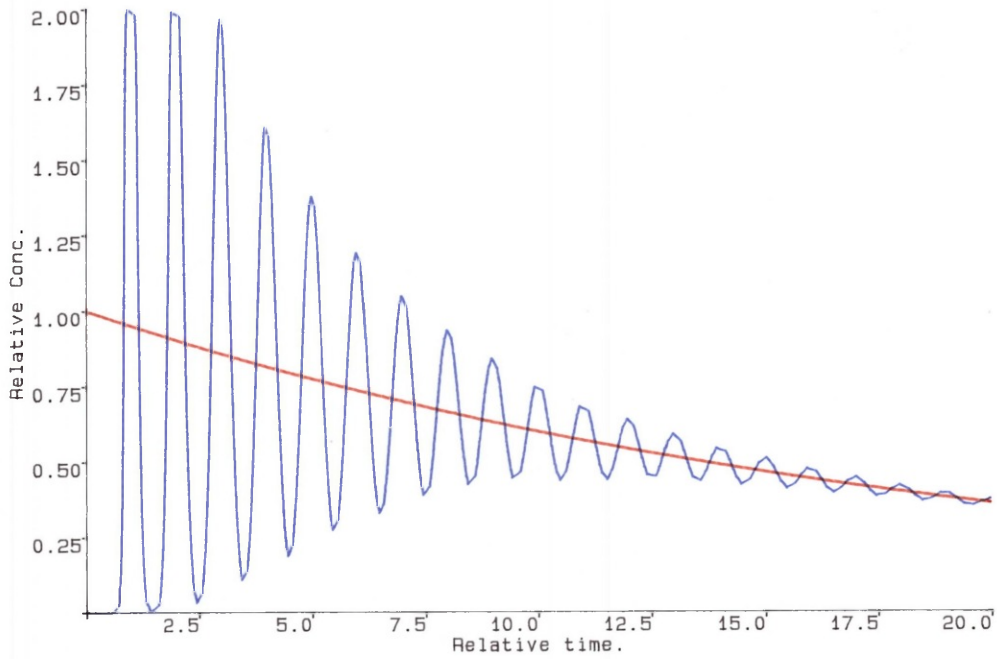




Bodenstein Number : 50.0
Circulation Number : 80.0

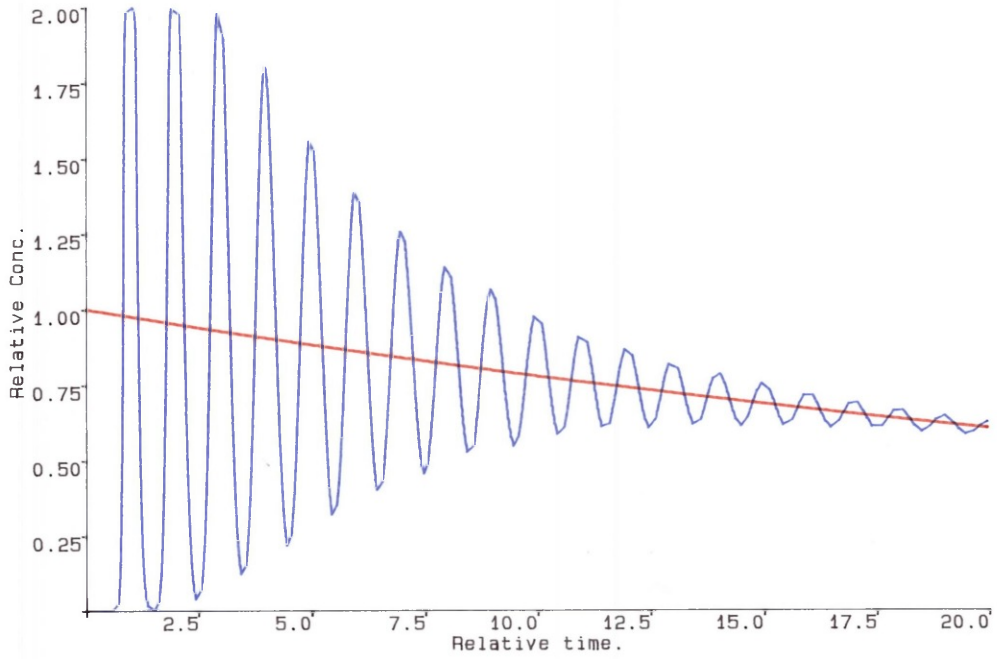
Figure 4.10
Mixing in a Continuous Loop Reactor
Bodenstein Number : 200.0
Circulation Number : 10.0

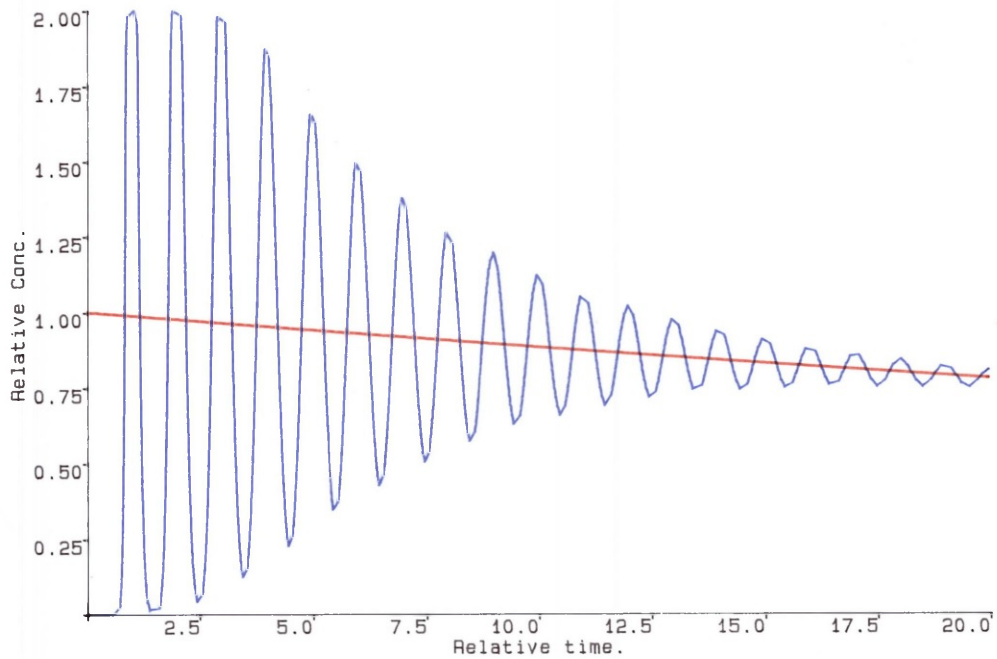




Bodenstein Number : 200.0
Circulation Number : 20.0

Figure 4.11
Mixing in a Continuous Loop Reactor
Bodenstein Number : 200.0
Circulation Number : 40.0





Bodenstein Number : 200.0
Circulation Number : 80.0

With this definition h is never greater than unity. Again referring to figures 4.4 & 4.5, it can be seen that large Bodenstein numbers cause the troughs to have flat bottoms at zero concentration, thus initially the estimate of the reference concentration is not good. The way this definition of inhomogeneity differs from equation 4.11 can be seen in figure 4.12. Broken line are the values from equation 4.11 and solid lines are values from equation 4.15. As the minimum concentration becomes greater than zero so the two definitions converge and give the same mixing time for useful values of inhomogeneity. In the second definition unity indicates plug flow conditions whereas the first definition values greater than unity can be used to indicate the extent of plug flow. In the range where the two converge, the second is useful in showing the affect that circulation number has upon mixing time. This can be seen in figure 4.13 for a Bodenstein number of 200 and a range of circulation numbers from two to infinity, the infinite circulation number corresponding to batch operation. It is interesting to note that mixing time is reduced with circulation number, due to a larger proportion of the inhomogeneity being lost at each circulation.

4.4 An Experimental Loop Reactor.

An investigation into mixing in loop reactors was performed on a loop reactor designed and built by Imperial Chemical Industries Plastics Division for the emulsion polymerisation of vinyl chloride, and which had been rebuilt in the Chemical Engineering Department of Imperial College. The design of the loop was based on evidence from the Gulf Oil patent, (4.2), that polymerisations were performed under laminar flow conditions, and this gave a reactor with the following specification:

Reactor Volume:	4.3 l
Length of Loop:	3.6 m
Internal Diameter of Tubing:	0.034 m
Volume of Tubing:	3.85 l
Circulation Flow Rate:	0.04 - 0.225 l/s

Figure 4.12
Comparison of Inhomogeneity Calculations
with Bodenstein Number as a Parameter.

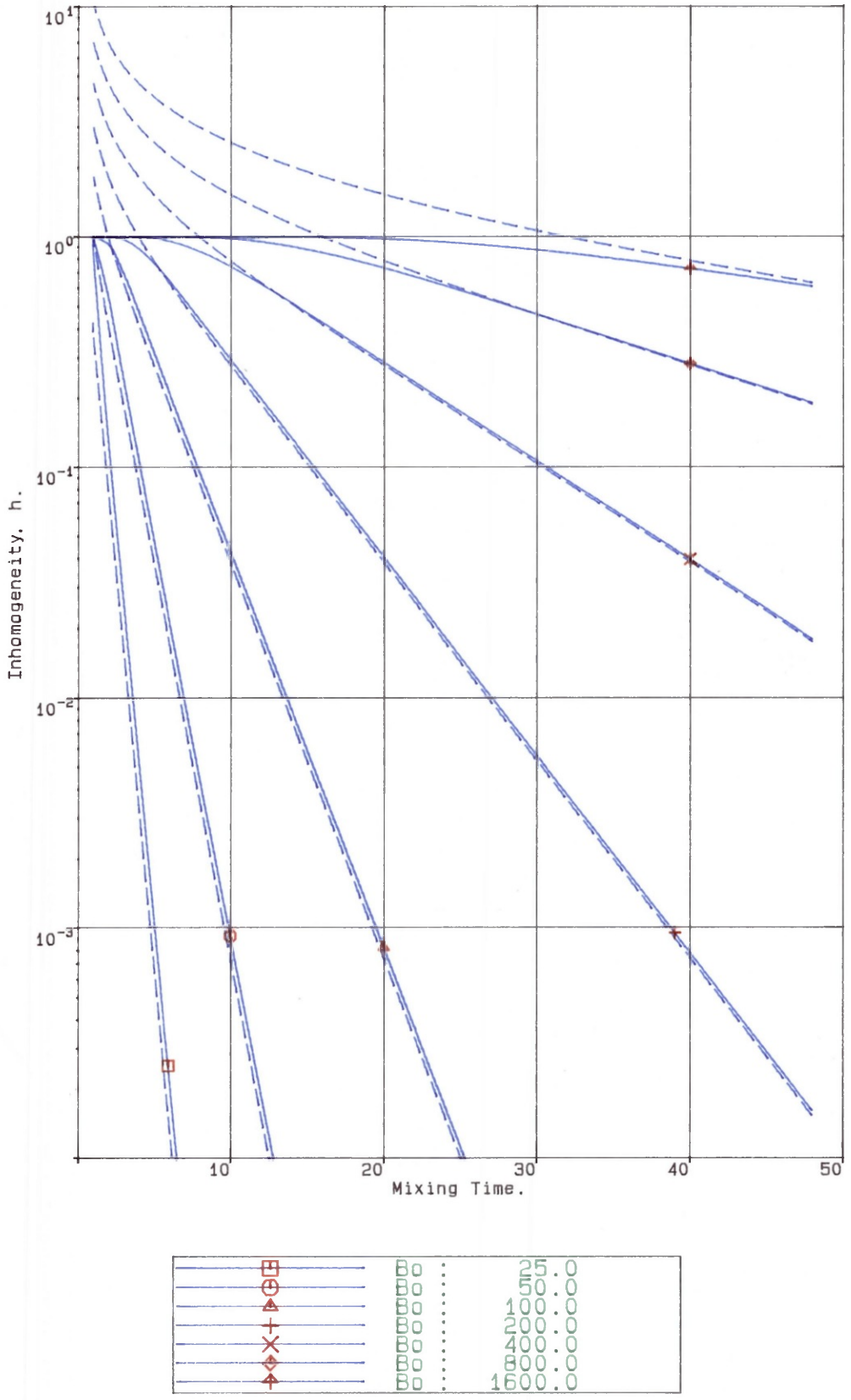
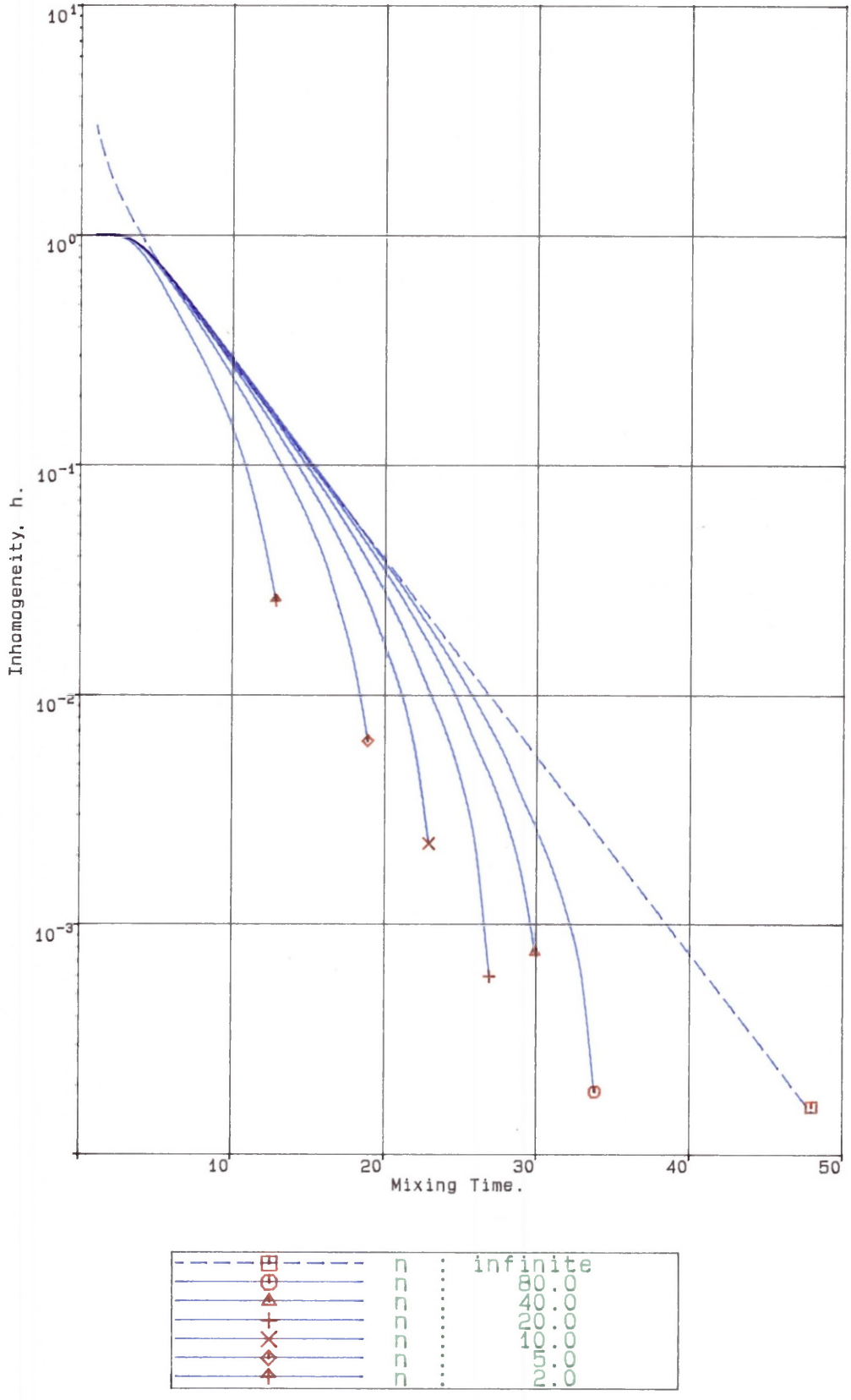


Figure 4.13
Mixing Time in a Continuous Loop Reactor
with Circulation Number as a Parameter.
Bodenstein Number : 200.0



An illustration of the main loop appears in figure 4.14. Circulation of reactant was provided by a positive displacement Monopump driven by an air motor, which, with a water charge, gave Reynolds numbers in the pipe from 1500 to 8500. These would be smaller with the increased viscosity of a reaction mixture, but shows that the flow could be laminar or turbulent. Reagents were fed into the reactor on the outlet side of the circulation pump via three metering pumps, one for the aqueous phase, one for the monomer and one for the initiator solution. These reagent were stored in vessels below the level of the loop to prevent any siphoning effect and thus give a constant delivery during the course of a reaction. Originally temperature control was provided by steam coils around the loop walls for heating and cold water sprays for cooling. In this work it was changed to a jacket system, through which a heating or cooling medium could be pumped. Temperature was measured using thermocouples placed around the loop and within the reactor stream, measurements being logged on a B.B.C. microcomputer.

Figure 4.15 is a line diagram of the loop reactor and peripheral equipment. Reactants are pumped from their storage vessels into the loop, in which the polymerisation takes place. The initiator solution and monomer are kept at room temperature to prevent chemical degradation, but the aqueous phase is heated with an immersion heater. When polymerising under pressure the overflow product stream passes through a filter to remove any large particles before it reaches a pressure let-down coil that has a small internal diameter. A secondary coil can be switched in line by a pressure activated valve if the back pressure exceeds a pre-set value. If polymerisations are performed at atmospheric pressure a by-pass line is used. The product stream then passes at reduced pressure into a storage vessel in which an anti-foaming agent can be added from a pressurised burette. The reactor is fitted with pressure gauges; a pressure relief valve and bursting disc are used for safety. If a blockage should occur in the feed lines a pressure activated switch will stop the pumps. A purge system consisting of a vacuum line and a nitrogen supply is provided to remove oxygen which would inhibit the reaction.

Figure 4.14 Loop Reactor.

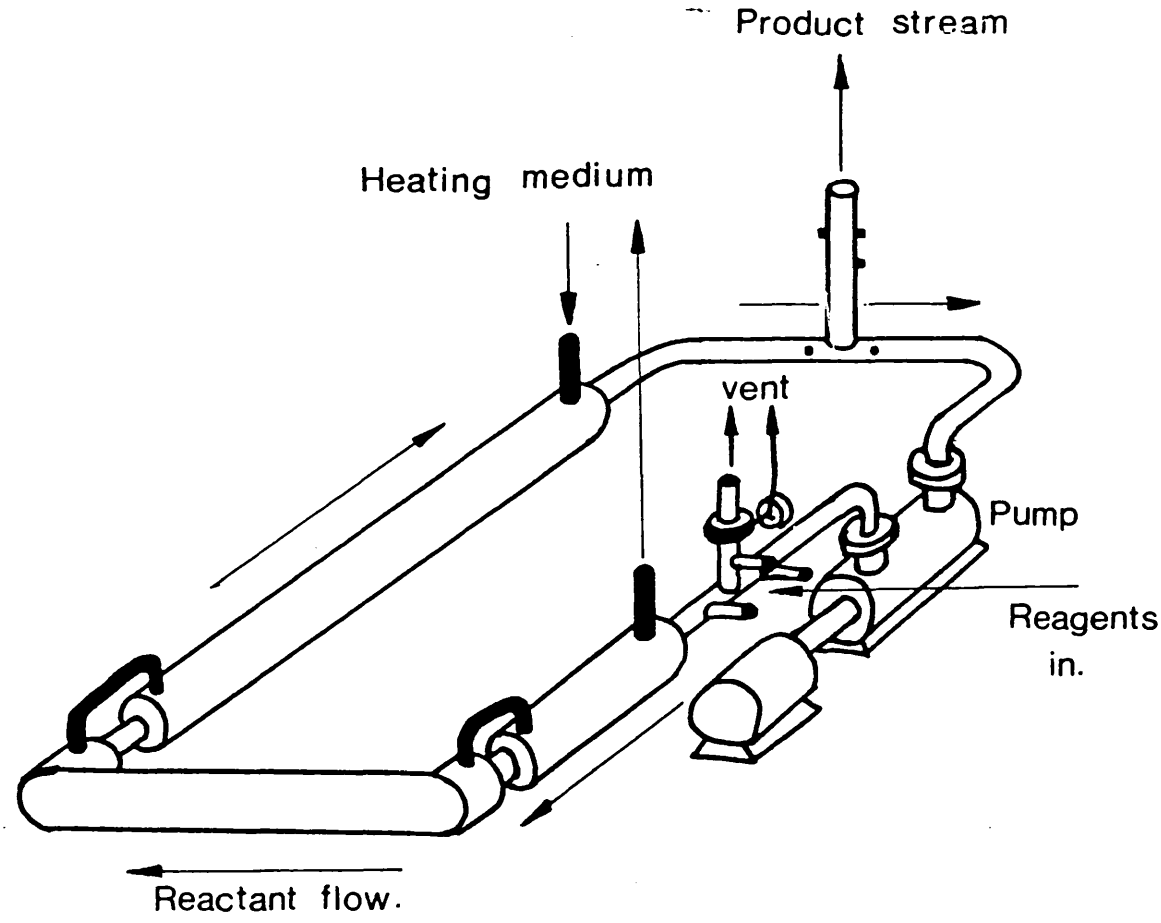
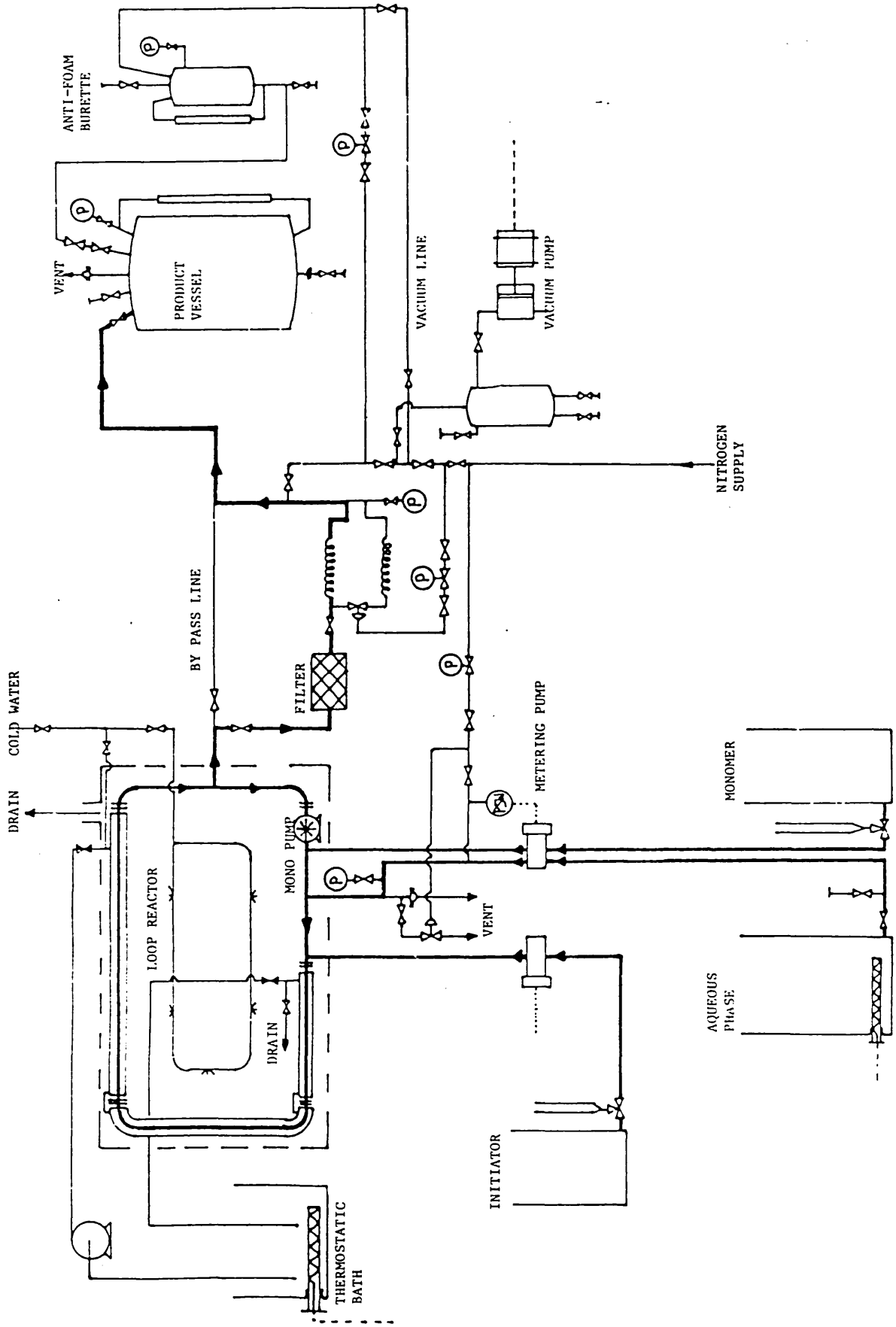


Figure 4.15

Line Diagram of the Experimental Loop Reactor.



Circulation flow rate was calibrated against the speed of rotation of the drive axle, measure with a tachometer. The flow rate was measured in two ways: directly, by measuring the time for a given volume to flow when the loop was opened; and in a closed loop by measuring the mean circulation time of a tracer and knowing the reactor volume. These two methods agreed very well, never being different by more than 1%. The second method, being easier, was used to check the calibration periodically.

4.5 Temperature Distribution.

A uniform temperature distribution is required in a polymerisation reactor to maintain uniform polymer properties. In the loop reactor there are two directions of distribution, the axial and radial temperature profiles. These two profiles were examined whilst a charge of water at 20°C was heated by water at 60°C circulating in the jacket, during batch operation. In order to take measurements within the loop, ports designed to take small measuring probes were fitted, figure 4.16.

The radial profile was examined every five minutes by moving a 1mm diameter sheathed thermocouple across the flow in steps and recording the temperature at each step. Examples of the temperature profile measured appear in figure 4.17. In laminar flow, figure 4.17A, the mid-stream temperature lagged the wall temperature by a maximum of 4°C. This could be reduced to 2°C, figure 4.17B, by the use of static mixers, figure 4.18, which repeatedly split the flow and so increased radial mixing. In turbulent flow conditions the measured temperature across the stream were all within 1°C of each other, figure 4.17C. The axial distribution was measured at points before and after the circulating pump, and all measurements were within 1°C of each other, independent of flow conditions.

Figure 4.16 Loop Reactor Measurement Port.

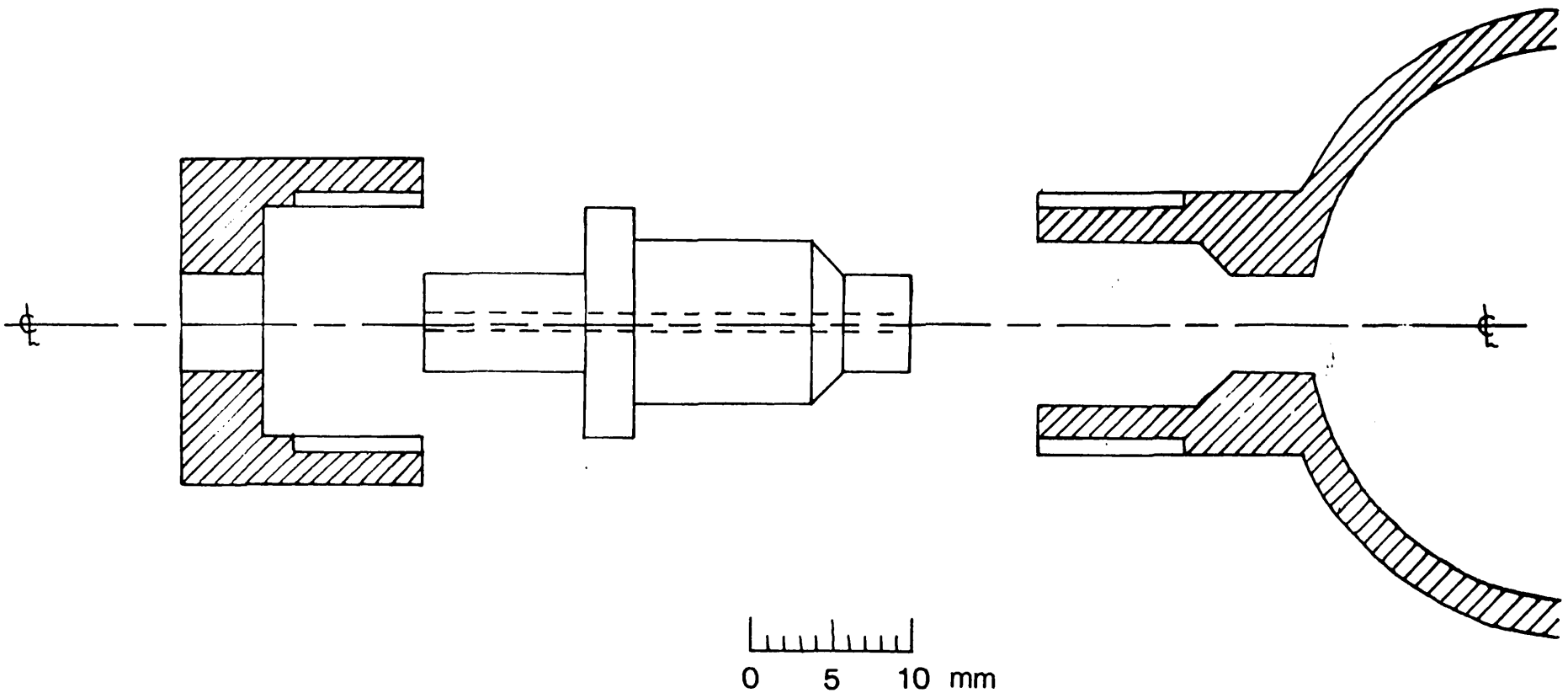
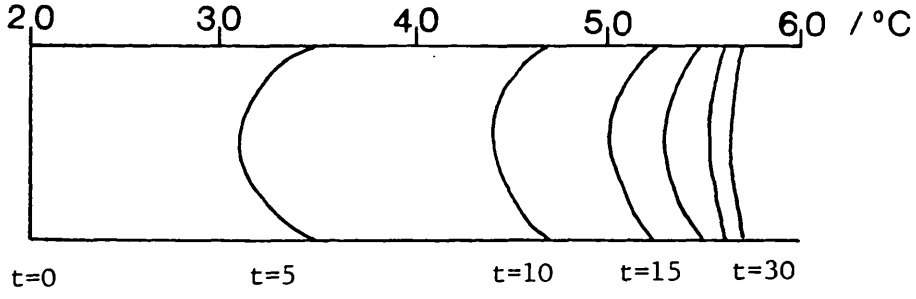
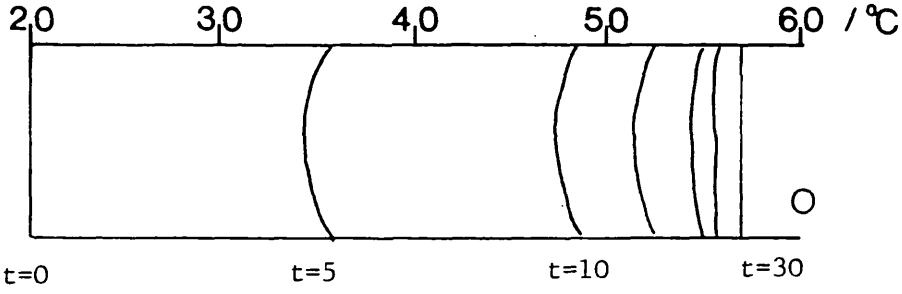


Figure 4.17 Radial Temperature Profiles.
- at five minute intervals.

A. R_e = 1500



B. R_e = 1500 with five static mixers.



C. R_e = 8500

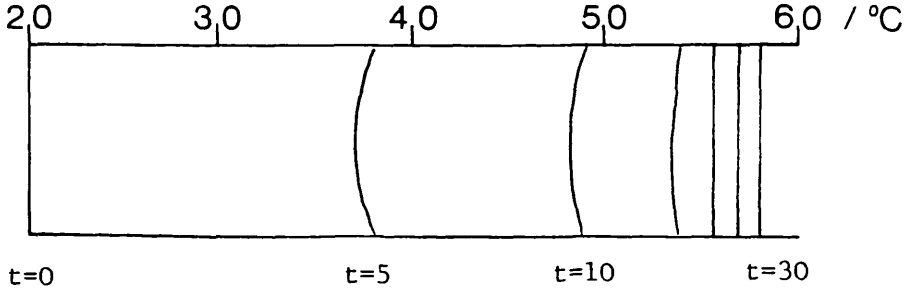
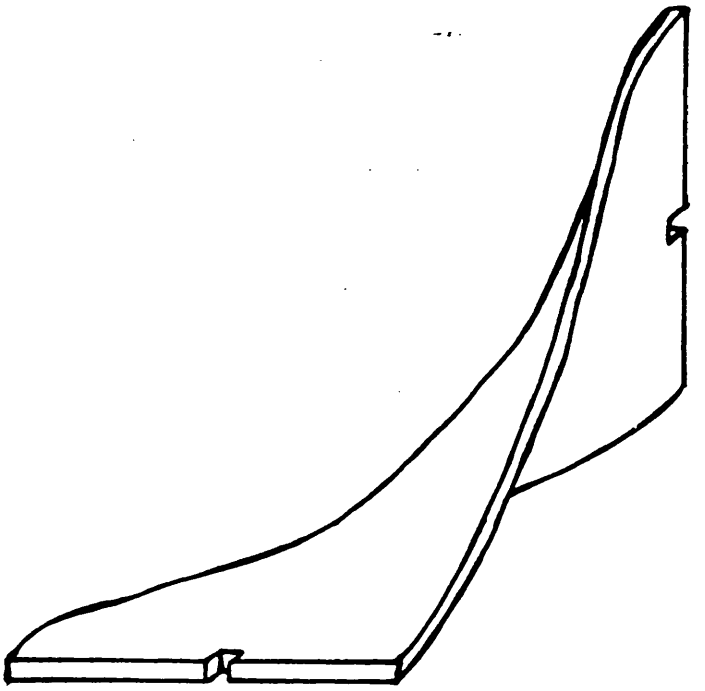
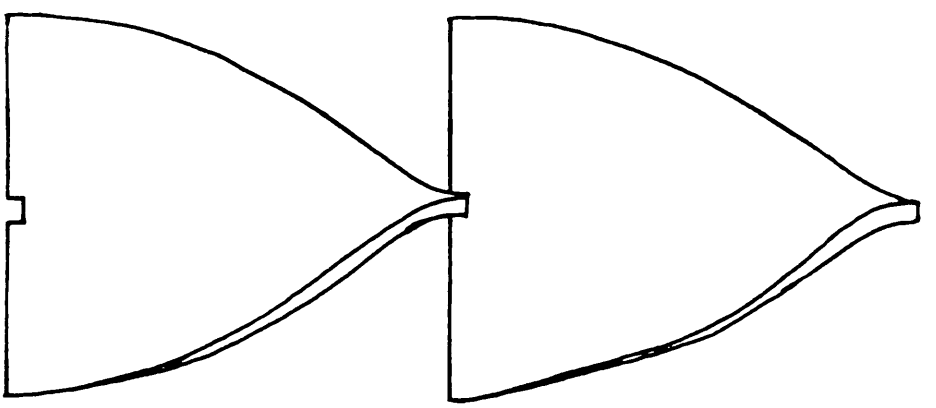


Figure 4.18 Static Mixers.

A.



B.



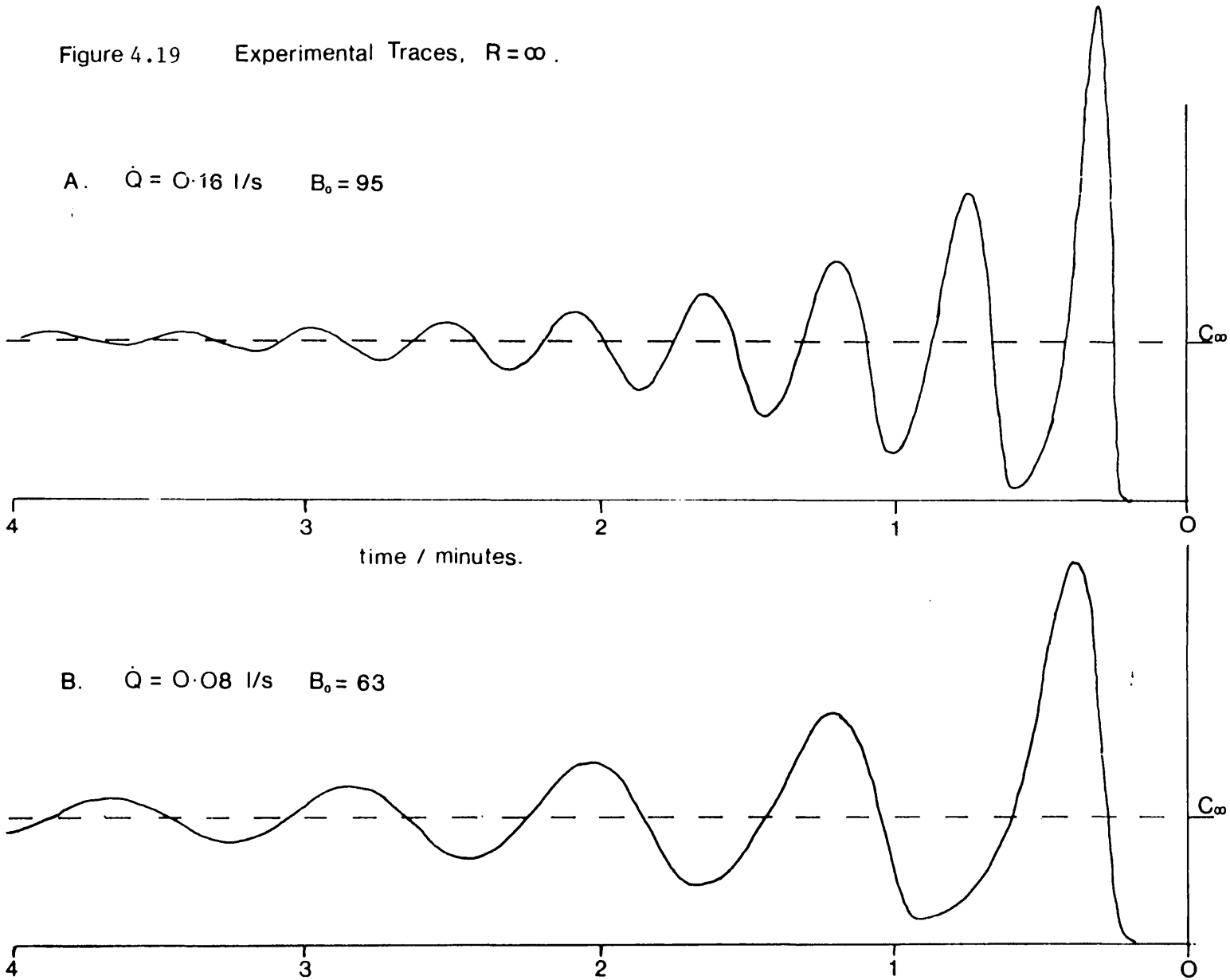
4.6 Mixing Measurements.

The mixing model already described imagines the change in concentration of a pulse of tracer being monitored at a fixed point. This situation was simulated by using a reactor filled with distilled water and an electrolytic solution as the tracer. A conductivity electrode made from two pieces of platinum foil, 4mm by 13mm, with a separation of 4mm, giving a cell constant of $0.769mm^{-1}$, was constructed. This was fitted into a measurement port 50mm before the over flow outlet, so that foils were parallel with the direction of flow. Conductivity was measured on a digital conductivity meter and recorded on a chart recorded. The tracer, one millilitre of one molar potassium chloride solution, was injected at a measurement port 50mm after the over flow outlet.

Once the reactor had been filled with distilled water the circulation pump would be set to the desired rate and the chart recorder allowed to come to a steady base line. Tracer was then injected as rapidly as possible, (less than 1 second), to obtain a pulse, and the concentration profile recorded. In batch operation the zero of the conductivity meter, and/or the chart recorder, could be reset to avoid using fresh distilled water at the end of each flow rate measurement. To obtain the distribution for continuous operation fresh distilled water could be added by the aqueous phase metering pump at a rate calculated to give the desired circulation number.

Two typical experimental charts for batch operation appear in figure 4.19, the time scale is actual time taken, not relative time as was used in the mixing model. In figure 4.19A, the mean circulation time was 26 seconds, giving a relative time of about 9 for four minutes. In figure 4.19B, the mean circulation time was 50 seconds, giving a relative time of about 5 for four minutes. It can be seen that the conditions in figure 4.19A have reached a more homogeneous state than in figure 4.19B, for the same period of time, although the Bodenstein number is greater. This would appear to be in contradiction to the theoretical results given in figures 4.6 & 4.7, where an increase in Bodenstein number increases relative mixing time. However, it must be

Figure 4.19 Experimental Traces, $R = \infty$.

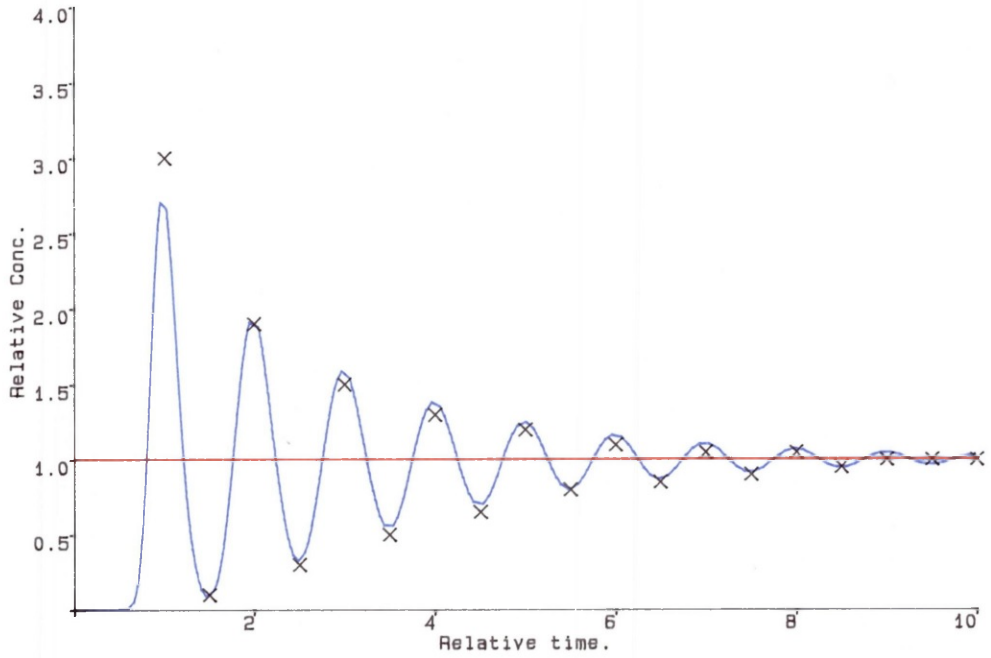


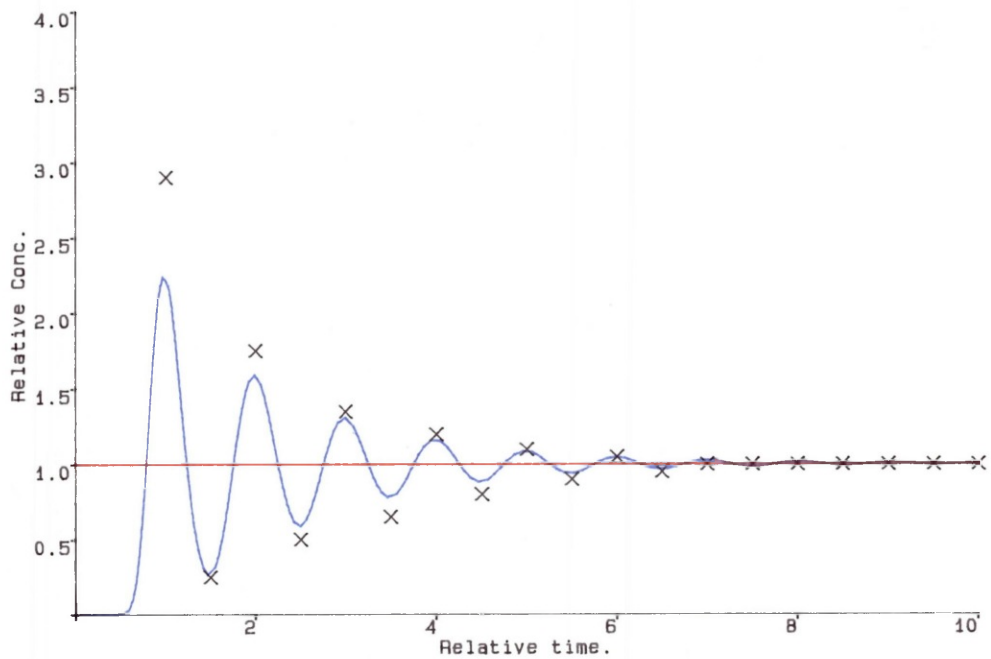
remembered that it is 'relative' mixing times that are used in the model and to get real time they must be multiplied by the mean circulation time. Increasing the Bodenstein number by increasing flow rate is accompanied by a reduction in mean circulation time which would reduce the real time taken to reach a specified inhomogeneity. Simulations of the two traces in figure 4.19 produced by the mixing model are given in figure 4.20. The peaks and troughs from the experimental traces, normalised by the reference concentration, are plotted along with the simulation results. The simulation shows very good agreement with the experimental results.

Examples of traces produced in continuous operation are given in figure 4.21 for the same Bodenstein number with two circulation numbers. Both of these traces were for a mean circulation time of 27 seconds, so in figure 4.21A renewal of the reactor contents occurred after a relative time of approximately 33, and in figure 4.21B after 67. Simulations from the mixing model, figure 4.22, show longer times for complete renewal. In mixing model for continuous operation the concentration will decay to zero in the limit of relative time tending to infinity as the renewal model used is the stream split ratio, which is less than unity, to the power of relative time, see equation 4.11. However in the practice the tracer will not always split in this ideal way and the sensitivity of measuring equipment will produces the effect of a more rapid decay.

In order to compare experimental and model results the inhomogeneity as defined in equation 4.8 is used. Inhomogeneity was evaluated from measurements taken off chart recorder traces for a range of flow rates and a number of mixing elements, and plotted against relative time together with calculated values from the mixing model, figures 4.23, 4.24, 4.25 & 4.26. The presence of static mixers causes the distribution of mixing times with respect to flow rate, for a give inhomogeneity, to be reduced, but there is no distinguishable affect between the number of static mixers used. This confirms that these static mixers only affect radial mixing, since the Bodenstein number, which characterises the effect of axial mixing, is not altered significantly by their presence. Since for a given flow rate the mean

Figure 4.20
Comparison with Experimental Results
Bodenstein Number : 95.0





Bodenstein Number : 63.0

Figure 4.21 Experimental Traces, Continuous Operation.

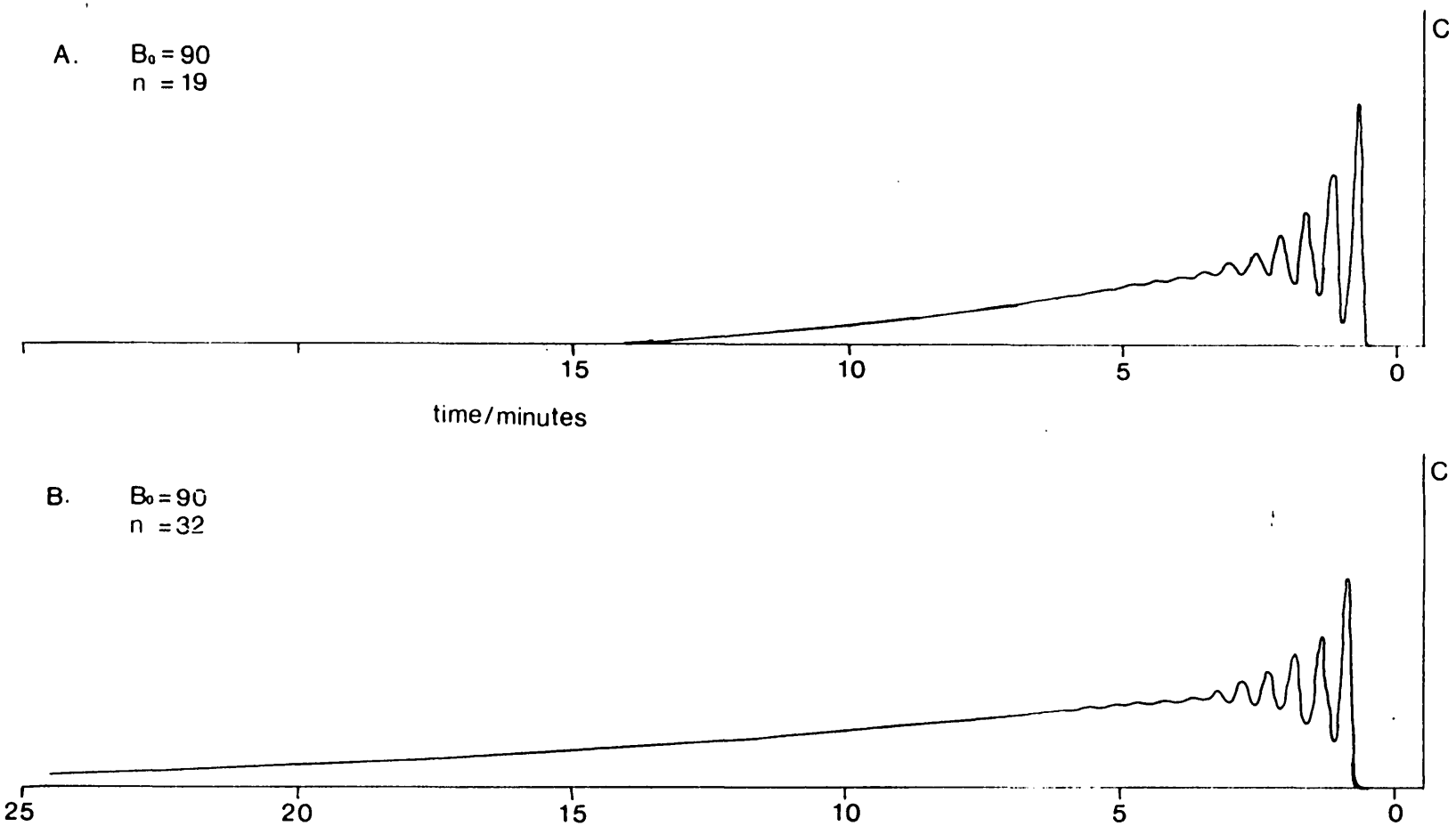
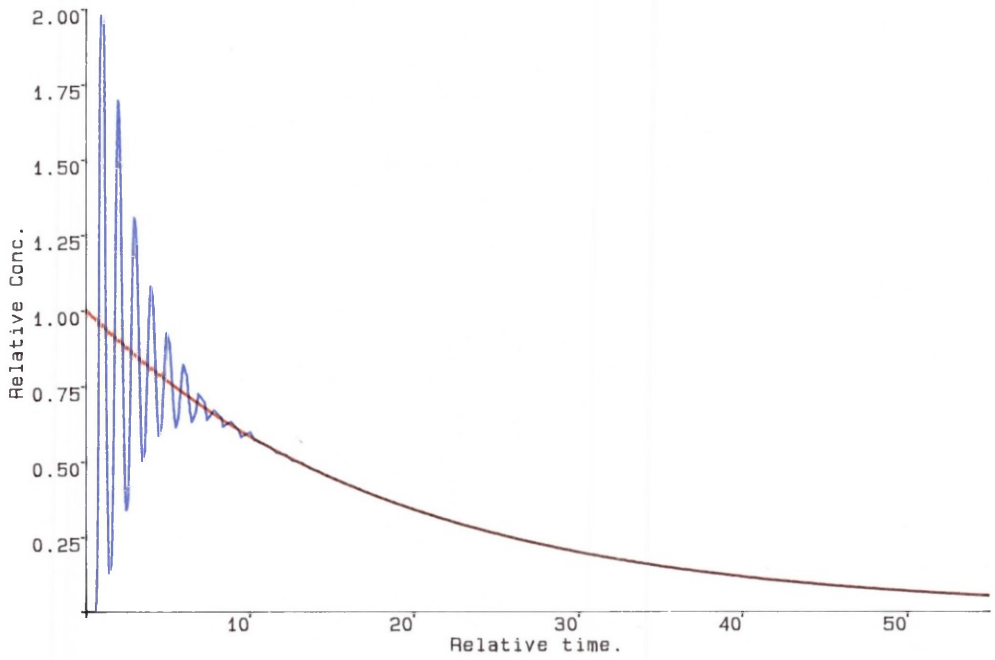
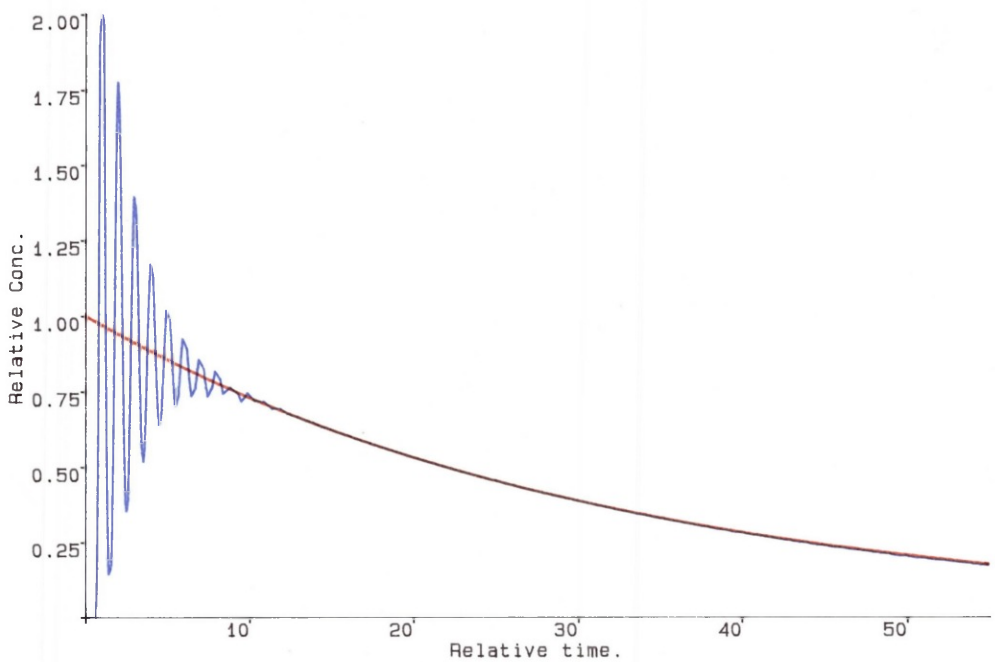


Figure 4.22
Comparison with Experimental Results
Bodenstein Number : 90.0
Circulation Number : 19.0





Bodenstein Number : 90.0
Circulation Number : 32.0

Figure 4.23

Experimental Mixing Times.

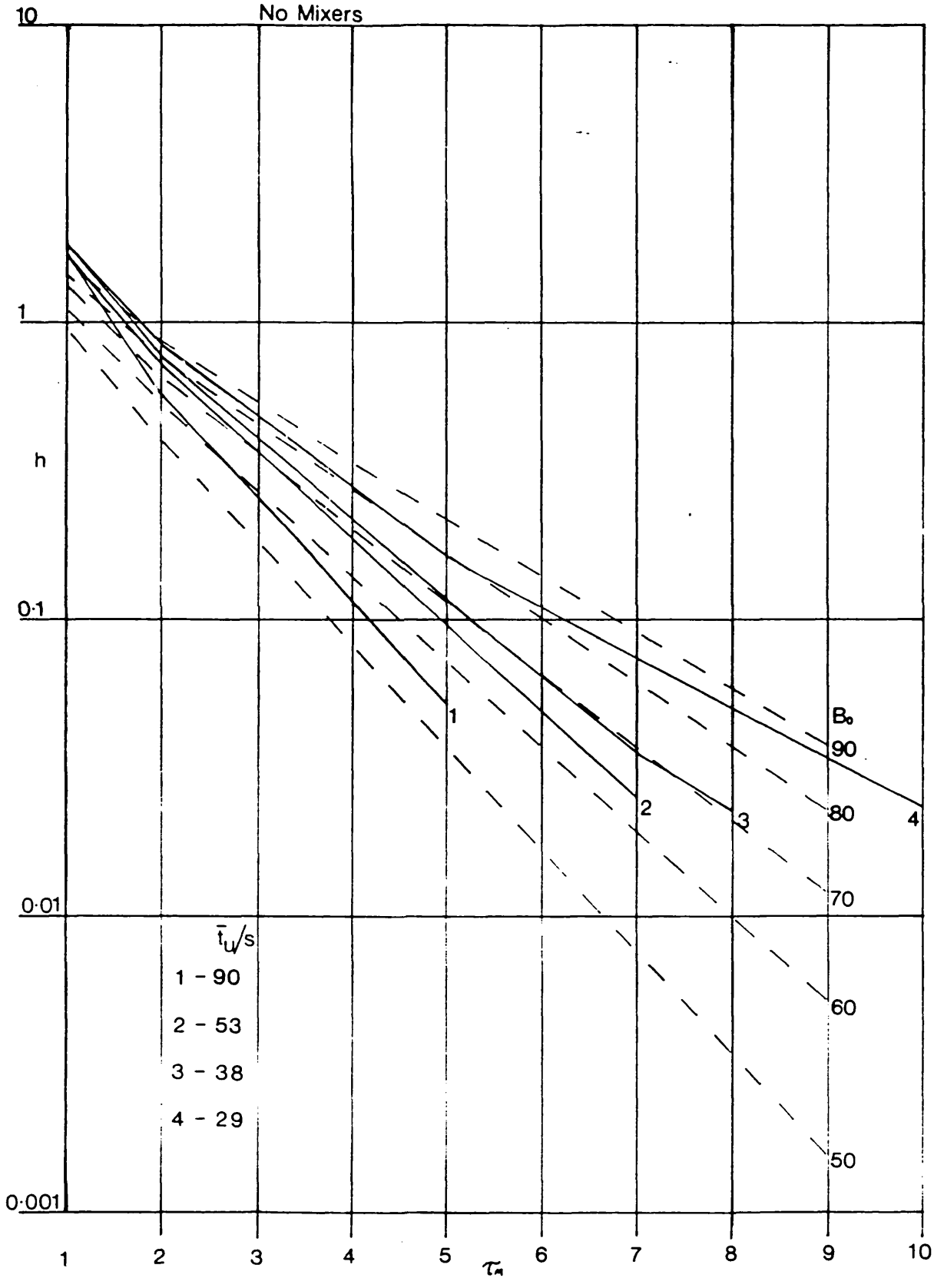


Figure 4.24

Experimental Mixing Times.

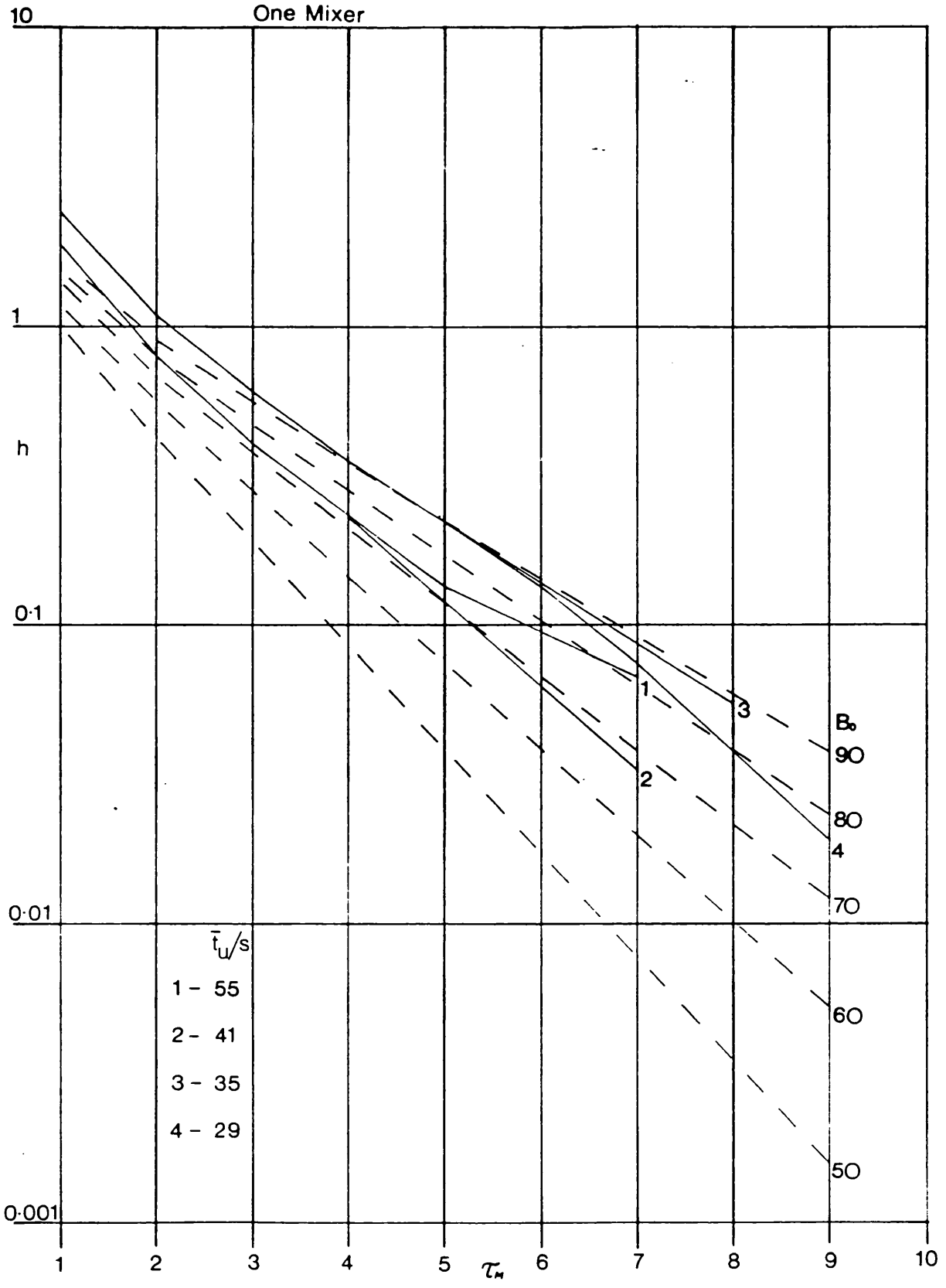


Figure 4.25

Experimental Mixing Times.

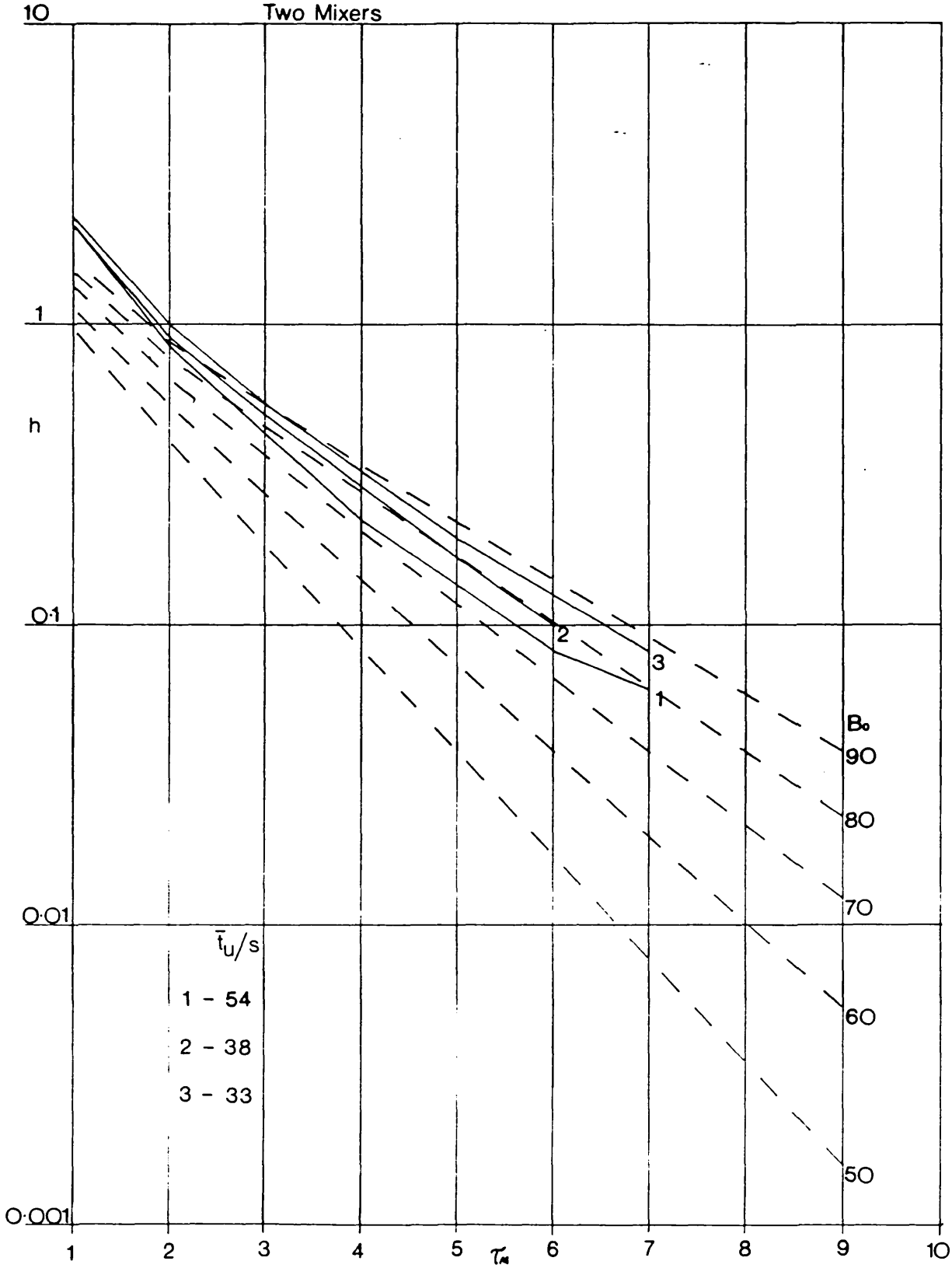
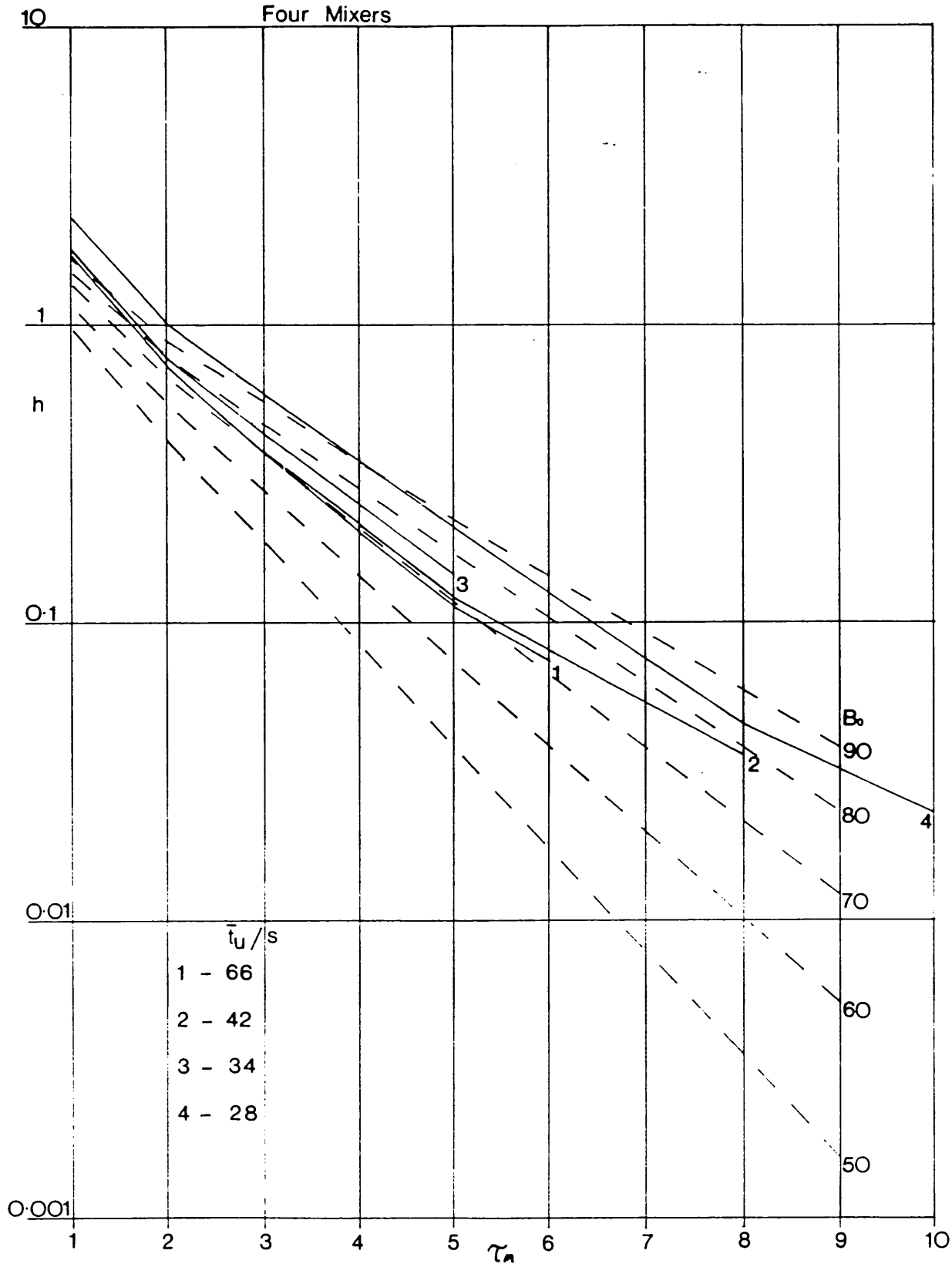


Figure 4.26

Experimental Mixing Times.



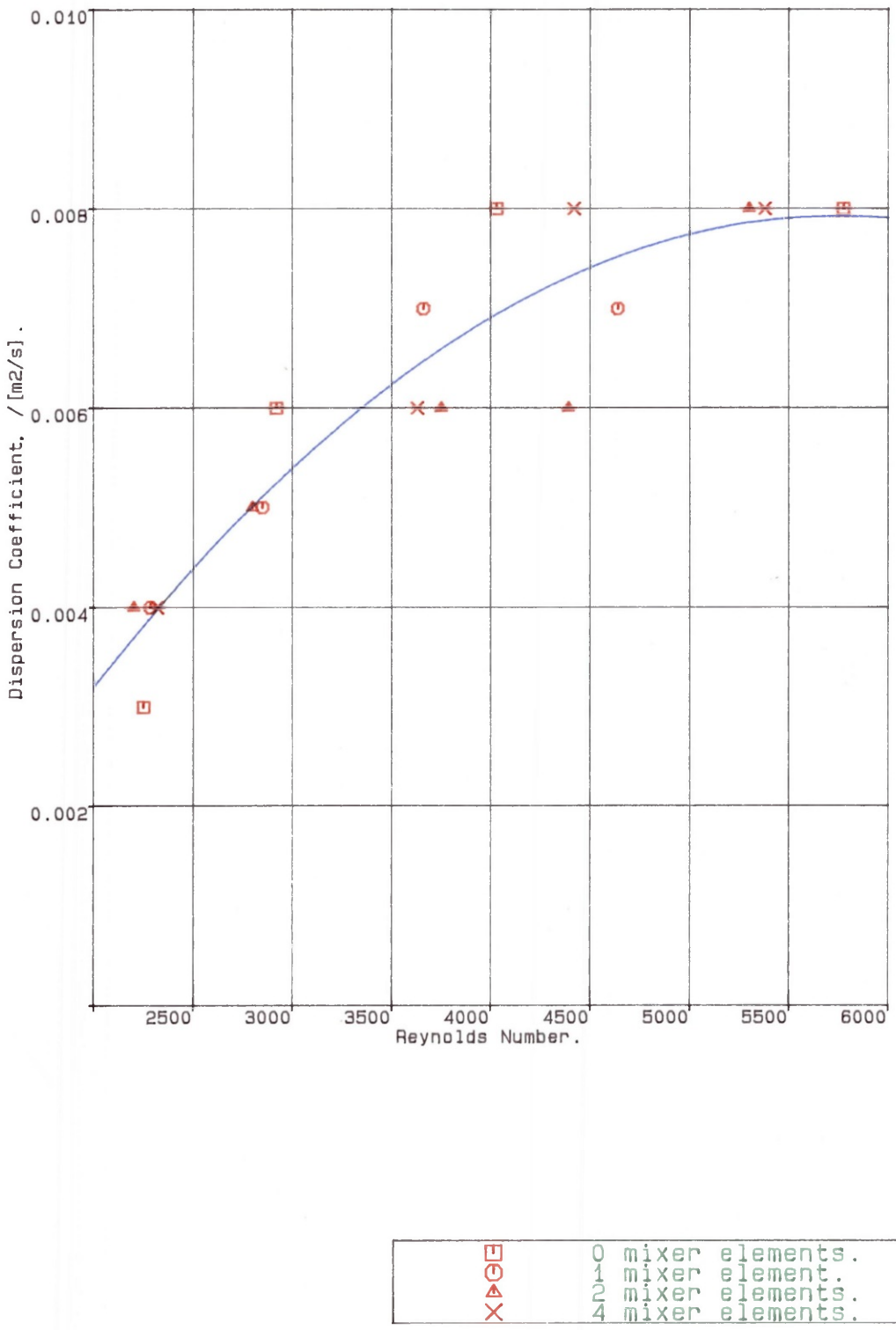
circulation velocity is constant, and the length of one circulation is fixed by the geometry of the reactor, it is only the effective longitudinal dispersion coefficient that changes the value of the Bodenstein number. The value of the effective longitudinal dispersion coefficient was evaluated for each curve by taking the mixing time to reach an inhomogeneity of 0.1 and, using figure 4.7, assigning a Bodenstein number, and thus the effective longitudinal dispersion coefficient. These were then plotted against Reynolds number to give figure 4.27, which show the effective longitudinal dispersion coefficient increasing with Reynolds number. The lower values observed were just in the laminar flow regime where there would be little or no back mixing due to the flow profile. With an increase in Reynolds number turbulent flow begins and so back mixing due to eddies in the unstable flow profile increases.

4.7 Emulsion Polymerisation of Styrene.

In order to examine the performance of the loop reactor for emulsion polymerisations, styrene monomer was polymerised with an aqueous continuous phase containing sodium dodecyl sulphate emulsifier and potassium persulphate initiator. Styrene was chosen as it insoluble in water and so will polymerise only be the emulsion polymerisation mechanism, whose kinetics should follow that of Smith and Ewart Case 2. Also it is relatively innocuous.

In a continuous polymerisation the loop would be operated initially as a batch reactor in order form seed latex, then reagents would be added and product taken off as continuous operation began. Thus to get successful batch operation is the first step in continuous operation, as a poor seed is unlikely to lead to a good quality latex. Badder and Brooks[4.6] have demonstrated that the start-up procedure for continuous stirred tank emulsion polymerisation reactors has a marked effect upon the stability of the long term reaction. Since it is the effect of agitation upon the polymerisation that is of interest here a constant start-up procedure on batch polymerisations was used.

Figure 4.27
Effective Longitudinal Dispersion Coefficient
against Reynolds Number.



4.8 Reagents and Procedure.

A simple recipe was used with only the basic components for an emulsion polymerisation. The recipe was initially tested in a glass autoclave at 50°C with a reaction time of three hours. It produced a stable polymer latex with at least a 98% conversion of monomer in to polymer. All the reagents were supplied by B.D.H. Ltd.:

Styrene - 1.5 litres was distilled under 20 mm of Hg pressure of nitrogen at 47°C.

Sodium dodecyl Sulphate - Used as supplied. 6 litres of 0.127M solution was made up with distilled water, this is fifteen time the critical micelle concentration.

Potassium persulphate - Used as supplied. 0.5 litres of 0.4M solution was made up with distilled water.

The loop reactor described above was used with the over flow pipe in a horizontal position to prevent the accumulation of less dense reagents in dead space, (Product stream in figure 4.14). A valve was fitted to the over flow pipe in order to vent nitrogen while filling and to remove the latex product. The start-up proceeded was as follows:

i. The reagents were stored in their respective vessels and their feed lines disconnected at the loop. The feed line were then filled by pumping the reagents from their vessels, then reconnected. This was done in order to remove air from the feed lines and so that a known volume could be pumped into the loop by the metering pumps.

ii. The reactor was purged with nitrogen in order to remove any oxygen which would inhibit the reaction.

iii. Emulsifier solution was pumped into the reactor until it was full, and the circulation pump started at the required rate.

iv. Hot water, at the required reaction temperature of 50°C, was pumped around the jacket to heat the emulsifier solution.

v. With the overflow valve open, 0.85 litres of monomer was pumped into the reactor.

vi. The monomer and continuous phase were circulated together and allowed to reach the reaction temperature, (one hour), before 0.1 litres of initiator solution was added.

The reaction then proceeded for three hours, the temperature being monitored and maintained at 50°C. When the reaction was completed cold tap water was circulated around the jacket to quench the reaction whilst circulation was maintained. The reactor would then be emptied and samples of the latex produced taken for analysis. Residual latex was washed out of the reactor, which was the dismantled for cleaning.

4.9 Observations and Results.

Polymerisations were performed over the range of circulation flow rates that could be achieved by the air motor drive. The physical properties of a sample latex produced at the highest flow rate were:

Density 996 kg/m^3.
Viscosity 15.2×10^{-3} Pa.s at 25°C.

These values give Reynolds numbers from 100 to 550 for the flow rates available, however, the polymerisation took place at 50°C, which would reduce the viscosity and so increase the Reynolds numbers. If this effect was to cause a ten fold increase the flow would still be laminar at the lower flow rates. The viscosity of water drops from 10^{-3} Pa.s at 20°C to 0.6×10^{-3} at 50°C, so a ten fold change seems unlikely.

Polymerisation were performed with circulation flow rates of 0.04, 0.08, 0.16, 0.20 & 0.225l/s. For the flow rates below 0.20l/s the majority of the monomer did not emulsify, but either remained as a separate organic phase, in which some polymerisation was observed to have taken place, since it had a noticeable increased viscosity or had formed solid polymer which fouled the inside of the reactor. The use of static mixers did not improve the radial mixing sufficiently to cause a significant improvement. When the flow rate was 0.20l/s, 15% by weight of the monomer was converted to solid polymer, which was recovered from the latex. The remainder of the monomer again formed a resin, as a separate organic phase, or solid fouling on the reactor surfaces. When the flow rate was 0.225l/s, the maximum monomer conversion to polymer obtained was 50%. In this experiment some of the un-polymerised monomer formed an unstable monomer emulsion that separated from the polymer latex on standing. These five experiments were repeated and similar results were obtained in each case. A summary of the flow conditions for each of these polymerisations appears in table 4.1. Here the Reynolds Number is calculated using the physical properties of pre-polymerised reagent, as these will be the initial conditions in the reactor. The dispersion coefficient is found using figure 4.27, and then the other values in table 4.1 are calculated from the flow rate and reactor geometry.

The results of these polymerisations suggest that turbulent flow is required in order to achieve successful emulsion polymerisation in a Loop Reactor. Monomer that is pumped into the reactor needs to be broken up into small droplets that will be stabilised by the surfactant, and then be the monomer reservoirs for the initiated micelles and growing polymer particles. If the monomer does not form these droplets but remains as a separate phase the supply of monomer to the polymerisation sites is severely restricted by the reduced effective surface area, and thus reduces the polymerisation rate. Polymerisation in the continuous monomer phase will take place when oligomeric radicals formed from the aqueous phase initiator and

Table 4.1

Flow Conditions for Styrene Emulsion Polymerisations.

Flowrate m^3/s	Reynolds Number	Mean Velocity m/s	Dispersion Coefficient m^2/s	Circulation Time s	Bodenstein Number
0.00004	1489	0.044	0.0020	82	79
0.00008	2979	0.088	0.0055	41	58
0.00016	5958	0.176	0.0080	20	79
0.00020	7448	0.220	0.0080	16	99
0.000225	8390	0.248	0.0080	14	111

solubilised monomer migrate into the monomer phase. The extent to which this happens will be relatively small as the effective surface area of the monomer swollen micelles will be much greater than the separate monomer phase and so will be more effective at capturing the radicals. Thus the rate of polymerisation in the continuous monomer phase will be slow.

To form small droplets high shear rates and good radial mixing are required. Good radial mixing is require because of the difference in the relative densities of the monomer and aqueous phases. As styrene is less dense than water it would tend to float on top of the water unless there was strong radial mixing in the loop to overcome its buoyancy. Although in laminar flow the parabolic velocity profile will produce an axial spread, there is no radial mixing and so the monomer and aqueous phase will stay separate. However, in turbulent flow there is radial mixing which is more important in the common situation where the monomer and aqueous phase have different densities.

The polymer latex formed at the highest flow rate obtainable in the Loop Reactor used in this work had a 50% conversion after three hours reaction time. This is significantly smaller than would be expected for an equivalent reaction in a stirred tank reactor, and thus the problems described above due to poor emulsification of monomer are still taking place. For this flow rate the Reynolds Number was 8390, table 4.1, which is in the turbulent flow regime, however the shear forces and radial mixing can not yet be of a sufficient magnitude to cause adequate mixing. As can be seen in table 4.1, an increase in the Reynolds Number causes an increase in the Bodenstein Number, once the flow is turbulent. A doubling of Reynolds Number will double the Bodenstein Number for constant physical properties and reactor geometry if the dispersion coefficient can be considered constant, which it can for high Reynolds Numbers as can be seen in Figure 4.27. Figure 4.4 shows that doubling the Bodenstein Number causes greater inhomogeneity in the reactor, and so increases the relative mixing time. However, Figure 4.6 shows that the relative mixing time does

not more than double for a two fold increase in Bodenstein Number, and since the mean mixing time halves for twice the flow rate the actual mixing time remains essentially the constant. Thus high Reynolds Numbers, which are desirable for emulsification, cause greater inhomogeneity in the Loop Reactor but do not increase the mixing time.

4.10 Comments on the Design of Loop Reactors for Emulsion Polymerisation.

Gulf Oil Ltd.'s patent specification indicated that emulsion polymerisation could be carried out successfully in laminar flow conditions. The above work suggests otherwise. The loop reactor used in the patent had major differences to the one used in this work, which may account for this. Firstly over 60% of their reactor volume was taken up by the centrifugal pump which would behave like a well stirred tank in which the new reactants will be well mixed with the reactor contents before going into the loop. The characteristic well defined flow field of a laminar or plug-flow loop reactor being lost, there will be little difference between this configuration and a continuous stirred tank reactor. The advantages of a positive displacement pump are that circulation is provided with minimal disruption to the flow profile and it can handle high viscosities with ease. However, in the reactor used in this work a sufficiently high flow rate could not be provided by the circulation pump to perform successful emulsion polymerisation or to examine high Reynolds Number flow.

The length to diameter ratio of the patented reactor was 400 whereas it was 106 in this work. A large length to diameter ratio is favourable because, for a given volume of reactor, a greater degree of turbulence, that is a larger Reynolds number, is obtained for a given flow rate. Also it gives a longer mean circulation time in which the longitudinal mixing effects have to act.

Finally the choice of vinyl acetate monomer, which has a relatively large solubility in water, would reduce the disadvantage of laminar flow since the radial concentration gradient produced by longitudinal dispersion would cause radial diffusion of monomer.

The problem when performing a continuous polymerisation is to get the mean residence time in the reactor to be of the same order as the time taken for polymerisation to reach an acceptable degree of conversion. This is done in a loop reactor by recycling a large proportion of the reactor contents, the affect of which was observed in figures 4.8, 4.9, 4.10 & 4.11. A required mass production rate of polymer latex, combined with a desired mean residence time from the polymerisation kinetics, will give the reaction mass the reactor must hold and, from physical properties of the reagents, the reactor volume. The desire for good mixing and heat transfer requires that the flow is turbulent[4.7], that is a Reynolds number well above 2000 with the physical properties of the fluid this will give the product of pipe diameter and mean circulation velocity. If the length to diameter ratio is specified, which geometrically must be greater than Pi and practically needs to be much greater than that, around 500, the geometry and flow rates of the loop reactor are set.

The role of the Bodenstein number in the modelling and description of the mixing effects in a loop reactor has been discussed, but it's role in design would depend upon knowledge of the effective longitudinal dispersion coefficient for a particular geometry and chemistry. Further work on the evaluation of the effective longitudinal dispersion coefficient from the contributory mechanisms and its behaviour under different flow conditions needs to be carried out if this mixing model is to be of use in design. The many advantages of the loop reactor make it valuable addition to the range of reactors that can be used for emulsion polymerisation, and worthy of further study.

5.0 Measurement of Molecular Weight Distribution.

Introduction.

In this chapter the measurement of polymer molecular weight distribution by Gel Permeation Chromatography, G.P.C., is described. A new convenient method for analysing data from G.P.C columns in order to obtain the true molecular weight distribution is presented.

Gel Permeation Chromatography.

The molecular weight of a polymer is not a unique value, but expressed as an average of the weights of a discrete distribution of polymer molecules. Each polymer molecule can be considered to be a chain of monomer units, so values in the distribution are each separated by the weight of one monomer unit. In order to obtain the molecular weight distribution the quantity of each length of polymer needs to by measured. Gel Permeation Chromatography, G.P.C., introduced by Moore[5.1] is a convenient method of doing this. It determines the full molecular weight distribution by the continuous separation of components in columns packed with beads of varying porosity. The polymer sample is dissolved in a solvent which is the same as the eluent flowing through the column. A sample of the polymer solution is then added to the eluent stream. Smaller polymer molecules diffuse into pores faster, and hence to a greater extent, than larger molecules, which are swept on by the eluent flow. This reverses the concentration gradient and smaller molecules then diffuse back into the eluent flow. This process is repeated continuously down the column, producing a steric separation of molecules, so larger molecules emerge before smaller ones. The effluent is then monitored, usually optically, to detect changes in the polymer concentration.

However, the resolution of this technique is not infinite. When a monodisperse, single molecular weight, sample is passed through the column a bell shaped Gaussian curve is produced, not a single spike. The position of the peak of the Gaussian curve depends upon the molecular weight of the compound, and the area is proportional to the concentration. This is due to a broadening of the peak by axial diffusion of the molecules. With a polydisperse sample axial mixing will produce a chromatogram that reflects not only the molecular weight distribution but also this diffusive mixing process. Its overall shape is broader than the true molecular weight distribution, being the sum of individual Gaussian curves for each component. The tails of the chromatogram represent components that do not exist in the sample and, although the area is still proportional to the total concentration, heights do not give the relative proportion of each component. In order to obtain the full molecular weight distribution it is necessary to remove the effect of the axial diffusion from the chromatogram. Tung[5.2] formulated the problem mathematically from a phenomenological point of view, arriving at his axial dispersion equation.

$$F(v) = \int_0^\infty W(y).(h/\pi)^{1/2}.e^{-h(v-y)^2}dy \qquad \text{equation 5.1}$$

Where:

F(v) : G.P.C. Chromatogram not corrected for dispersion.

W(y) : G.P.C. Chromatogram corrected for dispersion.

h : column resolution factor.

v,y : eluent volume.

Tung gives solutions of the dispersion equation for W(y), and points out problems with instability of the solution techniques. The graphical solutions presented by Tung show W(y) to be narrower than F(v), as would be expected, but on the same scale axis, the amplitude of W(y) is shown to be smaller than F(v). However, the dispersion equation indicates that W(y) should be narrower but taller than F(v), the areas under each curve being equal. Figure 5.1 shows F(v) evaluated from W(y) defined as a Gaussian distribution, and illustrates this point. This is confirmed by Chang and Huang's[5.3] solution to the axial diffusion problem. In this the integral equation which relates the true molecular weight distribution to the chromatogram is reformulated into an equivalent variational problem with a quadratic functional. The method of steepest descent is then applied to obtain the true molecular weight distribution, and the solutions presented are consistent with the dispersion equation. This method is efficient and reduces some of the problems of instability that Tung experienced by data smoothing.

Both these methods attempt to obtain the full molecular weight distribution from the chromatogram. When solving a set of differential equations for polymerisation kinetics, it is easier to obtain the moments of the distribution rather than the full molecular weight distribution. This is the approach of Hamielec and Ray in their analytical solution to Tung's axial dispersion equation[5.4]. Here the ratio of the corrected to uncorrected molecular weights is defined and analysed as follows. The height of the normalised G.P.C. chromatogram corrected for dispersion, W(v), for a given v, is proportional to the concentration of polymer with molecular mass given by M(v), the true molecular weight calibration curve. The number of molecules of molecular weight M(v), will be proportional to W(v)/M(v). Thus the k^{th} moment of the distribution with respect to molecular weight, will be:

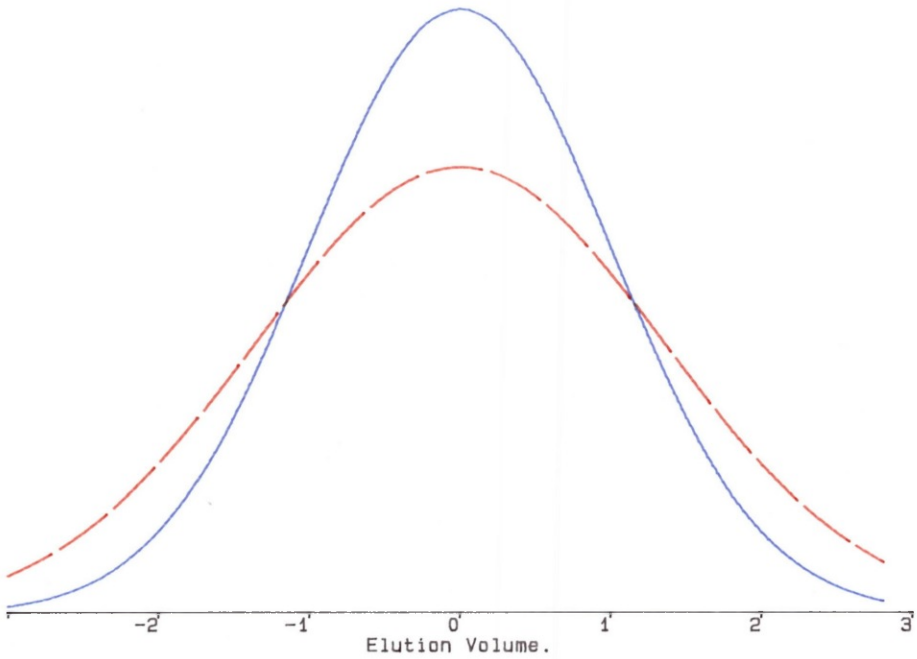
$$\lambda_k = \int_0^\infty \left(\frac{W(v)}{M(v)}\right) M(v)^k \, dv$$

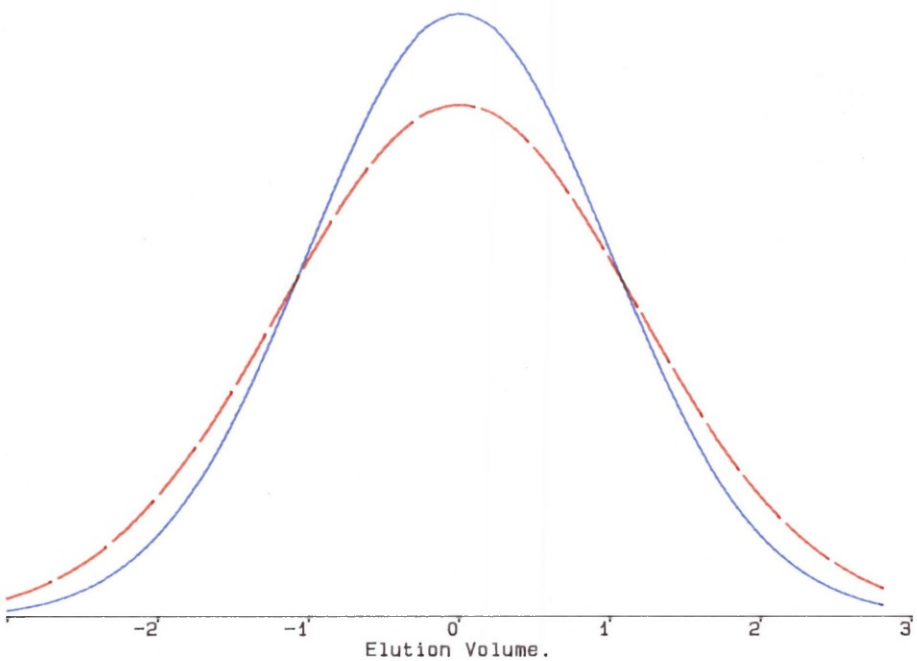
equation 5.2

Figure 5.1

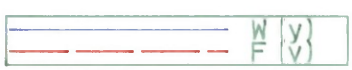
Column Dispersion of a Gaussian Distribution.

Column Resolution Factor : 0.6





Column Resolution Factor : 1.3



The molecular weight averages can be expressed in terms of these moments:

Number average chain length, $M_n = \lambda_1/\lambda_0$
Weight average chain lehgth, $M_w = \lambda_2/\lambda_1$

Substituting the normalised, but uncorrected G.P.C. chromatogram, F(v), for W(v), the uncorrected molecular weights are obtained, using Hamielec & Ray's notation:

$M_k(h)$ = dispersion corrected molecular weight average.

$M_k(\infty)$ = uncorrected molecular weight average.

where:

$M_k = \lambda_k/\lambda_{k-1}$

Now the ratio of the corrected to uncorrected molecular weights can be expressed as:

$$\frac{M_k(h)}{M_k(\infty)} = \frac{\int_a^b W(v).M(v)^{(k-1)}.dv / \int_a^b W(v).M(v)^{(k-2)}.dv}{\int_a^b F(v).M(v)^{(k-1)}.dv / \int_a^b F(v).M(v)^{(k-2)}.dv}$$

equation 5.3

where: a = initial elution volume.

b = final elution volume.

The calibration curve for a gel permeation chromatograph often can be well represented by:

$$M(v) = C.\exp(-D.v)$$

equation 5.4

where C and D are constants.

When equation 5.4 is substituted into equation 5.3 the ratio of the bilateral Laplace transforms of W(v) and F(v) is obtained. Tung's axial dispersion equation, equation 5.1, can be considered as the convolution integral of this transformation. The result of applying the convolution integral to the transformation is:

$$\frac{M_k(h)}{M_k(\infty)} = \exp((3-2k).D^2/4h)$$

equation 5.5

The ratio of the corrected to uncorrected moments is:

$$\frac{\lambda_k(h)}{\lambda_k(\infty)} = \exp(-D^2/4h). \prod_{j=0}^{(k-1)} \exp((3-2(k-j)).D^2/4h)$$

equation 5.6

Thus if the moments of the uncorrected chromatogram can be evaluated, then the corrected moments and true molecular weight averages are determined. Equation 5.6 shows that the axial dispersion is dependent only upon G.P.C. column parameter, D & h, which are determined experimentally.

From these moments it should be possible to reconstruct the full molecular weight distribution. The accuracy of reconstruction will depend upon the number of moments available. Bamford and Tompa[5.5] suggest that the molecular weight distribution can be calculated from its moments using a technique originally described by Margenau and Murphy[5.6]. The origin of the formula used and validity of this technique is not shown by Bamford and Tompa[5.5] but here the derivation will be outlined.

A continuous variable, x, will be used for the abscissa, which could represent elution volume or a continuous approximation to the discrete molecular weight. Since both these quantities vary from zero to infinity, and do not take negative values, the polynomials appropriate to this range are Laguerre polynomials. Taking Rodrigues formula for Laguerre polynomials from the National Bureau of Standards Handbook of Mathematical Functions[5.7].

$$L_n^a(x) = \frac{e^x\, x^{-a}}{n!} . \frac{d^n}{dx^n} (e^{-x}.x^{(a+n)})$$

equation 5.7

The explicit expression for Laguerre polynomials is

$$L_n^a(x) = \sum_{m=0}^{n} {}^{(n+a)}C_{(n-m)} . \frac{(-x)^m}{m!}$$

where:

$$^{(n+a)}C_{(n-m)} = \frac{(n+a)!}{(n-m)!\ (a+m)!}$$

equation 5.8

Note that there is an orthogonality relation:

$$\int_0^\infty e^{-x}.x^a.L_n^a(x).L_m^a(x).dx = \frac{(a+n)!}{n!} \quad \text{for } n = m$$
$$= 0 \quad \text{for } n \neq m$$

equation 5.9

The normalised distribution function, W(x), is then assumed to take the form:

$$W(x) = \frac{e^{-x}.x^a}{a!} \sum_{n=0}^{N} c(a,n).L_n^a(x)$$

equation 5.10

This assumes a base Gamma distribution, which is modified by the moments of the target distribution. N is the number of moments used in the modification. The coefficients, c(a,n), are then correlated in terms of the moments of the distribution by using the orthogonality relationship of Laguerre polynomials. Equation 5.10 is multiplied by $L_m^a(x)$ and integrated over the range zero to infinity, interchangeability of summation and integration is assumed:

$$\int_0^\infty L_m^a(x).W(x).dx = \frac{1}{a!} \sum_{n=0}^{N} c(a,n).\int_0^\infty e^{-x}.x^a.L_m^a(x).L_n^a(x).dx$$

equation 5.11

Applying equations 5.8 & 5.9 to equation 5.11 gives:

$$c(a,n) = \frac{n!a!}{(n+a)!} \int_0^\infty \sum_{j=0}^{n} {}^{(n+a)}C_{(n-j)} \frac{(-x)^j}{j!}.W(x).dx$$

equation 5.12

Re-arranging equation 5.12 results in

$$c(a,n) = \sum_{j=0}^{n} {}^{n}C_j \frac{a!}{(a+j)!} (-1)^j.\bar{\bar{W}}_j(x)$$

equation 5.13

where:

$$\bar{\bar{W}}_j(x) = \int_0^\infty x^j . W(x) . dx$$

equation 5.14

Equation 5.14 is the j-th moment of the distribution W(x), and a is a parameter yet to be determined.

Polymer chain length distributions are discrete distributions over a large range of values. Let x be the polymer chain length, n, scaled by the number average chain length, u, and considered it as a continuous variable. Taking the base Gamma distribution:

$$G(x) = \frac{e^{-x} . x^a}{a!}$$

using the scaling n=u.x we have

$$G(n) = \frac{e^{-(n/u)} . (n/u)^a}{a!}$$

equation 5.15

Now consider the moments of the Gamma distribution to find the relationship between the distributions:

$$\bar{\bar{G}}_k(x) = \int_0^\infty x^k . G(x) . dx = \frac{1}{a!} . \int_0^\infty e^{-x} . x^{(a+k)} . dx$$

$$= \frac{(a+k)!}{a!}$$

$$\bar{\bar{G}}_k(n) = \int_0^\infty n^k . G(n) . dn = \frac{1}{a!} . \int_0^\infty e^{-(n/u)} . (n/u)^{(a+k)} . u^k . dn$$

$$= u^k . \frac{(a+k)!}{a!}$$

Thus:

$$\bar{\bar{G}}_k(n) = u^k . \bar{\bar{G}}_k(x)$$

equation 5.16

To find the value of a, consider the mean and variance of the distribution, from equation 5.16:

mean : $\bar{\bar{G}}_1(n)/\bar{\bar{G}}_0(n) = u.(a+1)$

variance : $\bar{\bar{G}}_2(n)/\bar{\bar{G}}_0(n) - (\bar{\bar{G}}_1(n)/\bar{\bar{G}}_0(n))^2 = u^2.(a+1)$

Hence

$$a = \frac{(\bar{\bar{G}}_1(n))^2}{\bar{\bar{G}}_2(n) - (\bar{\bar{G}}_1(n))^2} - 1$$

equation 5.17

Equation 5.16 shows that the same result is obtained with the non-scaled distribution. The moments can now be used to evaluate all the coefficients required in equation 5.10 and so the distribution, W(x), can be reconstructed.

To examine how well this scheme of reconstruction works, the moments of a bi-modal Gamma distribution are used. Two distinct Gamma distributions:

$$G_1(x) = \frac{e^{-x}.x^{a_1}}{a_1!} \quad \& \quad G_2(x) = \frac{e^{-x}.x^{a_2}}{a_2!}$$

are added to produce the bi-modal distribution:

$$G(x) = f.G_1(x) + (1-f).G_2(x)$$

equation 5.18

where f is the fraction of the first distribution to be included in the bi-modal distribution, which maintains unit area under the curve. It is easily shown that the moments of the overall distribution are the scaled summation of the individual moments:

$$\bar{\bar{G}}_k(x) = f.\bar{\bar{G}}_{1,k}(x) + (1-f).\bar{\bar{G}}_{2,k}(x)$$

equation 5.19

Figures 5.2 & 5.3 illustrate how a Gamma distribution, as defined by equations 5.18 & 5.19, is reconstructed. Figure 5.2 is a mono-modal Gamma distribution. It can be seen that only three moments, zeroth, first and second, are needed to reproduce the curve over its full range. The six, nine and twelve moment reconstructions superimpose upon the three moment points, showing that divergence does not occur. Figure 5.3 shows a highly bi-modal Gamma distribution, with two clear peaks. In this extreme case twelve moments were sufficient to reproduce the curve.

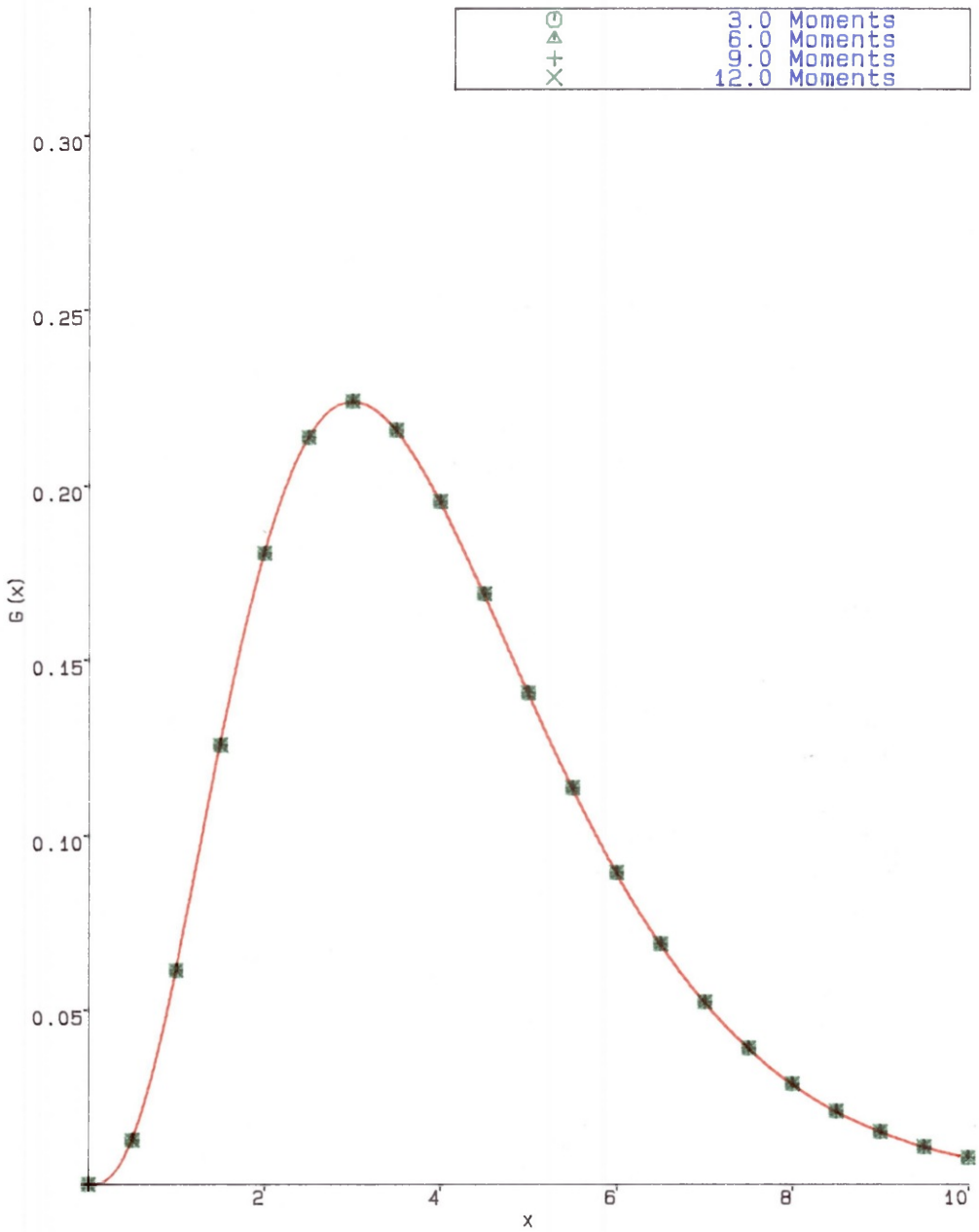
Increasing the number of moments used to reconstruct a distribution will improve the approximation to the original curve, but is limited by computational time, accuracy and capacity. The practical application of this method to determine molecular weight distributions will now be described.

5.1 Experimental Measurements.

Equipment and Procedure.

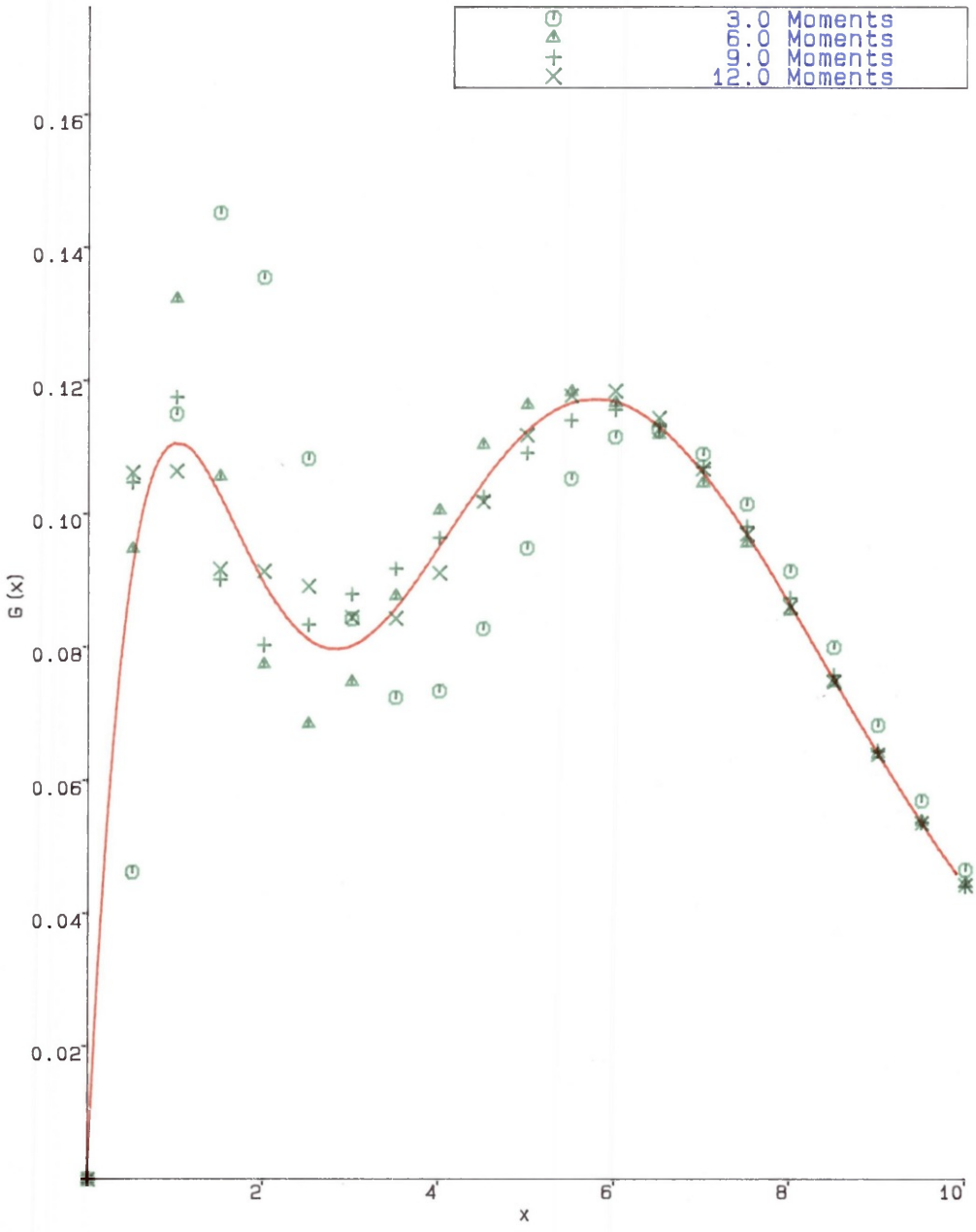
Molecular weight measurements were made on a Gel Permeation Chromatogram supplied by Applied Chromatography Systems Ltd. It consisted of a pumping unit, with a maximum operating pressure of 500 bar, which pumped solvent, via an injection valve, through columns in a column oven at 25°C. The effluent was monitored by a differential refractometer in which pure solvent was the reference, the changes in refractive index of the effluent being recorded on a chart recorder. Three columns were used, each packed with cross linked polystyrene beads, their mean pore sizes being 500 Å,100 Å and 10 Å.

Figure 5.2
Gamma Distribution from its Moments.



Mono-modal Gamma Distribution.
a = 3
All points are Coincident.

Figure 5.3
Gamma Distribution from its Moments.



Bi-modal Gamma Distribution.
$G(x) = f.G(x, a1) + (1-f).G(x, a2)$
$a1 = 3 \quad a2 = 6 \quad f = 0.3$

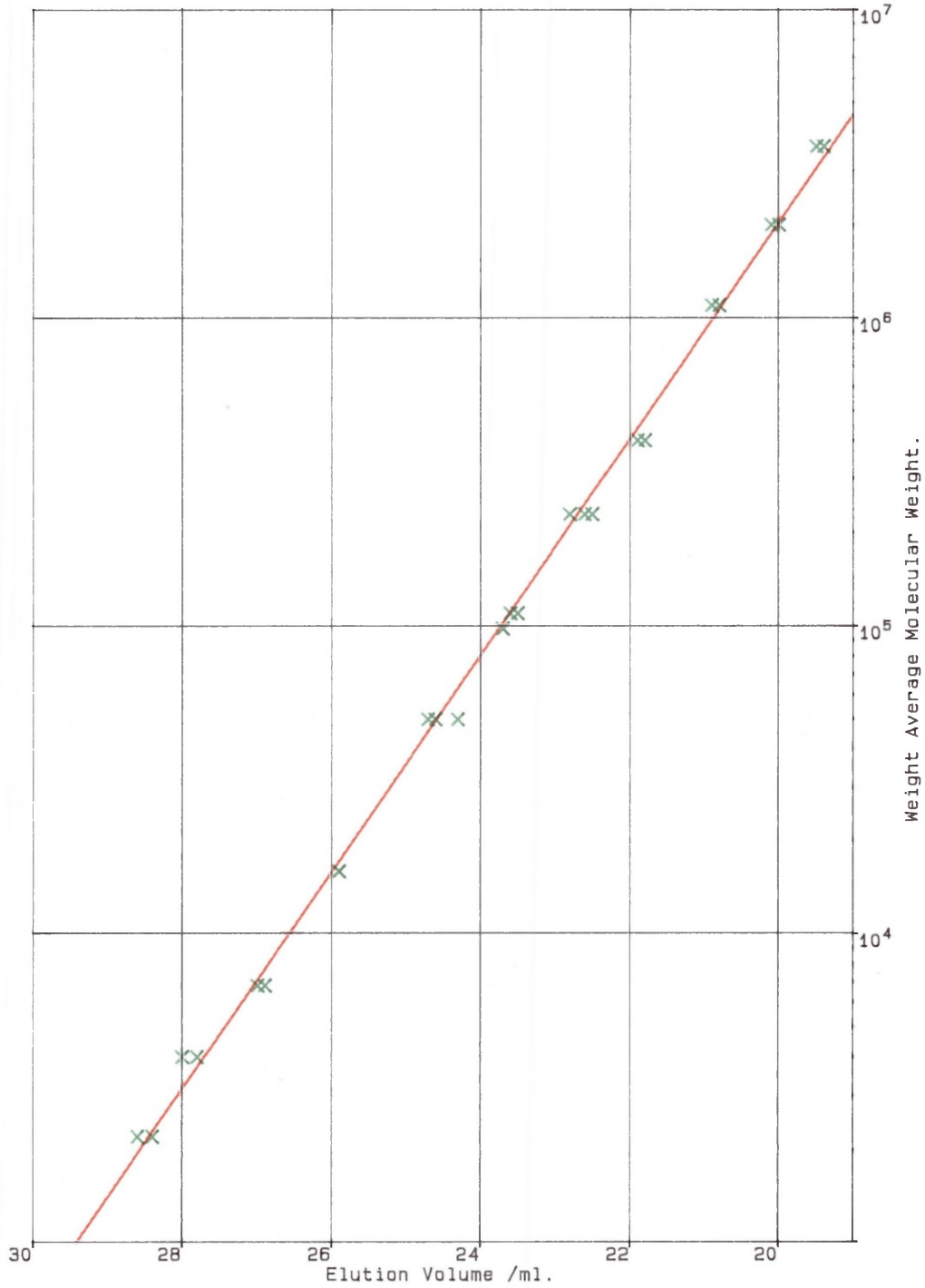
Tetrahydrofuran stabilised with 1% quinol was used as the solvent, supplied by B.D.H Ltd. The elution flow rate was 1.0 ml/min and the chart recorder speed was set to 10.0 mm/min so the chromatogram produced had a base axis of 10.0 mm/ml. Polymer samples were made up to a concentration of 2%, (weight to volume), and 0.05 ml/ml of 1% toluene in tetrahydrofuran was added as a marker. The injection valve was fitted with a 0.1 ml volume coil which was filled with the solution of polymer sample, so maintaining a constant injection volume.

Low polydisperity polystyrene samples of known molecular weight, supplied by Polymer Laboratories Ltd., were first used in order to calibrate the column for weight average molecular weight against elution volume. Figure 5.4 is the calibration curve, which was regularly checked throughout the course of measurements, and shows that equation 5.4 is a good representation of the calibration data. The values of C and D in equation 5.4 were obtained by fitting the calibration data.

5.2 Conversion of Chromatograms to Molecular Weight Distributions.

All the G.P.C. results were in the form of curves on chart paper. In order to remove the effect of axial dispersion using the scheme described, the information from the chromatogram was digitised for processing in a micro computer. A novel feature of the method used, which greatly enhances its practical utility, was the use of a B.B.C. model B micro computer was used with a "British Micro's Grafpad 2" to analyse the chromatograms. The Grafpad had an A4 area with 1280 by 1024 pixel resolution and a reproducibility of one pixel. The X and Y co-ordinates of the Grafpad pen were passed to the micro computer via the user port parallel interface. The programme that processed the data was in two parts, the first collected the data, the second calculated the moments:

Figure 5.4
Calibration Curve for G.P.C. Columns.



Data Collection.

i. Initiation of the Grafpad and setting the origin of the graphics area.

ii. Initiation of new chromatogram, which is placed on the graphics area and fixed with a cover. The X and Y co-ordinates of the initial and final elution volume were read in, together with the actual values in ml, via the computer keyboard. An array for the chromatographic data was then initiated.

iii. Data was collected by tracing the curve, which was drawn on the monitor screen and stored in the array.

iv. Base line drift often occurs on G.P.C. measurements, this was removed to give all ordinate values the same datum. When the initial and final elution volumes were entered the Y co-ordinates gave the end points of the base line that was used in this correction.

v. The X co-ordinate when tracing the curve gave the place in the array where the Y co-ordinate would be stored. If one of the array values was empty, equal to zero, due to that point not being covered during the tracing, then a discontinuity in the curve was produced which gave incorrect moments. This was overcome by scanning the data for unexpected zero values and using linear interpolation between neighbouring non-zero values to assign a reasonable value. A good correlation between the chromatogram and the digitised data on the monitor screen was produced by this technique.

vi. Finally the data was stored onto floppy disc as (volume, ordinate) data pairs, together with the number of point and the maximum ordinate value, for normalisation.

Moment Calculation.

i. Data points from the first part of the program were read in and normalised. The column calibration constants, C & D, and the column resolution factor, h, were entered so the correction coefficients and molecular weights for elution volumes used could be calculated.

ii. The normalised data was then used to calculate the uncorrected molecular weight moments using a Simpson type integration technique. This evaluated the moments using half the points and then all the points, Richardson's extrapolation method was then used to reduce the error.

iii. Correction of the moments for axial dispersion using equation 5.6 was then performed and the weight average and number average molecular weights and polydispersity were calculated and output to a printer, figure 5.5.

Three parameters were needed by the program to calculate the molecular weight and perform the correction. These are the calibration constants for the column as in equation 5.4, and the column resolution factor as in equation 5.1. The calibration constants were determined by least square fitting of the calibration data described above, to equation 5.4. The resolution factor can be determined by flow reversal experiments as described by Tung et al[5.8]. In this a sample of polymer is passed half way through the column and then the flow is reversed. The resultant chromatogram reflects the effect of axial dispersion only and is independent of the polydispersity of the polymer sample. Fitting this curve to a Gaussian distribution as is in equation 5.1 gives the value for column resolution. The process is then repeated for the other half of the column, and the overall resolution factor evaluated, similar to adding resistances in parallel.

$$\frac{1}{h_{column}} = \frac{1}{h_1} + \frac{1}{h_2}$$

Figure 5.4

Typical Output from Chromatogram Program.

Moments for data D.G170786

order	Uncorrected moments	Corrected momoents
0	6.52756685E-5	6.52756685E-5
1	5.54217848	5.54217847
2	1164240.83	1029972.33
3	5.3428108E11	3.27265878E11

Calibration curve: M(v)=D1.exp(-D2.v)
D1=8.858E12 D2=0.80192
Column Resolution factor, h=1.312

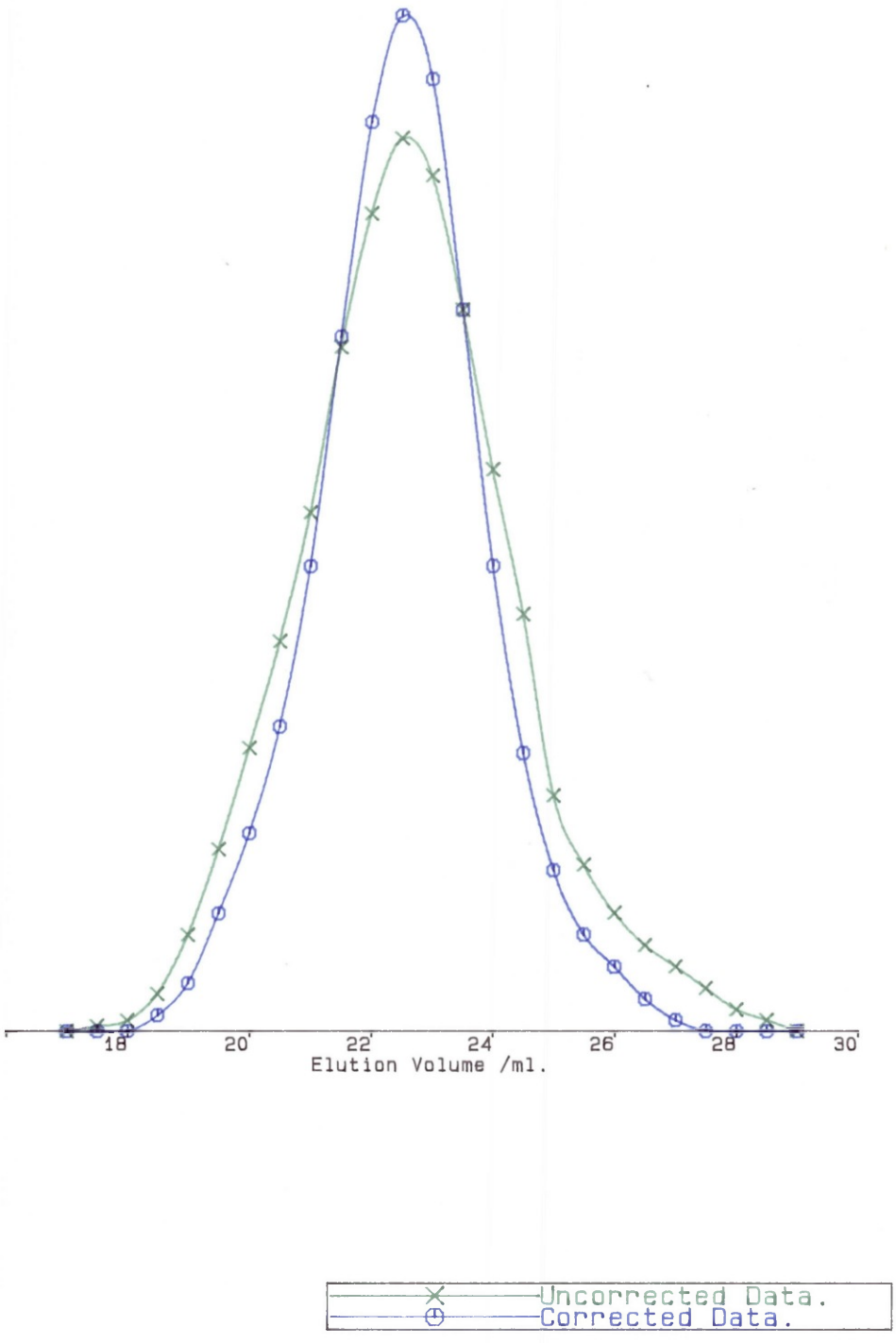
Number Average Molecular Weight
Mn=84904
Weight Average Molecular Weight
Mw=185842
Polydispersity, Zp=2.18884934

Since this method required a flow reversal valve, precise switching of flow half-way through the column and then curve fitting of the data, a more simple method was used here. Chromatograms of materials having known molecular weights and polydispersity, as used in the column calibration, were digitised and analysed in the programme described above. The value of the resolution factor used in the programme was adjusted until the calculated polydispersity corresponded with the manufacturers quoted value. This was done on each sample that was used to form the calibration, figure 5.4, the overall value used being the arithmetic mean of this range:

$$h = 1.312 \pm 0.052 \text{ ml}$$

The full molecular weight distribution of a polymer is seldom needed, the weight average molecular weight and polydispersity being sufficient to describe the polymer for most purposes. Equation 5.4 shows that the abscissa of the chromatogram is a logarithmic scale of molecular weight, and so would produce values of the sixth moment of the order 10^{38}. This causes overflow problems in the micro computer if the full molecular weight distribution is to be evaluated from its moments. However, if the moments of the chromatogram are used, in terms of volume /ml, this problem is avoided and comparison with the uncorrected chromatogram is possible. An example of such a reconstruction is given in figure 5.6. This shows that the true molecular weight distribution is narrower than the uncorrected distribution and taller as area is constant. Both curves are bell shaped with a low molecular weight tail. The base distribution chosen for the reconstruction was a Gamma distribution which proved suitable for these polymer samples as the original chromatogram had this form, but its suitability to other basic distributions would require more investigation.

Figure 5.6
Corrected G.P.C. Chromatogram.



The method described here probably has no advantage in accuracy over Tung's or Chang & Huang's method, and the use of Laguerre polynomials in the reconstruction is equivalent to the use of Hermite polynomials by Tung and the data smoothing used by Chang & Huang, in that detail is lost from the true distribution. However the advantages of this method of dispersion correction is that it is quick and avoids the problems with instability, caused by solving for the full molecular weight distribution, that were experienced by these other workers. Also it can be easily calibrated for the particular polymer/solvent system under study and is readily applied in a routine manner.

6.0 Conclusions.

It has been shown that the role of agitation in the course of an emulsion polymerisation is important, particularly at low surfactant concentrations. Monomer droplet formation relies on agitation to disperse the monomer in the continuous phase as droplets that will be stabilised by the surfactant present. The distribution of surfactant during the initial particle nucleation stage, Interval I, determines the number and size of the polymerisation loci, and thus the rate of polymerisation and molecular weight of the polymer, when other parameters are held constant. During the course of polymerisation agitation contributes to the mass transfer of reagents between the many phases involved in the emulsion system, as well as to the continual break up of large monomer droplets and the coagulation of polymer particles.

Further experiments have been suggested to investigate and quantify the extent to which agitation determines the formation of polymerisation loci, and controls the rate of reaction by restricted supply of monomer to the reaction loci. These experiments will determine the minimum agitation conditions, combined with surfactant concentrations, which will be required in order for the course of an emulsion polymerisation to be governed by the chemistry alone.

The feasibility of using a continuous Loop Reactor of emulsion polymerisation was investigated. Batch polymerisations of styrene in the Loop Reactor showed that the shear forces required to disperse the monomer for successful emulsion polymerisation dictated that the flow within the Loop Reactor must be well into the turbulent regime. Experimental measurement and modelling of the residence time distributions and the degree of mixing in in the Loop Reactor showed very good agreement. The experience gained from the batch polymerisations, and the mixing measurements and modelling, enabled the chemical kinetics and production requirements to be linked into guideline for the design of a loop reactor for successful continuous emulsion polymerisation.

Further work on the evaluation of the effective longitudinal dispersion coefficient from the contributory mechanisms needs to be performed for the mixing model developed here to be used in the design of Loop Reactors.

During the course of this work polymer samples were analysed for their molecular weight distribution by Gel Permeation Chromatography, G.P.C. A computational technique for removing the axial dispersion effect, that is inherent in G.P.C., from the chromatogram has been developed. The advantages of this technique are that it avoids numerical instability experienced by other methods, it is easily calibrated for the particular polymer/solvent system under study and is readily applied in a routine manner.

References.

1.1 Kiparissides, C., MacGregor,J.F. & Hamielec, A.E.
Can. J. Chem. Eng. 58 p48 (1980)
1.2 Kiparissides, C., MacGregor, J.F., Singh, S. & Hamielec, A.E.
Can. J. Chem. Eng. 58 p65 (1980)
1.3 Nomura, M., Narada, M., Eguiki, W., & Nagata, S.
J. Appl. Polym. Sci. 16 p835 (1972)
1.4 Donescu, D., Gosa, K. & Ciupitoiu, A.
J. Macromol. Sci. Chem. A22 p931 (1985)

2.1 Dismore, R.P. U.S. Patent 1732795 (1927).
2.2 Blackley, D.C. Emulsion Polymerisation Theory & Practice.
Applied Science Publishers Ltd. 1975.
2.3 Piirma, I. Ed. Emulsion Polymerisation.
Academic Press Inc. 1982.
2.4 Harkins, W.D. J. Chem. Phys. 13 p381 (1945).
2.5 Harkins, W.D. J. Chem. Phys. 14 p47 (1946).
2.6 Smith, W.V. & Ewart, R.H. J. Chem. Phys. 16 p592 (1948).
2.7 Friis, N. & Hamielec, A.E. J. Polym. Sci. 11 p3321 (1973)
2.8 Friis, N. & Hamielec, A.E. J. Polym. Sci. 12 p251 (1974)
2.9 Min, K.W. & Ray, W.H. J. Macromol. Sci.
Revs. Macromol. Chem. C11(2) 177 (1974).
2.10 Min, K.W. Ph.D. Thesis University of New York, Buffalo, 1976.
2.11 Min, K.W. & Ray, W.H. J. Appld. Poly. Sci. 22 pp89 (1978).
2.12 Kiparissides, C., MacGregor, J.F. & Hamielec, A.E.
Can. J. Chem. Eng. 58 p48 (1980)
2.13 Kiparissides, C., MacGregor, J.F. & Hamielec, A.E.
Can. J. Chem. Eng. 58 p65 (1980)
2.14 Nomura, M., Narada, M., Eguiki, W. & Nagata, S.
J. Appl. Polym. Sci. 5 p135 (1961)

3.1 Oldshue, J.Y. Fluid Mixing Technology. p49 Mc.Graw Hill Publication Co. N.Y. 1983.

3.2 Stepanek, P. & Konak, C. Advances in Colloid & Interface Science. 21 p195 (1984).

4.1 Geddes, K., Chemistry & Industry, 6 p23 (1983).

4.2 Gulf Oil Canada Ltd., British Patent Specification 1220777 (1971).

4.3 Warnecke, H.J., et al, Chem. Eng Sci. 40(12) pp2321 (1985).

4.4 Blenke, H., Advan. Biochem. Engng., 13 p121 (1979).

4.5 Carslaw, H.S. 'Introduction to the Mathematical Theory of Conduction of Heat in Solids.' 2nd Edition, Dover Publications, New York, 1945. p153

4.6 Badder, E.E. & Brooks, B.W., Chem. Eng. Sci., 39(10) p1499 (1984).

4.7 Massey, B.S. 'Mechanics of Fluids.', 4th Edition, Van Nostrand Reinhold. p193.

5.1 Moore, J.C. J. Poly. Sci. A2 p835 (1964).

5.2 Tung, L.H. J. Appl. Poly. Sci. 10 p375 (1966).

5.3 Chang, K. & Huang, R. J. Appl. Poly. Sci. 13 p1459 (1969).

5.4 Hamielec, A.E. & Ray, W.H. J. Appl. Poly. Sci. 13 p1319 (1969).

5.5 Bamford, C.H. & Tompa, H. J. Poly. Sci. 10 p345 (1953)

5.6 Margenau, H. & Murphy, G.M. The Mathematics of Physics and Chemistry. Van Nostrand, New York 1943, p421.

5.7 National Bureau of Standards, Handbook of Mathematical Functions.

5.8 Tung, L.H., Moore, J.C. & Knight, G.W. J. Appl. Poly. Sci. 10 p1261 (1966)